Deformation and aggregation of red blood cells and vesicles flowing in microchannels

Ing. Luca Lanotte

PhD in Chemical Engineering – XXV Ciclo
Dipartimento di Ingegneria Chimica, dei Materiali e
della Produzione Industriale
Università Federico II di Napoli

PhD in Physics
Laboratoire Interdisciplinaire de Physique (LIPhy)
Université Joseph Fourier de Grenoble

Vinci Program 2010–13

UNIVERSITÀ
ITALO
FRANCESE

Deformation and aggregation of red blood cells and vesicles flowing in microchannels

Ing. Luca Lanotte

Dottorato in Ingegneria Chimica – XXV Ciclo
Dipartimento di Ingegneria Chimica, dei Materiali e della Produzione Industriale
Università Federico II di Napoli

Tutor

Prof. Stefano Guido

Doctorat en Physique
Laboratoire Interdisciplinaire de Physique (LIPhy)
Université Joseph Fourier de Grenoble

Tutors

Dr. Lionel Bureau and Dr. Chaouqi Misbah

Vinci Program 2010–13

Wisdom is brilliant, she never fades.
By those who love her, she is readily seen,
by those who seek her, she is readily found.
She anticipates those who desire her by making herself known first.
Whoever gets up early to seek her will have no trouble
but will find her sitting at the door.
Meditating on her is understanding in its perfect form,
and anyone keeping awake for her will soon be free from care.
(Wisdom 6, 12–15)

La sapienza è radiosa e indefettibile,
facilmente è contemplata da chi l'ama
e trovata da chiunque la ricerca.
Previene, per farsi conoscere, quanti la desiderano.
Chi si leva per essa di buon mattino non faticherà,
la troverà seduta alla sua porta.
Riflettere su di essa è perfezione di saggezza,
chi veglia per lei sarà presto senza affanni.
(Sapienza 6, 12–15)

La Sagesse est resplendissante, elle est inaltérable.
Elle se laisse aisément contempler par ceux qui l'aiment,
elle se laisse trouver par ceux qui la cherchent.
Elle devance leurs désirs en se montrant à eux la première.
Celui qui la cherche dès l'aurore ne se fatiguera pas:
il la trouvera assise à sa porte.
Ne plus penser qu'è elle prouve un parfait jugement,
et celui qui veille en son honneursera bientôt délivré du souci.
(Sagesse 6, 12–15)

Abstract

Italian version

I globuli rossi (GR) rivestono un ruolo fondamentale nell'espletamento delle funzioni fisiologiche all'interno del corpo umano. Nel microcircolo, ad esempio, dove fluiscono in capillari dal diametro inferiore o, comunque, paragonabile alle loro stesse dimensioni, gli eritrociti sono responsabili dello scambio di ossigeno e sostanze nutritive tra il sangue ed i tessuti. Il rilascio di gas, secondo il parere pressocché unanime della comunità scientifica, si verifica grazie alla intima interazione tra i GR e l'endotelio che riveste i vasi sanguigni. È stato, inoltre, provato in numerosi lavori scientifici come disfunzioni nelle proprietà dei globuli rossi e il danneggiamento del tessuto endoteliale, in particolare dello strato glicoproteico che lo ricopre (glycocalyx), siano la causa principale di malattie vascolari molto diffuse oggigiorno, come la trombosi, il diabete, l'aterosclerosi. Lo studio del comportamento dei globuli rossi nel sistema microvascolare ha assunto, dunque, un'importanza sempre maggiore nel mondo della ricerca. La conoscenza delle proprietà meccaniche e reologiche che consentono agli eritrociti di deformarsi e organizzarsi in aggregati all'interno dei vasi, per esempio, consentirebbe di comprendere a pieno i meccanismi che governano il flusso sanguigno e, di conseguenza, facilitare la diagnosi di stati patologici.

In questo lavoro di tesi l'attenzione è focalizzata essenzialmente su due argomenti: l'aggregabilità dei globuli rossi durante il flusso in capillari e la funzione del glycocalyx endoteliale nel microcircolo. La formazione di treni di eritrociti all'interno di vasi di piccole dimensioni (diametro ≤ 20 μm) è del tutto normale all'interno del corpo umano e favorisce la coagulazione del sangue in caso di danneggiamento dei tessuti. L'alterazione del normale fenomeno di aggregazione dei GR, però, può portare all'insorgere di patologie diffuse quanto dannose, come la trombosi. Per quanto l'argomento sia attuale e di rilevante interesse scientifico, un'analisi quantitativa del fenomeno di formazione di aggregati di globuli rossi (cluster) non è ancora stata effettuata. Nella prima fase di tale progetto di dottorato, dunque, presso il laboratorio Chemems del Dipartimento di Ingegneria Chimica, dei Materiali e della Produzione Industriale di Napoli, sono stati condotti esperimenti *in vitro* su sospensioni di eritrociti, con ematocrito attorno al 10%,

per osservare la tendenza dei GR ad aggregarsi durante il moto in tubi in silica di diametro micrometrico (≈ 10 μm). È stata verificata questa attitudine in funzione del battente di pressione imposto e del tempo di residenza all'interno di segmenti di microcapillari, misurando la lunghezza degli aggregati e la loro composizione in numero. La campagna sperimentale è stata mirata a comprendere quale sia il tipo di interazione che si verifica tra le cellule componenti un cluster: si tratta di un'interazione di tipo puramente idrodinamico o intervengono anche forze di altra natura? Dai risultati sperimentali appare chiaro come la vera forza spingente del fenomeno sia la pressione imposta nei microtubi La visione più precisa del fenomeno, grazie ad un approccio microfluidico, consente di gettare le basi per la progettazione e la successiva messa a punto di dispositivi clinici atti a monitorare l'aggregabilità eritrocitaria a fini diagnostici, su sangue sano, ma anche in corrispondenza di stati infiammatori, ad esempio.

La seconda parte del progetto è stata effettuata in collaborazione tra il Dipartimento di Ingegneria Chimica, dei Materiali e della Produzione Industriale di Napoli ed il Laboratoire Interdisciplinaire de Physique di Grenoble. È stata effettuata una campagna sperimentale su microcapillari in vetro rivestiti da polymer brush, al fine di simulare le condizioni *in vivo* nel microcircolo. Si è verificato come la presenza di strati (layer) polimerici alteri non solo le proprietà idrodinamiche del flusso nei microtubi trattati, ma anche quelle dinamiche dei globuli rossi circolanti al loro interno. È stabilito con certezza che il lumen dei vasi sanguigni è rivestito da uno strato di glicopolimeri (glycocalyx) legati alla membrana delle cellule endoteliali che ricoprono le loro pareti. La conoscenza del ruolo idrodinamico del layer in questione sarebbe molto utile per (i) comprendere come le disfunzioni o i danneggiamenti del glycocalyx siano coinvolti in patologie vascolari (ad esempio l'aterosclerosi) e (ii) al fine di sviluppare test basati sulla microfluidica, in grado di rappresentare correttamente le interazioni tra pareti e componenti del sangue. I polymer brush, per la loro spiccata attitudine a modificare le proprietà chimico-fisiche delle superfici ed alterare il flusso in ambito micro e nanofluidico, rappresentano una opzione logica, allo scopo di riprodurre l'effetto del glycocalyx all'interno dei vasi nel microcircolo e le interazioni tra catene polimeriche e globuli rossi. Layer nanometrici di polyhydroxyethylmethacrylate (pHEMA) sono stati prodotti attraverso cosiddetta tecnica grafting-from e, dopo accurata caratterizzazione, utilizzati per rivestire le superfici interne di capillari in vetro dal diametro di 10 μm. In questo lavoro, si presentano i profili di velocità ottenuti investigando il flusso all'interno dei suddetti microcapillari rivestiti. Si mostra come la riduzione del flusso, causata dalla presenza delle spazzole polimeriche, è significativamente più grande rispetto a quanto si verificherebbe in seguito a una semplice riduzione geometrica del lumen disponibile o se considerassimo lo strato polimerico come un bordo poroso ed elastico, così come suggerito in precedenti lavori teorici. Inoltre, dall'osservazione del flusso di eritroc-

iti all'interno dei microcapillari rivestiti da polymer brush, si è riscontrato come, sia la velocità che la deformabilità dei GR, dipendano strettamente dalla presenza dei layer polimerici sulle pareti dei microtubi. Risulta anche evidente come il rallentamento riscontrato nel flusso dei globuli rossi non sia direttamente proporzionale allo spessore dei layer, al contrario di quanto verificato nelle misurazioni riguardanti il puro flusso idrodinamico.

French version

Les globules rouges (GR) jouent un rôle clé dans l'exercice de fonctions physiologiques dans le corps humain. Dans la microcirculation, par exemple, où ils s'écoulent dans des capillaires de diamètre comparable à leurs mêmes dimensions, voire de taille inférieure, les érythrocytes sont responsables de l'échange d'oxygène et de nutriments entre le sang et les tissus. Les émanations de gaz, selon l'avis unanime de la communauté scientifique, est due à l'interaction intime entre les GRs et l'endothélium recouvrant les vaisseaux sanguins. Il a également été montr'e dans de nombreux articles scientifiques que des dysfonctionnements dans les propriétés des globules rouges et des dommages du tissu endothélial, en particulier au niveau la couche de glycoprotéine qui le recouvre (glycocalyx), sont la principale cause de maladies vasculaires telles que: la thrombose , le diabète, l'athérosclérose. En conséquence, la recherche sur le comportement des globules rouges dans le système microvasculaire est devenu d'un intérêt scientifique majeur. La connaissance des propriétés mécaniques et rhéologiques qui permettent aux érythrocytes de se déformer et de s'organiser en agrégats à l'intérieur des vaisseaux permettrait, par exemple, de mieux comprendre les mécanismes qui gouvernent la circulation du sang et, par conséquent, de faciliter le diagnostic des états pathologiques.

Dans cette thèse l'attention s'est concentrée sur deux thèmes principaux: l'agrégation des globules rouges pendant l'écoulement dans les capillaires et la fonction du glycocalyx endothéliale dans la microcirculation. La formation de trains d'érythrocytes dans les récipients de petites dimensions (diamétre ≤ 20 μm) est tout à fait normal à l'intérieur du corps humain et favorise la coagulation du sang en cas de lésion tissulaire. L'altération du phénomène normal de l'agrégation des GR, cependant, peut conduire à l'apparition de maladies répandues et nocives, telles que la thrombose. Même si le sujet est à la fois opportun et d'intérêt scientifique considérable, une analyse quantitative de la formation d'agrégats de globules rouges (cluster) n'avait pas encore été réalisée. Dans la première phase de ce projet de thèse au sein du laboratoire Chemems du Département de Ingénierie Chimique, de Matériaux e de la Production Industrielle de Naples des expériences *in vitro* ont été réalisés sur des suspensions de globules rouges avec un hématocrite $\approx 10\%$, afin d'observer la tendance des GR à s'agréger au cours de leur déplacement dans des tubes de silice avec un diamètre de quelque micromètre (≈ 10 μm). Ce comportement a été évalué en fonction de la pression imposée et du temps de résidence à l'intérieur de segments de microcapillaires, en mesurant la longueur des agrégats et leur composition numérique. La campagne expérimentale avait pour but de comprendre le type d'interaction qui se produit entre les celules composants un cluster: il s'agit d'une interaction purement hydrodynamiques ou des autres forces sont également impliqués? À partir des résultats expérimentaux, il est clair

que la véritable force motrice du phénomène est la pression imposée dans des microtubes. Le point de vue plus précise du phénomène, grâce à une approche microfluidique, permet de jeter les bases pour la conception et le développement ultérieur de dispositifs cliniques adaptés pour contrôler l'agrégabilité érythrocytes à des fins diagnostiques, tant du sang sain, que aussi en correspondance de des états inflammatoires, par exemple.

La deuxième partie du projet a été réalisée en collaboration entre le Département de Ingénierie Chimique, de Matériaux e de la Production Industrielle de Naples et le Laboratoire Interdisciplinaire de Physique de Grenoble. Une campagne expérimentale a été réalisée sur microcapillaires en verre, revêtues de brosses de polymères, afin de simuler les conditions *in vivo* dans la microcirculation. Il a été observé que la présence de couches de polymére modifie non seulement les propriétés hydrodynamiques de l'écoulement dans des microtubes traités, mais aussi la dynamique des globules rouges circulant dans eux. Il a été établi avec certitude que le lumen des vaisseaux sanguins est revêtue d'une couche de glyco-polymères (glycocalyx) liées à la membrane de cellules endothéliales qui tapissent les parois. La compréhension du rôle hydrodynamique de la couche en question apparaît d'un intérêt essentiel pour (i) comprendre comment le dysfonctionnement et/ou l'endommagement du glycocalyx sont impliqués dans les maladies vasculaires (l'athérosclérose, par exemple) et (ii) pour développer des tests basés sur la microfluidique, capables de représenter correctement les interactions entre les parois et les composants sanguins. Les brosses de polymères représentent une option logique, pour reproduire l'effet du glycocalyx à l'intérieur des vaisseaux de la microcirculation et les interactions entre les chaînes de polymères et les globules rouges, grâce à leur aptitude à modifier les propriétés physico-chimiques de surfaces et le champ d'écoulement micro et nanofluidique. Les couches nanométriques de polyhydroxyéthylméthacrylate (PHEMA) ont été produites par ce qu'on appelle technique de greffage "*grafting-from*", et, après une caractérisation approfondie, utilisées pour revêtir les surfaces internes des capillaires en verre d'un diamètre de 10 μm. Dans cette thèse, nous présentons les profils de vitesse obtenus en étudiant la circulation au sein de ces microcapillaires recouverts de brosse de polymères. On montre que la réduction de l'écoulement, provoquée par la présence de brosses de polymres est significativement plus grande par rapport à ce qui se produirait à la suite d'une simple réduction géométrique de lumen disponible ou si on considère la couche de polymère comme une bordure poreuse et élastique, telle que suggéré dans des articles théoriques déjà publiés. De plus, à partir de l'observation de l'écoulement de globules rouges à l'intérieur des microcapillaires revêtues par la brosse de polymère, il a été constaté que la vitesse et la capacité de déformation de globules rouges, dépendent strictement de la présence de la couche de polymère sur les parois des microtubes. Il est également évident que le ralentissement de l'écoulement des globules rouges n'est pas directement

proportionnel à l'épaisseur des couches, contrairement à ce qui s'est produit dans les mesures concernant l'écoulement hydrodynamique pur.

Contents

1 Introduction **13**
- 1.1 Microvascular system . . . 14
  - 1.1.1 Structure . . . 14
  - 1.1.2 Functions . . . 14
  - 1.1.3 Pathologies . . . 16
- 1.2 Human blood . . . 17
  - 1.2.1 Platelets . . . 20
  - 1.2.2 White Blood Cells . . . 20
- 1.3 Red blood cells . . . 20
  - 1.3.1 Geometry and mechanical properties . . . 20
  - 1.3.2 Hemorheology . . . 23
- 1.4 Blood observation in microfluidics . . . 28
  - 1.4.1 Historical background . . . 28
  - 1.4.2 Imaging technologies for blood cells observation . . . 30
  - 1.4.3 Microfluidic point-of-care . . . 31
- 1.5 Endothelial glycocalyx . . . 32
  - 1.5.1 Endothelium . . . 32
  - 1.5.2 Glycocalyx . . . 35
- 1.6 Modeling of red blood cells . . . 38
  - 1.6.1 Historical background . . . 38
  - 1.6.2 Basic modeling of RBCs under flow . . . 40
  - 1.6.3 Different methods of solutions . . . 41
- 1.7 Aim of the thesis . . . 43

2 Red blood cell clustering **45**
- 2.1 Introduction . . . 45
- 2.2 Materials and methods . . . 46
  - 2.2.1 Experimental apparatus . . . 46
  - 2.2.2 Blood samples . . . 47
- 2.3 Results and discussion . . . 48
  - 2.3.1 Experimental investigation . . . 48
  - 2.3.2 Numerical simulation . . . 56
- 2.4 Conclusions . . . 59

3 Flow in brush-coated channels **63**
3.1 Introduction . . . 63
3.1.1 Polymer brushes . . . 63
3.1.2 Biocompatible polymer brushes as endothelial glycocalyx model . . . 66
3.2 Materials and methods . . . 67
3.2.1 Materials . . . 67
3.2.2 Samples preparation . . . 68
3.2.3 Characterization techniques . . . 69
3.2.4 Experimental apparatus for flow measurements . . . 71
3.3 Results and discussion . . . 72
3.3.1 Samples characterization . . . 72
3.3.2 Flow velocity in brush-coated capillaries . . . 76
3.3.3 Interpretation of experimental results . . . 78
3.4 Conclusions . . . 81

4 RBC flow in "hairy" microcapillaries **83**
4.1 Introduction . . . 83
4.1.1 Endothelial glycocalyx: properties and main functions 83
4.1.2 Red blood cell flow in microvascularity: the interaction with glycocalyx . . . 84
4.2 Materials and methods . . . 85
4.2.1 Experimental apparatus . . . 85
4.2.2 Blood samples . . . 86
4.3 Results and discussion . . . 86
4.3.1 Red blood cell velocity . . . 86
4.3.2 Red blood cell deformation . . . 90
4.4 Conclusions . . . 92

5 Conclusions **95**
5.1 Achieved results . . . 95
5.2 Possible developments . . . 97

6 Acknowledgments **99**

A Publications **117**

B Conferences **119**

Chapter 1

Introduction

The role of red blood cells (RBCs or erythrocytes) in microcirculation is a topic of fundamental importance in scientific research. In fact, RBCs are involved in O_2 and nutrients delivery to all human tissues, thanks to their ability to deform and flow even in very narrow vessels. Therefore, alterations of their physical properties are the reason of many pathological disfunctions and most of vascular diseases. Although there have been vast improvements in the last century, and especially in the last thirty years, many open questions have still to be handled:

- *Which are the reasons and mechanisms that lead RBCs to aggregate during their flow, mostly in microvessels?*
- *Is there a connection that links erythrocytes aggregation and nutrients delivery in microcirculation?*
- *What is the interaction between red blood cells and capillary walls (i.e. the so-called glycocalyx that lines endothelium)?*
- *How do glycocalyx damages affect blood flow and RBCs properties?*

The development of suitable techniques to investigate RBCs flow in microcapillaries, taking in account the interaction with the endothelial cells coating vessel inner walls, is a central point to give insights and solve these questions. In parallel with the *in vivo* approach, realistic, but also complicated to realize, and *in vitro* experiments, easier to carry out, but more distant to reality, is taking place the attempt to develop artificial systems that could simulate the presence of glycocalyx.

The first chapter of this thesis has the purpose to introduce the audience to its main topics and aims. A first section will provide a general overview about structure and functions of the microcirculatory system and possible disorders and disfunctions in microcirculation. Afterwards, the attention will be focused on human blood, its suspending phase, its corpuscolar parts

and, in particular, red blood cells (RBCs). The state of the art about *in vivo* and *in vitro* techniques, in order to observe RBCs flow in microcapillaries and their interaction with glycocalyx, will be provided.

1.1 Microvascular system

1.1.1 Structure

The microcirculation is referred to as the small branches of the circulatory system with diameters ranging from few micrometers (4–8 μm) up to one hundred micrometers [26]. The total number of such dimensioned capillaries in human body is probably higher than 10^9 and they play a key role in human physiological functions, since 80% of total pressure drop between the aorta and the vena cava occurs in the smaller size vessels, approximately. In macrocirculation, the larger vessels serve as tubes to and from the heart and the peripheral organs and as pressure reservoirs, essential to cardiac functions. On the contrary, microvessels differentiate the microcirculation because they are in close contact or embedded within the organs, whereas most of the large vessels are not. Microvessels are organized in a complex network [41]. In some tissues, such as mesentery, the microcirculation can be approximated as a diverging tree of arterioles, which feed blood to the capillaries, that in turn drain into a converging tree of venules. It is simplistically possible to schematize microcirculation as a network of tubes in series or in parallel, the latter exhibiting identical properties [26, 27], but the reality is much more complex. In fact, the structure is highly heterogeneous[43]. A parameter to quantify this heterogeneity is the so called *generation number*, defined as the number of branch points between the main feeding arteries and a given vessel. In mesentery networks, the generation number is ranging between 2 and 25 (Figure 1.1). By means of computer simulation it is possible to reconstruct microvascular networks and have an idea of the structural heterogeneity in microcirculation.

As a consequence, the microcapillaries cannot be regarded as a set of equivalent vessels, since they experience many widely changing hemodynamic conditions. The same is for venules and arterioles. The vessels heterogeneity has a deep influence on the functional behavior of microcirculation [28]. Recent studies try to associate both experimental results, theoretical point of view and computational models, since each individual approach cannot understand and explain by itself the complexity of microvessel network structures and the resulting flow patterns.

1.1.2 Functions

The main function of the circulatory system is to transport nutrients and other corpuscolar materials throughout the body. Diffusion could appear

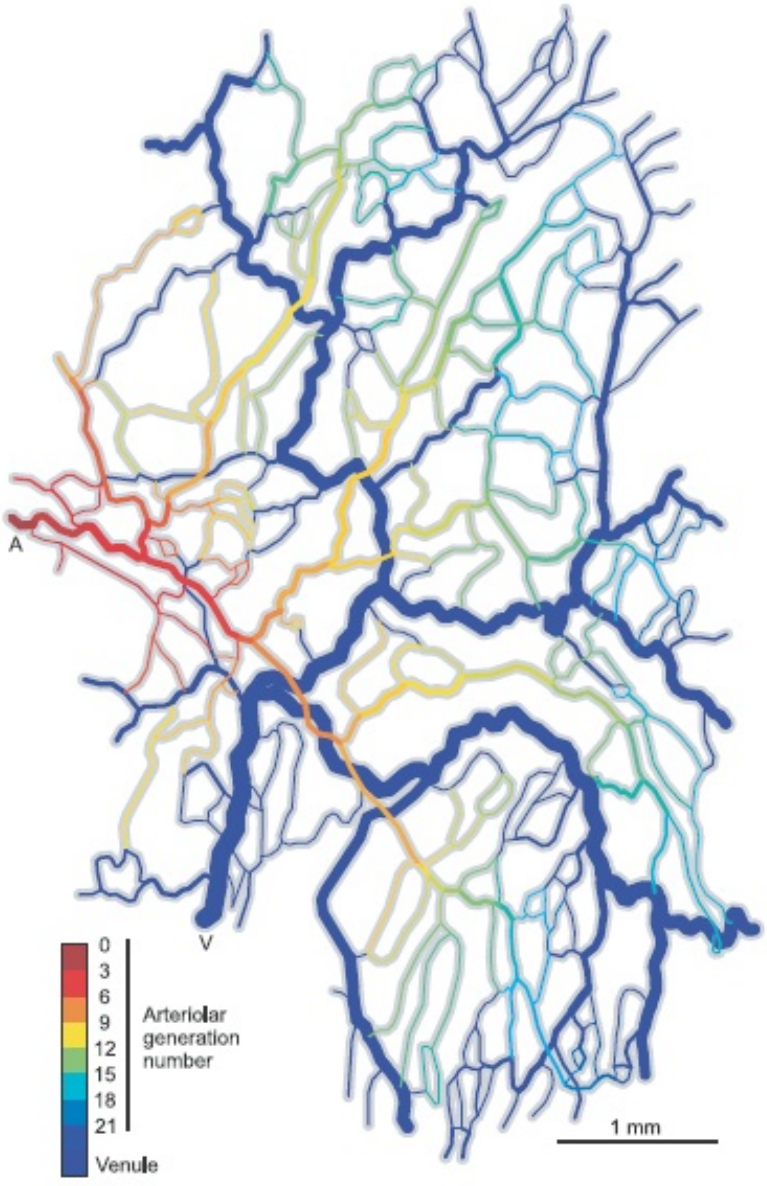

Figure 1.1: Computer-generated image of a mesenteric network of microcapillaries [29].

the most efficient way to do it, but in human body the delivery of materials mostly occurs thanks to convection. In fact, diffusion is effective only over very short distances, like in narrow capillaries, while convection, that is defined as the transport by a flowing fluid, has no such limitation, and is really useful for mass transport in macrocirculation. In other words, convection is easier and efficient in large tubes, since flow resistance rapidly increases with decreasing conduit diameter, but a large number of small capillaries, densely distributed throughout all body, is necessary to efficiently transport substances to tissues and organs by diffusion.

Oxygen is one of the most important substances that have to be distributed and removed by blood. In particular, brain and heart have a high and continuous need for O_2 and, if the supply fails or is slowed down, permanent damages may occur. Because of its scarse solubility in water and subsequently in tissues, ensuring an adequate oxygen supply causes heavy demands on the circulatory system. For instance, it is necessary to bring oxygen within a very small distance of all cells needing O_2. Then, very steep gradients between blood cells and tissues are generated, in order to have adequate diffusive fluxes. In summary, oxygen level in tissues is closely depending on the microvascular architecture and the flow distribution [29].

Supplying an adequate blood flow to all body parts, accordingly to requirements that can vary with time and positions on a large variety of scales [30], is not the only function of the circulatory system. In order to satisfy all the changing demands, the vascular network is capable of wide variations in perfusion in blood flow (metabolic regulation) [42], or keeping an almost constant flow over a range of perfusion pressures (autoregulation) [31, 32]. To realize this, the vascular system is able to answer to many different stimuli, such as pressure and shear forces on vessel walls generated by the flow and the level of some fundamental substances (oxygen, metabolites and vasoactive agents). By considering short time scales, blood flow is locally controlled through the contraction and relaxation of smooth muscles that line the inner walls of arterioles. In this regard, cell-cell communication via gap junctions, in particular between endothelial cells (ECs), is a fundamental component in the ability of vasculature to respond to varying demands in a coordinate way [33].

The analysis of the circulatory system requires consideration of multiple interacting biological factors, linked to one another, as it is possible to see in Figure 1.2 [29].

1.1.3 Pathologies

Significant blood loss, if not rapidly replenished, can lead to irreversible malfunctions in the microcirculation and, consequently, death. The microcirculation represents a mesoscale in the circulatory system, linking smaller and larger scale phenomena one to another. Microvascular disfunctions can

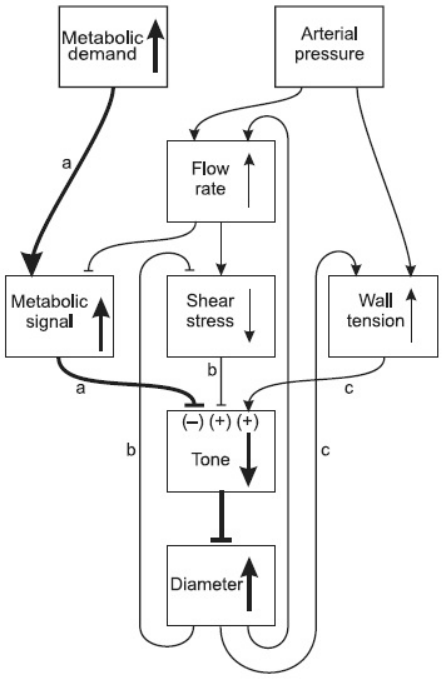

Figure 1.2: Interaction of factors involved in blood flow regulation [29].

be caused by the deleterious consequences of other pathologies, like hypertension, sickle cell anemia and diabetes, or by factors involving the network itself. Microcirculatory disorders are major determinants of morbidity and mortality in the modern society. For instance, the heterogeneous vascular network structure can lead to regions of hypoxia, even in normally well-oxygenated tissues. The hypoxic regions can affect tissue physiological functions and compromise eventual therapies, as in the case of radiotherapy in tumors [34]. This is a typical example of macro—consequences of microcirculation-scale phenomena. That is why, both basic and clinical research focus their attention on the methods to prevent and treat the damaging effects of microvascular disorders on bodily functions.

1.2 Human blood

Human blood is a specialized connective tissue flowing in our veins and arteries [44]. An average adult has roughly 5 liters of blood circulating in his body. It is essentially a suspension of living cells in a liquid called plasma. Plasma has a straw yellow color and is consisting of water ($\approx 92\%$), mineral ions, nutrients, (glucose, amino acids, fatty acids), hormones that lend to blood the function of messenger and the ability of signaling tissue damages, waste products (carbon dioxide), electrolytes (mainly sodium and

chloride) and dissipated proteins. The protein mostly present in plasma is albumin, that is important to regulate the colloidal osmotic pressure in blood vessels. Plasma constitutes the 55% of blood, the remaining 45% is mainly constituted by red blood cells and a low percentage ($\approx 1\%$) of white blood cells and platelets (Figure 1.3). Blood performs many important functions:

- *Delivery of oxygen and nutrients to tissues and removal of waste.* Oxygen deliver occurs thanks to red cells, since O_2 is mainly bound to the hemoglobin carried in erythrocytes. About 98.5% of the oxygen in a sample of arterial blood in a healthy human breathing air at sea-level pressure is chemically combined with the hemoglobin (Hgb), which is certainly the primary transporter of oxygen. The remaining 1.5% is simply dissolved in the other blood liquids. With the exception of pulmonary and umbilical arteries and their corresponding veins, arteries carry oxygenated blood away from the heart and deliver it to the body via arterioles and capillaries (4–5 microns in diameter), where the oxygen is consumed. Afterwards, venules and veins carry deoxygenated blood back to the heart. Under normal conditions in humans at rest, hemoglobin in blood leaving the lungs is about 98–99% saturated with oxygen. In a healthy adult at rest, deoxygenated blood returning to the lungs is still approximately 75% saturated. Nutrients, such as amino acids and fatty acids, are dissolved in plasma, or bound to its proteins. During the flow in circulatory system, blood provide to remove waste substances, such as carbon dioxide, urea and lactic acid.

- *Coagulation*, that is a fundamental part of the body's self-repair mechanism. Basic notions about coagulation will be reported in the following, just to shed light on the dynamics and link vascular pathologies to coagulative disfunctions.

- *Immunological functions.* They include mainly circulation of white cells and detection of foreign material by antibodies (immunoglobulins). In mammals, blood is in equilibrium with lymph, which is continuously formed in tissues from blood by capillary ultrafiltration. Lymph is collected by a system of small lymphatic vessels and directed to the thoracic duct, which drains into the left subclavian vein where lymph rejoins the systemic blood circulation.

- *Regulation of body pH.* The normal pH of blood is in the range of 7.35–7.45, which means slightly alkaline. Blood pH, partial pressure of oxygen (P_{O2}, partial pressure of carbon dioxide (P_{CO2}) and bicarbonate (HCO_3) are thoroughly regulated by homeostatic mechanisms, that influence and control the acid—base balance through respiratory and urinary system.

- *Regulation of body temperature.* Blood circulation transports heat throughout the body, and adjustments to this flow are an important part of thermoregulation. Increasing blood flow to the surface (e.g. during warm weather or strenuous exercise) causes warmer skin, resulting in faster heat loss, while decreasing surface blood flow lowers heat transport.

- *Hydraulic functions.* The restriction of blood flow can be used in specialized tissues to cause engorgement resulting in an erection of those tissues.

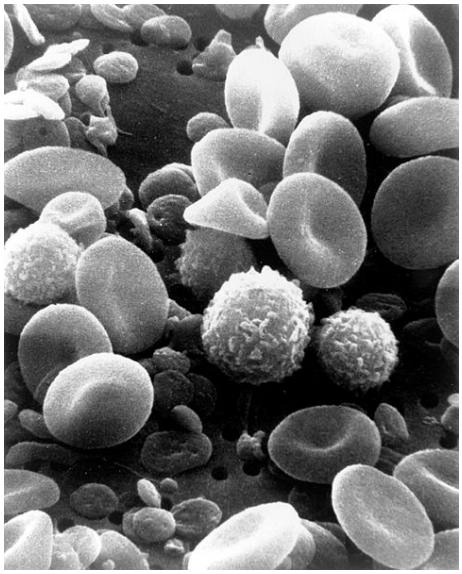

Figure 1.3: Circulating human whole blood elaborated by Scanning Electron Microscope (SEM) at the National Cancer Institute of U.S. in February 1982.

All blood cells are produced in the bone marrow in a process called hematopoiesis, which comprises erythropoiesis (production of red blood cells) and myelopoiesis (production of white blood cells and platelets). Excluding the childhood period, when all human bones produce RBCs, only larger ones are able to lead hematopoiesis in the adult phase. In addition, during childhood, the thymus gland, placed in mediastinum, is an important source of lymphocytes. Blood proteinaceous components (including clotting proteins) are mainly produced by the liver, hormones by the endocrine glands, while watery fraction is regulated by the hypothalamus and maintained by the kidney.

1.2.1 Platelets

Platelets (or thrombocytes) are cell fragments (i.e. they have not a nucleus containing DNA) derived from precursors megakaryocytes fragmentation, during blood cells formation in bone marrow. Thrombocytes have a diameter of 2–3 μm and an approximate life span of 5–9 days. They are known as natural growth factors, but, most of all, they are important because of their involvement in hemostasis and subsequent clots formation in mammalian blood. They change fibrinogen to fibrin. Fibrin subsequently creates a mean onto erythrocytes collect and clot, implementing a dual action: stopping more blood from leaving the body and preventing bacteria from entering the body.

Many pathologies are linked to an abnormal amount of platelets in our blood and to their dysfunctional behavior (thrombasthenia). The physiological concentration of thrombocytes in healthy blood is 150–400 $\times$ 10^9 per liter. If there is an insufficient number of platelets, problems in hemostasis can occur (thrombocytopenia). When there is an outrageous presence of thrombocytes in blood vessels (thrombocytosis), they can cause obstructions and, subsequently, strokes, myocardial infarction, pulmonary embolism or vessel blockage of body extremities.

1.2.2 White Blood Cells

White blood cells (or leukocytes) represent a fundamental part of the immune system, involved in defending individuals against diseases and foreign bodies. They destroy and remove old or aberrant cells and cellular debris, as well as attack infectious agents (pathogens) and foreign substances. There are five different types of white cells (neutrophil, eosinophil, basophil, lymphocyte, monocyte) with an average life span of 3–4 days. They are spread throughout human body, lymphatic system and blood too.

Normally, there are 4000–7000 white blood cells $\times$ μl of healthy human blood, i.e. they make up less 1% of the whole blood. This number is usually one of the indicators of patients health, together with some changes in physical properties of the cells, such as volume, conductivity and granularity, that reveal the presence of immature cells or malignant leukocytes, like in leukemia, known as the cancer of leukocytes.

1.3 Red blood cells

1.3.1 Geometry and mechanical properties

Red blood cells represent a large percentage of the cells present in human body ($\approx$ 25%). The amount of erythrocytes in healthy blood is in the range of 4–6 millions $\times$ μl, depending on the sex of the individual. In mammals, mature red blood cells lack nucleus and organelles. Each complete cycle of

circulation takes on average 20 seconds, considering a single erythrocyte, and the life span is about 120 days. RBCs are the main carrier to deliver oxygen and nutrients to human tissues through the circulatory system, thanks to their particular ability to deform and flow even in capillaries smaller in size than the cells themselves [35, 36]. The high deformability can be attributed to many factors, and, in particular, to: cell shape and dimensions, viscosity of intracellular fluid and rheological properties of cell membrane. Below, in this section, the attention will be focused on these three factors, in order to have an overview of physical and rheological properties of red blood cells.

Red blood cells rest shape is a biconcave disk with a major diameter of ≈ 8 μm and thickness of ≈ 2 μm (Figure 1.4). In fact, the discoid-like geometry is an equilibrium configuration between stomatocyte (cup shape) and echinocyte (crenated shape), which are also observed in healthy blood.

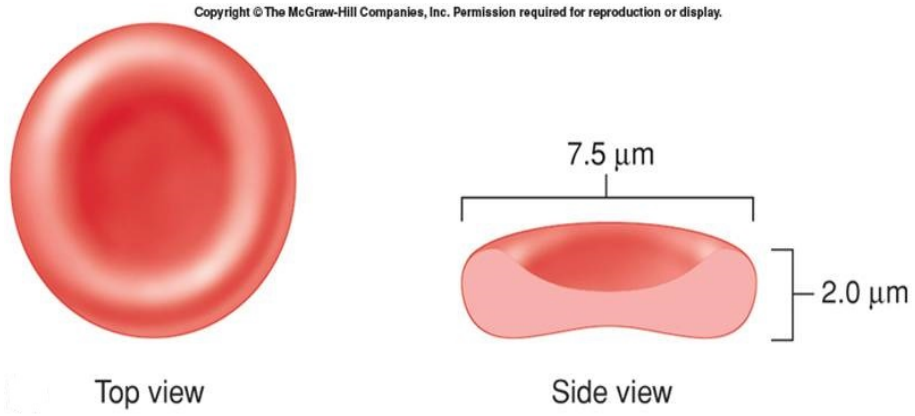

Figure 1.4: Average dimensions of a red blood cell at rest.

Mean cell volume (MCV) is ≈ 90 fl and mean surface area (MSA) is ≈ 135 μm^2 [37]. The MSA of an erythrocyte is significantly greater than the surface area (97 μm^2) of a hypothetical sphere enclosing a volume of 90 fl and this excess of area ($\approx 40\%$) partially influences RBC deformability, since RBC surface area and volume keep constant during the flow in microconfined geometries.

RBCs have a typical purple color due to the presence of hemoglobin into the intracellular fluid. Each molecule of hemoglobin has four heme groups, and their interaction with various molecules alters the exact color. A single red blood cell within a capillary contains about 3×10^9 hemoglobin. More than for chromatic reasons, hemoglobin is important because it imports a viscous rheological behavior to erythrocytes. The ageing of red blood cells entails a decrease of both MCV and MSA though their ratio remains constant. So, this is associated with an increase of the corpuscolar concentration and, consequently, of the inner viscosity [38].

The cell membrane of red blood cells consists of two main parts: an

envelope, made of a lipid bilayer containing integral proteins and a sort of membrane skeleton, consisting of an underlying protein network [39]. The former has the ability to resist bending (an important property in driving rest shape changes) without having shear resistance, while the latter, which is mainly composed of spectrin, actin, tropomyosin and proteins 4.1 and 4.9, is responsible for the resistance to stretch and shear deformation.

The rheological behavior of the cell membrane is another key factor affecting RBC deformability [40]. In a two-dimensional continuum mechanics description, the elastic behavior of the RBC membrane is expressed in terms of three fundamental moduli:

- *The shear modulus* μ, [N/m]: it is associated with constant area elongation or shear of the membrane [45]. The most commonly used methods for measuring μ are the micropipette aspiration, which consists of reading the length of the cell portion aspirated into a pipette under a given aspiration pressure, or through optical tweezers.

- *The area expansion modulus* K, [N/m]: corresponding to surface dilation (isotropic expansion), without either shear or bending [47]. As well as for the shear modulus, the micropipette aspiration is the main technique to measure K. The obtained values are relatively high (≈ 450 mN/m), and this justify the assumption of constant surface for red blood cells. Recently, by using fluorescence-imaged micropipette aspiration, the membrane skeleton alone has been investigated, after removal of the lipid bilayer, and regions of local dilation and compressibility were noticed.

- *The bending modulus* B, [N m]: without either shear or expansion. The membrane buckling instability is measured to estimate B, by using micropipette aspiration [40, 46]. This is a classical technique, but similar values are found by the analysis of thermal fluctuations of the membrane thickness (the flicker phenomenon) [48], tether formation and membrane pulling by atomic force microscopy.

The following table (Table 1.1) presents a summary of RBCs mechanical properties.

Finally, red blood cells have an elastic behavior. An evidence of their elasticity is the capacity to recover the rest shape when deforming forces are removed. But the erythrocytes rheological properties are not purely elastic [53], since the mechanical cell response has a viscous character due to the membrane fluidity and the intracellular viscous fluid [49, 50]. The force needed to deform a RBC increases with both the extent and the rate of deformation: this is an evidence of the viscous behavior of erythrocytes. Under some pathological conditions, a permanent deformation of the cells

	Value
RBC volume (μm^3)	88.4–107
Membrane surface area (μm^3)	129.9–141.4
Membrane surface viscosity (μN s/m)	0.47–1
Cytoplasmic viscosity (mPa s)	6–7
Membrane shear elastic modulus (μN/m)	1–13
Bending elastic modulus ($\times 10^{-}9$ N m)	0.13–3
Time for shape recovery (s)	0.1–0.27
Area compressibility modulus (mN/m)	300–500

Table 1.1: RBC mechanical properties [59].

can occur because of the excessive shear forces they are subjected to. Pathological alterations of red blood cell deformability are known to be implicated in several diseases, including diabetes, thalassemia and sickle cell disease. A method to investigate the viscous character is to measure the rest shape recovery time upon sudden removal of an applied deformation, such as in micropipette aspiration. The experimental results show that the recovery time varies from cell to cell, in the range 0.1–0.3 s, but it is not depending on the initial deformation. Other features that indicate a viscoelastic behavior of erythrocytes are formation of thin filaments (tethers) induced by yielding of the membrane above a critical stress value and permanent membrane deformation upon application of a small force for a time scale of few minutes. In conclusion, it is reasonable to say that RBCs have a viscoelastic rheological behavior.

1.3.2 Hemorheology

Rheology is the scientific field that studies flow and deformation of materials. Usually, fluids, including liquids and gas, are investigated, but solids can be under consideration too. Since the flow of red blood cells is a main topic of this thesis, and it is clear that viscous mechanical properties and deformability are fundamental to understand RBC behavior in the circulatory system, it is important to shed light on the rheological properties of blood and its corpuscolar elements. Hemorheology has a scientific and clinical interest, since the details of blood rheology and the alteration of the normal blood flow are helpful to understand and treat many disease states. There is an increasing amount of clinical and experimental data clearly indicating that the flow behavior of blood is a major determinant of proper tissue perfusion. From a rheological point of view, blood can be defined as a non-Newtonian two-phase liquid, or a liquid-liquid emulsion, considering the liquid-like behavior of red blood cells under flow. However, the definition of solid-liquid suspension, with the cellular elements being the solid phase, is very often used too.

Because of its complex nature, blood fluidity cannot be described by a single value of viscosity, with the exception of the apparent viscosity (AV, η), that considers blood as a whole fluid. AV shows higher values at low shear rates or shear stress, whereas a decrease and a subsequent approach to a minimum value (≈4–5 cP at 37 °C) is noticed for increasing shear rate (shear-thinning behavior) [13, 55, 56].

Figure 1.5 shows the shear rate-viscosity curves for three different conditions: normal blood, RBCs suspended in protein-free buffer (a medium that does not induce RBC aggregation), and chemically rigified RBCs suspended in plasma.

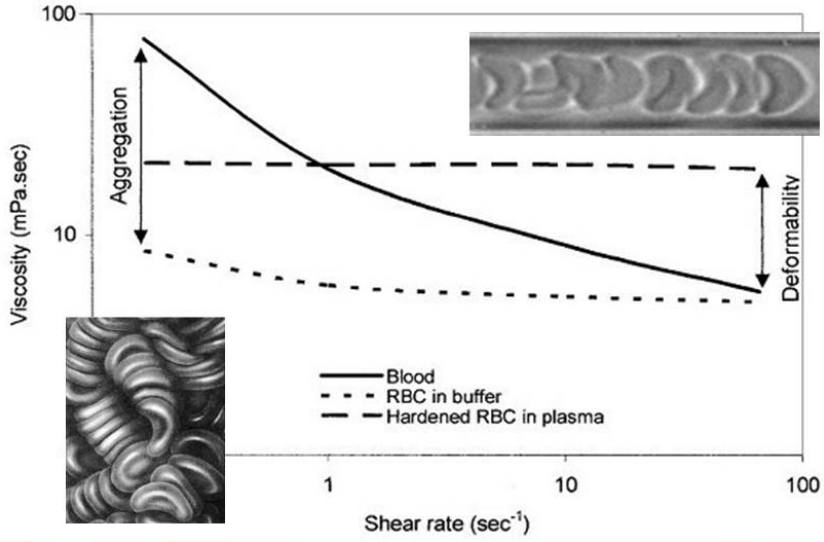

Figure 1.5: Shear rate-viscosity curves for normal blood, RBCs suspended in protein-free buffer and rigified RBCs suspended in plasma [51].

Taking into account the non-Newtonian behavior, the viscosity of blood depends on the existing shear forces and is determined by plasma viscosity, hematocrit, RBC deformability and RBC aggregation [51, 52]. First of all, the effects of changes in plasma viscosity and hematocrit value on blood fluidity will be briefly investigated. In order to better understand the experimental results presented in the following and the aims of this thesis, the attention will be mainly focused on the link between blood viscosity and RBC deformability and aggregation [57].

Plasma is a Newtonian fluid and can be referred to as the suspending phase of the cellular elements present in blood. Changes in plasma viscosity determine evident changes in blood viscosity too, obviously. Usually, plasma viscosity is in the range of 1.10–1.35 cP at 37 °C. Significant deviations from these values can be explained by the variation of proteins content in plasma. This can occur in case of tissue injuries or diseases. The abnormal

protein level (in pathophysiological conditions, plasma viscosity can range between 5–6 cP), called paraproteinemias, is closely linked with the clinical individual state. In addition, in laminar flow conditions, streamlines are disturbed by the presence of corpuscolar elements suspended in plasma. It is clear that the cellular portion of blood is the primary reason why its viscosity is higher than plasma one. The degree of flow disturbance depends on the concentration of flow elements. There are two main ways to quantify the concentration of corpuscolar elements and, subsequently, the flow disturbance: hematocrit (Ht) and relative viscosity (η_{rel}). The first parameter measures the percentage of red blood cells suspended in a blood sample, the second one represents the magnitude of viscosity difference between blood viscosity and plasma viscosity and is defined as the ratio $\frac{\eta_{blood}}{\eta_{plasma}}$. The value of relative viscosity rises with the increasing amount of cells. As Figure 1.6 clearly shows, the higher is the value of hematocrit the higher is the alteration of blood flow. For example, in correspondence of medium-high values of shear rate, an unit increase of Ht causes a 4% rise in blood viscosity.

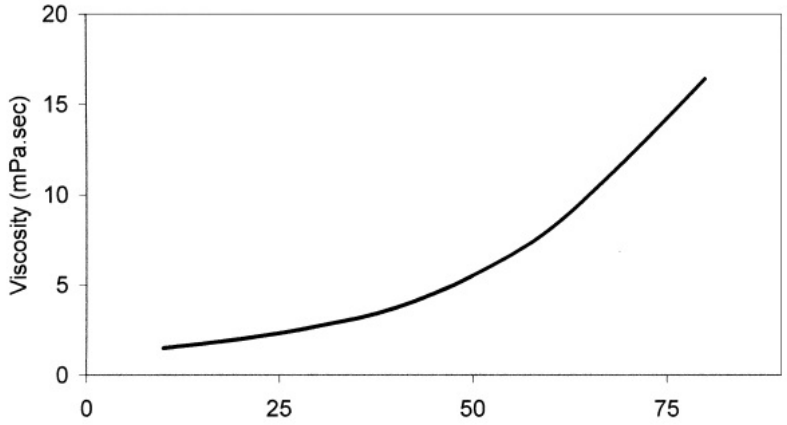

Figure 1.6: Effect of hematocrit on blood viscosity at an imposed value of the shear rate [51].

Red blood cell deformability

The disturbance of flow streamlines depends not only on the concentration of blood cells but also on the behavior of these cells under shear forces. RBCs are the major determinant of this effect, with these cells exhibiting a very special rheological behavior. RBCs are high deformable bodies and significantly contribute aiding blood to flow both under bulk flow condition and in the microcirculation [58, 59]. Deformability is sensitive to many factors, such as: local and general homeostasis, changes in the ratio RBC

membrane surface area to cell volume, cell morphology, cytoplasmic viscosity, combination and association of membrane skeletal proteins. Alterations of the normal values of these parameters and properties can be caused by genetic disorders, but by abnormal local tissue metabolism, oxidative stress or activated leukocytes too. Healthy RBCs tend to orient themselves with the flow streamlines, especially if the shear forces are high enough to slightly deform these cells. In fact, it has been experimentally observed that RBCs behave like fluid drops under most flow conditions. Thus, RBC deformation and orientation are the primary cellular factors affecting blood viscosity at high shear rates [44].

In static conditions (i.e. without external stresses and constraints), normal human red blood cells have a typical biconcave disk shape, due to cytoskeleton properties. When erythrocytes flow in vessels a deformation and consequently a change in shape can occur. In tubes with slightly larger diameters than cell size, the deformation of a flexible and buoyant RBC takes place in presence of significant shear and pressure fields in the flowing plasma. As far as the flow in capillaries with a diameter comparable to erythrocyte size is concerning [62, 63], it is necessary to consider the effect of two main factors, that will be described hereafter. The deformation of a static cell in a static fluid is due to the surrounding constraining walls. When the cell is moving in a tube, the effects of resulting pressure and shear fields in plasma have to be considered. In brief, the degree of deformation, referred to as deformability, of a red blood cell depends on the tube diameter and the strength of the flow in the channel. It is intuitive to deduce that higher deformability is noticed for small capillaries, in presence of high flow rate, while undeformed rest shape is observed in large tubes at low flow rates.

Why is RBC ability to deform so important? An example of the physiological relevance of erythrocyte tendency to deform is blood filtration through spleen vasculature, where older cells removal is mostly due to trapping in the fenestrated walls of venous sinuses [60]. In fact, in these sinuses RBCs are forced to squeeze in narrow rectangular slits between endothelial cells having width around 6 μm and height around 1 μm (i.e. one of the dimensions is quite smaller than cell size). RBC deformability is also an important parameter in evaluating hemocompability of artificial devices, such as rotary blood pumps [61]. Although the importance of these physiological and scientific functions, the most fundamental role of red blood cells is to keep high blood fluidity and aid high efficiency in oxygen delivery to human tissues, especially in microcirculation [65], where flowing cells and vessel walls are in close contact. Thus, a high deformability is an evident index of both properties. Erythrocytes usually assume a parachute-like shape during flow in microtubes. Extent and geometry of shape changes depend on magnitude and orientation of applied forces [62, 64].

Red blood cell aggregability

The tendency to aggregate of red blood cells is another property that plays an important role in hemorheology. At rest, RBCs tend to arrange in linear arrays, like stack of coins. Linear aggregates interact to form three—dimensional structures, as it is possible to observe via SEM microscopy (Figure 1.7). This phenomenon does not occur in all suspending solutions and it is evident from many scientific papers. The special composition of plasma promote RBC aggregation. In particular, type and concentration of fibrinogen, a fibrous protein, is important to encourage rouleaux formation, together with other macromolecules, such as high—molecular weight dextran and water-soluble polymers, even if the specific mechanism has not been fully elucidated [66]. The application of shear forces prevent aggregate organization: rouleaux are easily dispersed by fluid forces, but they are able to reform when the external forces disappear. At low shear rate flow and, consequently, high RBCs aggregability conditions, higher blood viscosity is pointed out. The reason of this change in viscosity value is the increase of particle size in vessels, that causes a flow streamlines disturbance. So, red blood cell aggregability represent the main determinant of blood viscosity at low shear conditions [67] and is implicated in important diseases, like clotting and thrombus formation , likely due to vascular obstruction [68, 69].

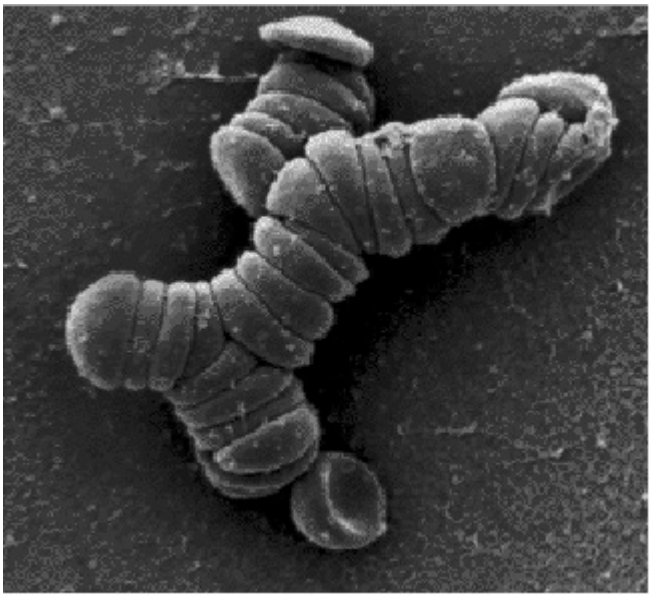

Figure 1.7: Rouleaux formation in static conditions (http://www.deroeck.co.uk/Research.htm).

As regards the better understanding of physiological functions of erythrocytes, it is important to focus on RBC aggregation during the flow in

microcirculation and not only in static conditions. As it has been observed both experimentally, *in vivo* and *in vitro*, and by numerical simulations, red blood cells tend to form trains (clusters) when they flow in microcapillaries, where the distance between consecutive cells is comparable to cell length. The cluster formation is closely linked to vascular diseases, like thrombosis, and clotting, more in dynamic than in static conditions. RBCs aggregation is also promoted by chemical signaling coming from RBCs, such as the release of ATP and ADP under low pO_2, low pH and in response to mechanical deformation [70]. If fibrinogen is the main determinant of rouleaux formation at rest condition, which is the driving reason for cluster formation in microvessels [71, 72]? The clustering phenomenon is often attributed to the slower motion of some cells down the capillary, thus creating a train of trailing cells. This is clearly true in presence of white blood cells. WBCs are larger and less deformable, so they move at significantly lower speeds in confined geometries and can be found at leading position of RBC clusters. There are no conclusive evidences to explain train formation in presence of RBCs only and many basic questions about physics of cluster formation remain open.

Finally, the rheological properties of erythrocytes that allow them to deform and aggregate are responsible of the non-Newtonian behavior of whole blood in large vessels and influence blood flow in microcirculation. The other cellular elements have no significant effects on the macroscopic flow (i.e. large geometry systems), while they influence flow resistance and dynamic in small capillaries (diameter lower than 100 μm, because of their low elasticity, especially white blood cells).

1.4 Blood observation in microfluidics

1.4.1 Historical background

Historically, the first experiments on microvessels took place in the seventeenth century, in parallel with the advent of the microscope. With respect to chronology, Malpighi was the first to discover the capillary system, while van Leeuvenhoek developed a first, pioneering technique to measure the velocity of red blood cells in a complex branching network of eel microcapillaries, and in a good agreement with the current measured values. The real breakthrough in microvascular research occurs after 1830, when Poiseuille, a French physicist, performed experiments on the hydrodynamics of the flow in tubes. His experimental results are now the basis to understand the mechanism of blood flow both in large than in micro-vessels. Of course, another cornerstone in research about microcirculation and hemorheology was the Swedish physiologist Fåhræus, who investigated blood flow properties in small tubes [73, 74], in 1930s. He carried out his experiments thanks to optical microscopy, observing RBCs flow in glass microcapillaries and regu-

lating under tight control the pressure drop in the tubes. By means of his experimental investigation, Fåhræus found out one of the most important anomalous properties of blood: RBCs concentration in narrow capillaries is lower than in outflowing blood (Fåhræus effect). He hypothesized that this effect is the consequence of two main factors: red blood cells and suspending fluid (plasma) have different traveling speeds and, in turn, the non uniform distribution of flowing cells along the tube. Many consecutive papers [75] confirmed the results of Fåhræus. It is now well established that erythrocytes mainly occupy the regions close to tube axis, that is the zone where a peak of flow velocity is reached. So, since red blood cells move in the central region of the capillaries, there is a confinement of the suspending fluid to the slowly moving marginal regions of the flow. Finally, the radial distribution of red blood cells and the shape of velocity profile inside the capillary closely influence two interrelated effects: not only the change in RBC volume concentration (dynamic tube hematocrit, Ht), but, in turn, the precipitous slowing down of the apparent viscosity of blood with the decreasing tube diameter too (Figure 1.7).

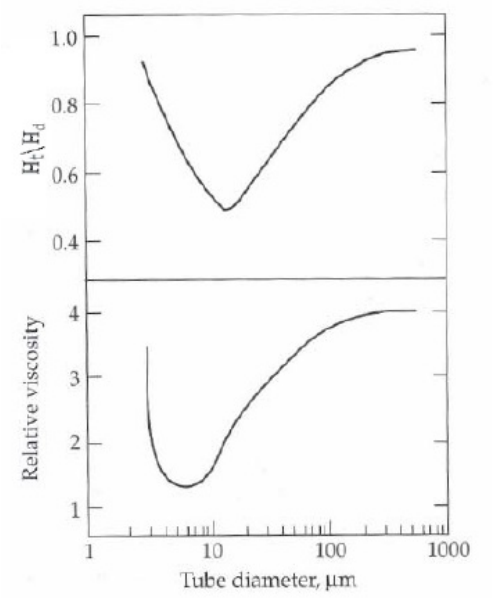

Figure 1.8: Fåhræus effect in narrow capillaries [180].

Following the footsteps of Fåhræus and Lindqvist classical works, RBC confined flow behavior in microcapillaries has been the subject of many investigations [41, 58, 76]. From the experimental point of view, the main physical observable characteristics are cell shape, velocity and thickness of the suspending fluid film separating RBCs from the capillary wall, as a function of diameter, pressure drop and Ht.

1.4.2 Imaging technologies for blood cells observation

The development of *in vivo* high-speed imaging technologies allowed to observe the deformation of red blood cells in narrow capillaries [77, 78], most of all in dogs, rats and other test animals. In order to adapt to a vessel size equal or smaller than cell dimension, RBC shape departs from the biconcave disk and acquire a bullet- or parachute-like shape or, as it is evident from later *in vivo* studies at low speed values [79], a deformed shape better described by a shallow bowl with a bulging of the forward edge and a thinning of the back end. These results have been acquired thanks to a simultaneous observation of erythrocyte motion by means of two microscope at right angles. In parallel with *in vivo* experiments, *in vitro* techniques have greatly improved. Recently, red blood cells have been imaged at velocities up to ≈5 cm/s in glass microcapillaries [64] with a diameter ranging between 4.7–10 μm by using a high resolution camera (Figure 1.9). Very interesting experimental investigation focused on the causes that lead to RBC asymmetric shape, in parallel with numerical simulations [83]. In 10 μm capillaries, asymmetric and axisymmetric structures coexist. At low velocities (up to ≈0.1 cm/s), asymmetry is apparently due to cell membrane folding, while at higher RBC speeds, asymmetric shapes are the result of out-of-axis cell position, that is prevented in smaller capillaries by the significant confinement [80].

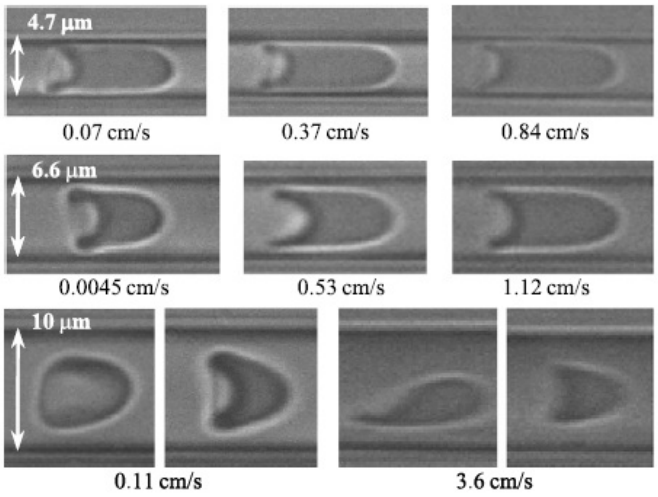

Figure 1.9: RBC deformation in glass microcapillaries of different diameter [64].

1.4.3 Microfluidic point-of-care

Nowadays, a fundamental part of diseases prevention and treatment is based on detection of biochemical parameters in samples of blood and urine. There are several available diagnostic tests in medical laboratories at relative low cost. They provide precise results for routine analysis in a variable range of time (from few hours to some days), depending on the measured parameters Table 1.2. As regards blood tests, there are specific situations in which a continuous or frequent monitoring is necessary in order to detect the amount of blood gases, glucose, neurotransmitters, ions and hormones dispersed in plasma. In other cases, such as for metabolic parameters or biomolecules (i.e. cholesterol), a medium- long-range time scale is indispensable for detection, since the samples have to be sent to diagnostic laboratories for analysis. Time delay and logistic problems in central laboratories can be serious deficiencies for classical routine tests. In fact, diseases are diagnosed by performing biochemical analysis and observing specific symptoms. Even small changes in biochemical parameters of blood and urine can be a significant signal of organ damages or dysfunctions [126]. Therefore, a more rapid and precise detection of pathological states is a fundamental goal in order to have early diagnosis and subsequently efficient treatments.

seconds/minutes	hours	days
O_2	Creatinine	Iron
CO_2	Bilirubin	Albumin
K^+	Urea	Globulin
Glucose	Sodium	Cholesterol
Lactate	Chloride	
Cortisol	Triglyceride	
Neurotransmitters		

Table 1.2: Typical time scale necessary to monitor various clinical parameters [119].

Microfluidics represents a new approach in order to improve medical tests and enable a more widespread monitoring of health parameters. Thanks to the breakthrough in this research field of the last 20 years, it is possible to think about small, fast and easy-to-operate devices with minimum invasion, able to bring costs and human mistakes down. A new frontier of so-designed systems are the point-of-care (POV) testings [119], since they offer an innovative way to carry out compact and flexible clinical chemistry tests closer to the patients and out of clinical centers [118]. POC apparatus take advantage of miniaturization of total analysis systems (μTAS) and development of lab-on-a-chip devices, elaborating small amount of samples and having small size and weight [119, 120]. Point-of-care applications are useful in specific areas where a faster monitoring and detection is neces-

sary to improve medical decisions and following treatments [121], such as intensive care units, operating theaters and patient's home. For instance, miniaturization of devices will allow to detect cardiac markers to diagnose acute myocardial infarction [122] and or monitor whole blood chemistry during intensive care treatments [123]. Moreover, since costs play an important role in scientific applications and POC systems introduce 35% expense saving per analysis and additional economy in manpower [124], it is reasonable to say that they will become increasingly important. For example, Table 1.3 shows the necessary steps in traditional tests in laboratories as compared to the ones in point-of-care diagnostic systems: the saving in sample handling and decision making steps make POC tests very useful [125].

Laboratory based system	Point-of-care system
1. Test is ordered	1. Test is ordered
2. Test request is processed	2. Nurse draws blood sample
3. Nurse draws blood sample	3. Sample is analysed
4. Sample is transported to the lab	4. Results are reviewed
5. Sample is labelled and stored	5. Clinicians act on results
6. Sample is centrifuged	
7. Serum sample is sorted to analysers	
8. Sample is analysed	
9. Results are reviewed by the lab staff	
10. Results are reported to the department	
11. Clinician acts on results	

Table 1.3: Comparison of classical routine blood tests and point-of-care-systems [119].

In Figure 1.10, an example of point-of-care blood testing is showed [126]. After the sample solution is fed to the biosensor array, the circuits present in the analyser are able to detect the concentration of various analytes. In this specific case, the biochip has the function of identifying and determining three metabolic parameters from blood: the partial pressure of oxygen (pO_2), and lactate and glucose concentrations.

1.5 Endothelial glycocalyx

1.5.1 Endothelium

Capillaries, venules and arterioles are the site of nutrients exchange between intra- and extravascular compartments in microcirculation. Physiological

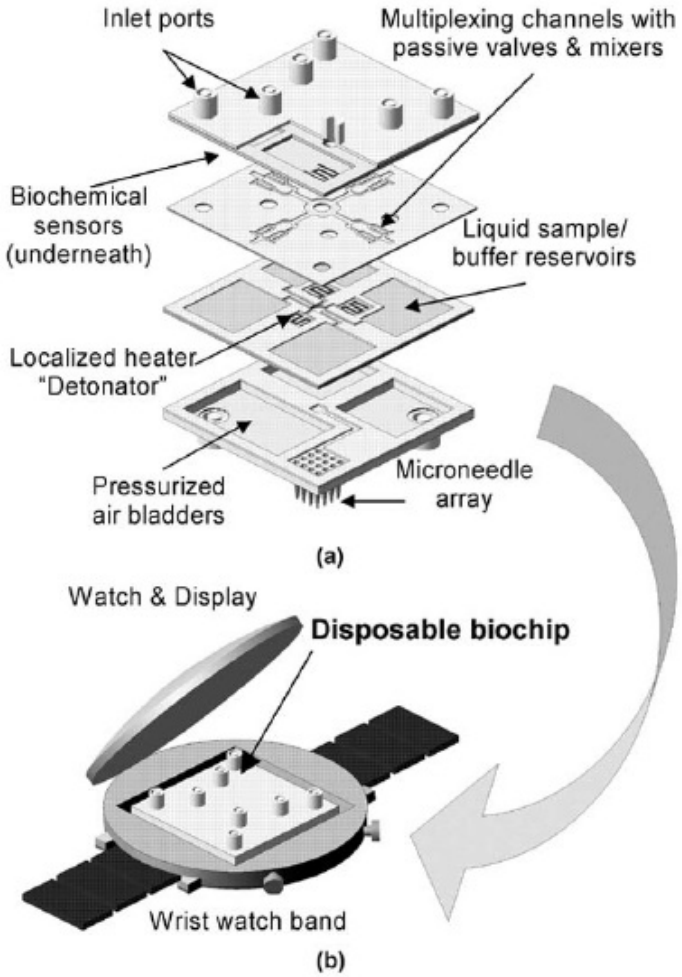

Figure 1.10: Sketch of a point-of-care system: a) details of a multilayer disposable biochip and b) wristwatch analyser for detecting point-of-care testing with biochip [126].

regulation of this fundamental exchange involves many aspects of hemodynamics, including pressure, flow rate, the available surface area for the solute delivery and the permeability of the microvascular walls themselves. All capillaries are lined by endothelial cells (ECs) rif177, which organize themselves in different basic structures. Adhesion molecules form tight junctions which are interspersed within the so-called interendothelial clefts [15], that occupy approximately the 0.2% of the endothelial cell surface. The organization and the density of these cell-cell junctions is extremely variable and confers special permeability properties. Permeability defines the intrinsic property of capillary inner surfaces to slow down or obstruct the flow of fluids or corpuscolar particles through intercellular clefts. For instance, tight junctions predominate in specialized capillaries with particularly low permeability, such as in retina and brain [16, 17]. The multilayer arrangement of capillary walls ensures that they behave as multicomponent, composite exchange barriers, considering that they can support different kind of cells too [1]. The endothelium present on vessel walls can be organized in three different ways [2, 3]:

1. *Continuous*: each cell directly contacts the next at intercellular junctions. Continuous endothelial cells may show fenestrations, transcellular cytoplasmic holes, that may or may not contain diaphragms [3].

2. *Fenestrated*: it is a glomerular mature endothelium, characterized by fenestrations and no diaphragms [4].

3. *Discontinuous*: there are significant gaps between adjacent cells, where basement membrane may also be absent.

There are significant biological interactions between blood cells and endothelial cells in vessels of diameter ranging from 10 to 50 μm [5]. In this case, the size of red blood cells is comparable to the diameter of the vessels. In fact, one of the most important properties of blood is the easiness in flowing through microvasculature. If the vessel is large enough, blood may be almost considered as a Newtonian fluid, like the plasma. Since in this thesis the attention is focused on microcirculation, it is necessary to consider the flow resistance in microvessels and take in account *apparent* and *relative viscosity*, which estimate the non-Newtonian behavior and relate blood flow properties in microcapillaries to the Newtonian fluid peculiarities.

The luminal surface of vascular endothelium is lined by a hydrated mesh rich in carbohydrates, in dynamic equilibrium with plasma constituents, called glycocalyx [6, 7]. The endothelial glycocalyx has an important role in transduction of shear stress, regulation of leukocyte-endothelial cell interactions, regulation of clotting and complement cascades, growth factor binding and regulating the permeability of the capillary walls [8, 9].

1.5.2 Glycocalyx

The concept that vessel walls are lined with an extracellular layer dates back more than 60 years. Initially, studies of endothelial permeability initiated an interest in the structure and composition of the material on the endothelial surface and in the inter-endothelial clefts. In 1966, Luft [10] used ruthenium red staining for an electron microscopic study of the endothelial surface. Using this technique, he directly demonstrated the existence of an endocapillary layer that was not observable by light or electron microscopy (Figure 1.11). Since the 1970s, several methods for the quantitative intravital study of microvascular blood flow using light microscopy have become increasingly well developed [11, 12]. Although many progresses had been made in these years, there are still many open questions to completely understand the structure and the role of the glycocalyx in the circulatory system.

Figure 1.11: Visualization of the endothelial glycocalyx of a rat by Scanning Electron Microscopy [8].

Nowadays, it is well established that the luminal surface of the endothelial cells that line human vasculature is coated with a glycocalyx of membrane-bound macromolecules (EGL) [7, 13, 14]. This layer has a thickness estimated in the range 100–1000 nm and is basically made of sulfated proteoglycans, hyaluronan, and glycoproteins . These components form a network in which soluble molecules, either derived from plasma or endothelium, are incorporated (Figure 1.12). A dynamic equilibrium exists between glycocalyx and the flowing blood, that continuously influences composition and thickness of EGL. Furthermore, an enzymatic or shear-induced loss can affect the endothelial glycocalyx. So, a sort of dynamic balance between

biosynthesis and loss makes it hard to define EGL structure with certainty. The total area of interface between blood and endothelium in humans can be estimated to be about 350 m^2. For an estimated average endothelial thickness of about 0.3 μm, this correspond to a total endothelial mass of only $\approx$ 110 g. Nevertheless, the EGL is not a passive membrane or barrier between blood and tissues.

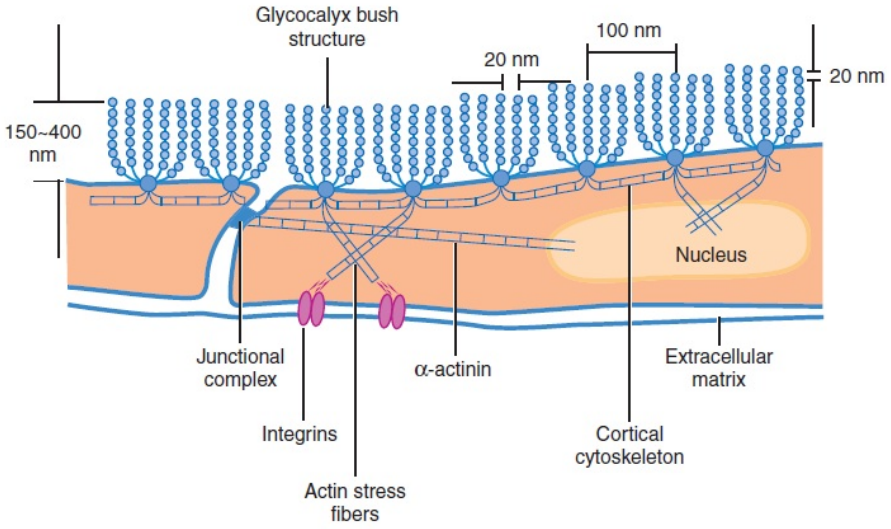

Figure 1.12: Structural model for the endothelial glycocalyx [9].

The hydrated gel-like structure provides to glycocalyx three fundamental functions [7] that it plays as the interface between the ECs and the flowing blood with its plasma and cellular components:

- Modulator of permeability in the transcapillary exchange of water;
- Mechanotransducer of fluid shear stress to the endothelial cytoskeleton, including the resulting biochemical responses;
- Regulator of red and white blood cell interactions, with emphasis on the inflammatory response.

In this work, the main goal is to focus the attention on the interaction between blood cells, and in particular red blood cells, and endothelial glycocalyx. Thus, without minimizing the other important roles of EGL, in next sections the influence on blood flow will be discussed in more details. The vascular endothelium is currently believed to be actively involved in the majority of cardiac pathologies. Since the glycocalyx have a strong influence on most interactions between flowing blood and endothelial cells, it is evident that it can affect many pathological processes.

First of all, it is well established that the presence of the endothelial surface layer influence hematocrit and flow resistance in narrow capillaries [11]. Any structure that interferes with the free movement in microvessels can be assumed to increase resistance to blood flow. Observations of blood flow in networks of microvessels pointed out that the resistance in these capillaries is higher than expected, when considering the rheological behavior of whole blood in glass tubes [12, 14]. This significant difference was attributed to the presence of the EGL. In fact, the functional capillary diameter for blood flow *in vivo* is narrower than the anatomical width of the vessel, which is usually used to estimate tube hematocrit. The latter results to be much less than half of systemic hematocrit, in microvessels. It is not still very clear which is the consequence of this decrease in Ht values. In first instance, while a dramatic effect, it does not appear to be of primary physiological importance, even if there is a significant probability that the presence of the layer influences oxygen delivery in microcirculation. High flow conditions could cause the flattening of glycocalyx against the endothelial surface, reducing resistance to blood flow. This is a possibility, yet to be experimentally verified, but it is probable that endothelial glycocalyx is able to rapidly change in structure, in order to respond to hemodynamic conditions. This hypothesis could indicate a feedback regulation between hemodynamic and metabolic conditions and EGL structure and density [7].

As regards the interaction between endothelial glycocalyx and red blood cells, it is clearly shown [18] that an erythrocyte at rest expands to fill the entire available lumen of the capillary, crushing the EGL. In presence of flow, the cell exhibits a pop-out phenomenon: as the flow strength is increased, the cell rises through the glycocalyx, until a critical velocity is reached beyond which the RBC and EGL are not still in contact and a thin lubricating layer separate the cell from the endothelial surface layer.

The first realistic attempts to analyze the RBCs flow in glycocalyx-lined capillaries appeared in works of Damiano [19] and Secomb [20], who adopted similar approaches to explain the effect of EGL on the capillary resistance and hematocrit, as it was described previously. The predicted retard of the flow through EGL-lined capillaries could causes problems in maintaining a continuity of mass. So, in order to avoid microvascular disorders, more elongated RBC shapes, than in smooth tubes with the same size, are noticed. In skeletal muscle capillaries, red cell velocities are often in the range of 100–200 μm/s in steady flow and can drop to zero during intermittent flow conditions. These intermittent and varying flow conditions have been introduced in theoretical models [21, 22], refining the red cell model and including the effect of bending elasticity in RBC membrane. By virtue of the almost well-understood mechanical properties of red blood cells, Secomb was able to provide a quantitative description of the flow-dependent exclusion of erythrocytes from the endothelial glycocalyx (lubrication theory), closely linked to the mechanical properties of EGL.

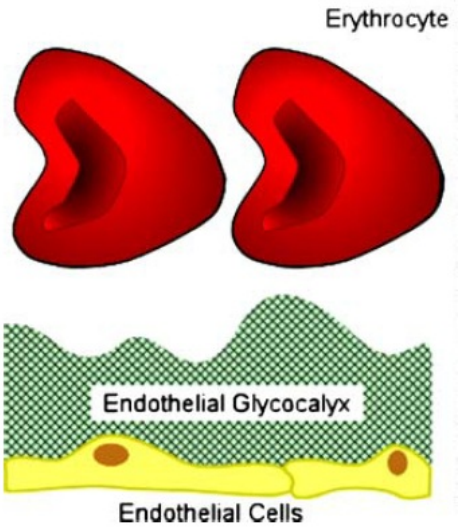

Figure 1.13: Schematic representation of blood flow in microvessels, showing its main components [8].

Experimental investigation showed that damages and loss of the endothelial glycocalyx resulted in the loss of EGL properties that were enumerated before. In the last few years, evidence is emerging that a disrupted glycocalyx plays a fundamental role in several vascular pathologies, such as diabetes [23], ischemia [24] and atherosclerosis [25].

1.6 Modeling of red blood cells

1.6.1 Historical background

As already written in the previous sections, blood can be referred as to a complex fluid, because of the intimate coupling between the shape of dispersed cells (mostly red blood cells) and the suspending plasma. One of the most common consequence of this continuous interaction is the rich set of RBCs morphologies in the blood circulatory system. The significative complexity of blood is a characteristic property of non-equilibrium dissipative systems, in which general thermodynamic laws (e.g. minimization of energy, maximization of entropy) cannot be applied.

The challenging question of finding the equilibrium shape of a red blood cell was the main topic of several studies in 70's and 80's. For instance, Helfrich [136] elaborated a simple geometrical model that represents the basis of modern theoretical works, in which he assumed that the most of the RBC membrane energy is stored in its bending modes. He hypothesized that the energy of the cell is a quadratic functional of the mean membrane curvature H and he proposed to obtain the cell shape by minimizing its cur-

vature energy, that is subject to two constraints: the constancy of both area and enclosed volume of an erythrocyte, the internal fluid being incompressible. In Helfrich model, the two constraints are imposed by two Lagrange multipliers (λ_1 and λ_2) and the total "free energy" to be minimized is:

$$F = \frac{k}{2}\int H^2 dA + \lambda_1 \int dA + \lambda_2 \int dV$$

where A is the total surface of the membrane, V the enclosed volume and k is the membrane bending rigidity (this parameter has the same dimension of an energy). The first term represents the curvature energy, that is found to be invariant with changes in cell size. This implies that the energy stored does not depend on the size itself, but only on the swelling ratio, also called reduced volume. In agreement with the definition we already provided in the previous sections, the reduced volume can be expressed as:

$$\nu = \frac{V/(4\pi/3)}{[A/4\pi]^{3/2}}$$

Usually, $\nu \approx 0.65$ for a human RBC. Thanks to this model, it was possible to predict not only the biconcave shape at rest of red blood cells, but many other morphological configurations corresponding to different values of ν.

A turning point in red blood cell modeling was mimicking their behavior by vesicles. The main difference between RBCs and vesicles is that the latter have a membrane simply made of a phospholipids bilayer, unlike red blood cells that have in addition the well known cytoskeleton, a network of organized proteins. Although the lack of the cytoskeleton, vesicles proved to be useful in simulating erythrocytes and checking the prediction of the theoretical model, since it is possible to vary their swelling ratio at will. The good agreement between experimental investigation with vesicles and theoretical predictions allowed to improve the precision of the model, that was enriched with a spontaneous curvature H_0, for example. In fact, it is reasonable to think that an open membrane have a minimal curvature energy equal to H_0 and so the term H in the "free energy" expression had to be substituted by (H - H_0). In conclusion, the Helfrich model was refined by adding two more parameters, ν and H_0 and, as a consequence of this addition, the variety of predicted shapes increased dramatically. Nowadays, the problem of RBCs equilibrium shape is well understood both experimentally and theoretically [137].

From the end of the 90's, the attention of theorists focused on the study of red blood cells and vesicles in non-equilibrium conditions, basically under an imposed flow strength. These problems have still to be completely solved.

1.6.2 Basic modeling of RBCs under flow

With the exception of arterioles and at some sites of aneurysms [148], *in vivo* vessels at the RBC scale exhibit a Reynolds number (Re) small enough so that the inertia is often negligible. Thus, experiments on vesicles and red blood cells in microcirculation are often performed in correspondence of such small values of Re. The fluid inside and outside the flowing cells can be described by the Stokes equations:

$$\eta \nabla \mathbf{u} - \nabla P = 0$$

$$\nabla \cdot \mathbf{u} = 0$$

where $\mathbf{u}$ is the velocity field and P is the pressure. The quantities associated with the internal fluids of the cells are denoted with a prime. For instance, the internal viscosity of a red blood cell is usually different from that of the external fluid and is denoted as η'. At the membrane, we have the following three boundary conditions:

- The continuity of the velocity field

  $$\mathbf{u} = \mathbf{u}'$$

  This condition induces the continuity of the normal component as a consequence of the mass conservation and of the tangential one, since we make the assumption of no-slip condition.

- The equality of fluid and membrane velocity, $\mathbf{u}_m$

  $$\mathbf{u} = \mathbf{u}' = \mathbf{u}_m$$

  This can be considered valid only under the assumption of osmotic equilibrium, in which the membrane is not permeable to water flow. In order to determine the evolution of the membrane, it is sufficient to know the normal component of the velocity, but if one is interested in the fluid motion along the membrane (the so-called tank-treading), the adjacent fluid tangential velocity has to be determined. To this end, the equality of the tangential velocity of membrane and adjacent fluid is imposed (no-slip condition).

- The continuity of the stress

  $$\sigma \cdot \mathbf{n} - \sigma' \cdot \mathbf{n} + \mathbf{f} = 0$$

where σ = -P$\mathbf{I}$ + η (∇ $\mathbf{u}$ + ∇ $\mathbf{u}^T$) is the stress tensor. P represents the pressure value, $\mathbf{I}$ the unit tensor, the superscript T designates the transpose and $\mathbf{f}$ is the membrane force. This force is composed of two contributions: the bending force ($\mathbf{f}_b$) and the membrane in-plane elasticity ($\mathbf{f}_e$) (for example membrane shear elasticity), that has to be introduced separately.

1.6.3 Different methods of solutions

In this section a general overview on the different methods used to solve the above set of equations is provided. The analytical method is limited to situations in which the shape of the objects is close to a sphere and, moreover, the reductive perturbation methods become adoptable (the set of partial differential equations (PDE's) can be transformed into ordinary differential equations (ODE's)). This method succeeded in studying the motion of a single vesicles [150, 151, 152], compressible/incompressible capsules [153, 154] under unbounded shear and Poiseuille flows. Recently, pairs interactions have been investigated by this method [155]. Globally, the analytical method was really useful in last decades in order to gain insights into the phenomena concerning quasi-spherical shapes.

Nowadays, all the other cell shapes in flow are studied by means of numerical simulations. Along these lines, one of the most common method is the boundary integral one, that is based on the use of the Green's function techniques, thanks to the linearity of the Stokes equations [156]. It has been applied in case of vesicles (both in 2D and in 3D) [149, 157] and capsules [158]. The main advantage of this method is that there is no need to solve the equations for the fluid domain, since the whole cell dynamics is encoded in the membrane itself. On the contrary, its weakness relies in the so-called nonlocality: in fact, in order to move one membrane point, we must have information on the location of all the other points. The complexity of the method in terms of numerical schemes is of order N^2, N being the number of dicretization points on the membrane and eventually boundaries. In order to reduce the complexity, the use of fast multipole methods is useful, lowering it down to N [159].

Another class of methods consists in either meshing the fluid domains (finite differences, finite elements), or using spectral methods, and solve the fluid equations subjected to boundary conditions. Thus, the cell is considered to be immersed in that domain (indeed, the associated method is called immersed boundary method). The determination of the velocity field of the membrane is realized thanks to an interpolation on the neighboring lattice points, where the velocity field is fully computed. Once this step is completed, the calculated velocity takes the place of the point and the method is reiterated for all the membrane. In the problems solved by the immersed boundary method, the membrane is explicitly displaced in the

Lagrangian sense. Although it can be considered on of the oldest methods [160], it has been used only recently to investigate vesicles and capsules [161]. Usually, in the immersed boundary method the membrane is considered as a continuum and then membrane forces are discretized. However, there are some cases in which the membrane of the objects is treated as a system of connected beads and springs (with stretching and bending stiffness) [162].

Other quite popular methods that have been adapted to vesicles, and cells in general, are the phase-field [163, 164] and the level set methods [148], in which the membrane is implicitly defined by introducing a scalar field (the phase field or the level set function), and all geometrical properties (like mean curvature, normal, etc.) can be expressed in terms of this field. Contrary to the previous method, this one is fully Eulerian and it is often used in order to study vesicles. The main deficiency of this kind of methods is that, to our knowledge, it is still not working when membrane shear elasticity is included. When phase-field or level set methods are used, the fluid/structure coupling is studied and solved by using finite differences [165], in Fourier space [163], or using the finite element methods [148].

Finally, there are methods which consist not in solving the fluid equations directly, but just by mimicking them via kinetic equations. In this category, three fundamental methods can be mentioned:

- Dissipative particle dynamics (DPD), which can be considered as an implementation of molecular dynamics (MD), consists in viewing fluid particles as "atoms" or "molecules" to which basic Newton laws are applied with pairwise interactions. DPD is viewed as a coarse-grained method where each "particle" represents a cluster of atoms or molecules. As a result of internal degree of freedoms associated with each cluster, the particle-particle interactions, which are relatively weak in comparison with the real atom-atom ones, includes both random and dissipative contributions [166]. In conclusion, the DPD method can be considered a highly efficient method, as long as the coarse-graining degree is adequately chosen, if concentrated suspensions are investigated. On the contrary, it has not yet been quantitatively used for the simple case of single vesicle/RBC under linear shear flow.

- Multiparticle collision dynamics (MPCD), that is a particle-based mesoscale simulation technique which incorporates thermal fluctuations and hydrodynamic interactions. The coupling of embedded particles to coarse-grained solvents is achieved through MD [167] and can be applied to vesicles and capsules [168]. The limits of this kind of method are the high cost and some serious discrepancies with the boundary integral method (that uses directly the Stokes equations), that have been pointed out for vesicles under a linear shear flow [149], for example.

- Lattice-Boltzmann method (LBM), which is a hydrodynamics solver

in which each cell is treated in an immersed boundary method, as discussed above [169]. In LBM, the fluid is investigated as a set of particles laying on lattice. In this spirit, a fluid is seen as a cluster of pseudofluid particles that can collide with each other when they spread under the influence of external applied forces. The Lattice-Boltzmann method offer some advantages, like the ease of implementation and a good versatility to quite arbitrary geometries, but, as for the previous case of DPD no quantitative phase diagram even in a simple situation (linear shear flow) has been reported yet.

1.7 Aim of the thesis

The purpose of this thesis is trying to shed light on some of the basic topics that are still not very well understood about the mechanisms governing blood flow in microcirculatory system: red blood cells aggregation in microvessels and the role of RBC interaction with the endothelial glycocalyx in microcirculation.

First and foremost, the preliminary efforts will be concentrated on the improvement and development of an *in vitro* technique suitable to study red blood cells aggregation (clustering) in microconfined geometries, by using small amounts of fresh blood. RBC motion in a flow cell elaborating few milliliters of solution will be observed by optical microscopy. In last decades, RBCs aggregability in dynamic conditions attracted scientific attention, since it is deeply linked to clotting in microcirculation, that depends on inflammatory states in turn, and some important pathologies (i.e. diabetes and thrombosis). The aim of the experimental investigation is to understand which are the factors governing red blood cells aggregation during the flow in microcapillaries. The challenging goal is to monitor and estimate the hydrodynamic interactions between consecutive flowing cells and prove if other interaction forces influence the formation of RBC trains. Therefore, dimensions and statistical distribution of clusters will be provided as a function of flow parameters, like pressure drop and residence time. As it was amply explained in the previous sections, the understanding of RBC clustering would have outlets in medical research, not only to understand onset and evolution of pathological states. In fact, this project of thesis aspires to set the basis for innovative microdevices that will be able to monitor and quickly estimate dynamic RBCs aggregability, both in healthy and pathological blood, especially in inflammatory states.

In the second part of the thesis, the interaction between erythrocytes and endothelial glycocalyx will be studied. An artificial system to simulate the presence of the endothelium on the inner walls of human microcapillaries is presented in the following sections. Glass microtubes lined by nanometric polymer brush are produced by a grafting-from technique. The challenging

goal of this experimental investigation is to verify if biocompatible polymer brushes are really able to mimic *in vivo* conditions in microcirculation. In the early experiments, the main purpose is to understand how flow conditions (such as flow resistance) are modified in "hairy" capillaries in comparison with bare tubes, normally used in *in vitro* experiments. In a second step, the purpose is to check which is the influence of such polymer layers on RBCs motion and their physical properties. The experimental outcomes will be compared with theoretical works available in the literature and with recent results obtained on rats *in vivo*. The development of methods to mimic *in vivo* conditions would be extremely useful to better understand the role of EGL in microvasculature, especially in the onset of vascular diseases, like atherosclerosis, where the glycocalyx layer suffers evident damages. Moreover, the set up of such microdevices could be a breakthrough in clinical research, in order to make *in vitro* medical tests more and more realistic, and for eventual further implants in human body.

Chapter 2

Red blood cell clustering in Poiseuille microcapillary flow

2.1 Introduction

Red blood cells are fundamental in physiological essential functions, such as oxygen delivery and CO_2 removal from tissues, thanks to their ability to deform and flow in the microvascular network. In this section, the investigation will be focused on RBC clustering in microcapillary flow, i.e., the formation of trains of RBCs where the distance between consecutive cells is comparable to cell length. The RBC clustering phenomenon has been observed both experimentally [71, 81] and by numerical simulations [72] and is significantly involved in the well-known process of RBC aggregation [66], whose specific mechanism is not fully elucidated. A formation of packed RBC structures plays an important physiological role, being one of the main factors leading to the non-Newtonian behavior of blood, especially to the increase of viscosity at low shear rates and, in turn, to vascular obstructions. The higher viscosity is implicated in clotting and thrombus formation [66, 67, 68]. It should be noticed that RBCs can promote platelet aggregation also by chemical signaling, such as the release of ATP [70] and ADP under low pO_2, low pH and in response to mechanical deformation [68, 69]. In previous works, RBC cluster formation has been attributed to the slower motion of some cells along the channel, which act to slow down the faster cells, thus creating a train of trailing cells. This effect has been clearly established in presence of white blood cells [82], which, being larger and less deformable than RBCs, move at significantly lower velocities in confined geometries and are found at the leading front of RBC clusters. However, an unquestionable evidence supporting this explanation, in case of RBCs only, has not been provided so far. Furthermore in general, several basic questions concerning the physics of RBC clustering under confined flow remain open.

- *What are the most probable cluster sizes for a given flow condition?*

- *How does the length of a cluster, having a given number of cells, evolve by varying flow conditions (such as the flow strength)?*
- *What is the mechanism of cluster formation?*

In this work, we take on the challenge of these questions by presenting the first systematic experimental investigation on human RBC cluster dynamics in microcapillaries, associated with preliminary numerical simulation results.

2.2 Materials and methods

2.2.1 Experimental apparatus

In order to carry out a systematic investigation, an already tested experimental apparatus has been used [64]. Silica cylindrical microcapillaries (Polymicro Technologies) with a diameter of 10 μm and length of few millimeters were placed in a flow cell, schematically shown in Figure 2.1. The flow cell is made of two Plexiglass plates separated by a rectangular rubber frame. The RBC suspension was fed to the flow cell using flexible tubing connected to a glass reservoir on a vertical rail, and collected at the exit in a second glass reservoir. The pressure drop in the microcapillaries was taken to be equal to the distance between the liquid menisci of the two reservoirs, the other losses being negligible (an accurate calibration of the flow cell has been performed in previous studies [64]).

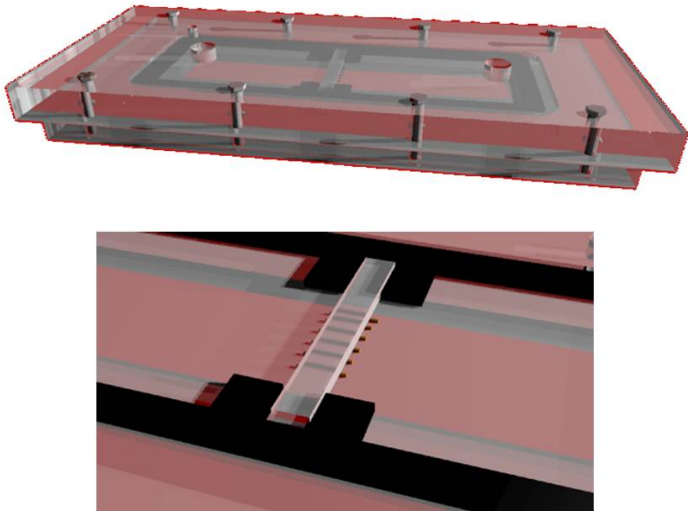

Figure 2.1: Flow cell schematic: details of the glass microcapillaries.

The flow cell was placed on the motorized x-y stage (Ludl) of an inverted microscope (Zeiss Axiovert 100) equipped with a motor assembly for remote

focus control (Ludl) (Figure 2.2). A glass cover slip inserted into a window cut in the bottom plate of the flow cell allows observations. Images of the flowing RBCs are acquired by a high speed video camera (Phantom 4.3, operated up to 1000 frames/s) and by using a 100x high magnification oil immersion objective. The microcapillaries are sandwiched between the cover slip glass surface and a silicone spacer having a similar refractive index and thus reducing optical distortions (Figure 2.1), so as to avoid the movement of the silica pieces of microtubes as result of the imposed flow strength.

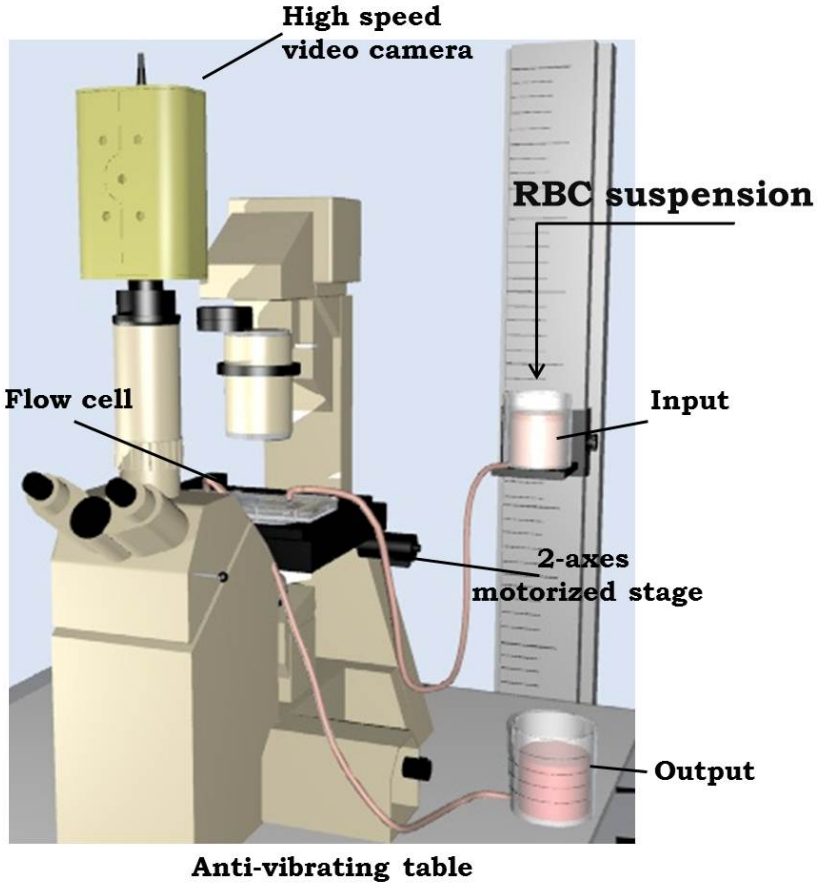

Figure 2.2: Set up of the experimental apparatus.

2.2.2 Blood samples

Fresh venous blood samples, drawn from healthy consenting donors and used within 4 h from collection, are centrifuged to separate RBCs from white cells and platelets. Afterwards, RBCs are resuspended in plasma and diluted to a volume concentration of 10% with ACD anticoagulant (96% water,

2.3% sodium citrate, 1.1% anhydrous dextrose, 0.6% citric acid) and human albumin. This concentration has been selected in order to have the typical hematocrit value found in microcirculation. The higher values of Ht ($\approx 45\%$) measured in healthy blood analysis are associated with large vessels, whereas in going from the macro- to the microvasculature, the hematocrit decreases because of entrance effects and the inhomogeneous radial distribution of red blood cells, which tend to migrate and concentrate along the central axis (the so called Fåhræus-Lindqvist effect [84].

2.3 Results and discussion

2.3.1 Experimental investigation

This section is essentially divided in two parts. The first one is mainly based on experimental investigations carried out in the rheology laboratory of the Dipartimento di Ingegneria Chimica in Napoli. By means of optical microscopy we were able to observe the flow of dense RBC suspensions. Afterwards, an off-line analysis of the acquired data has been performed by a commercial software (Image Pro Plus), that allowed to measure morphological and kinetic properties of the flowing RBCs (Figure 2.3). Thanks to the interpretation of image analysis, it was possible to provide a plausible explanation of the observed phenomenon in agreement with the recent theoretical assumptions. The reliability of the experimental results have been tested by numerical simulations elaborated at the Laboratoire Interdisciplinaire de Physique (LIPhy) in Grenoble.

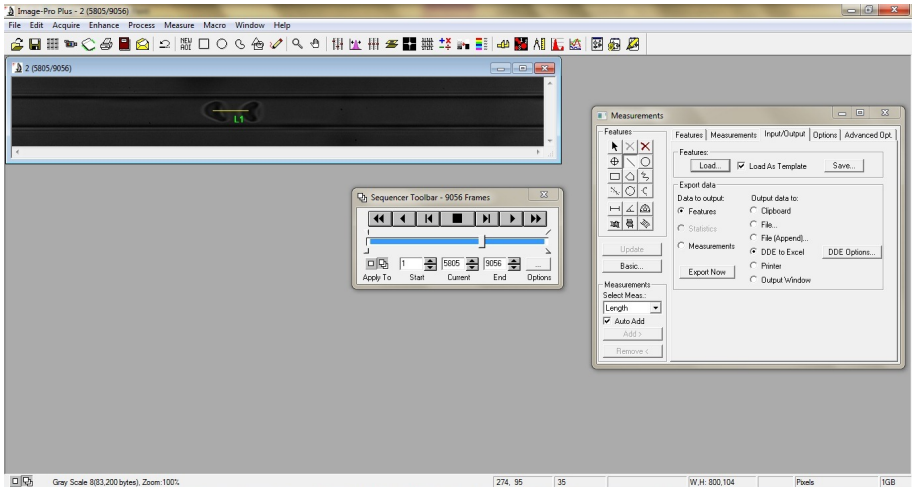

Figure 2.3: Measurement of the distance between two consecutive RBCs by Image Pro Plus.

Since an official definition still lacks, the first step was to precisely define

a RBC cluster in our experimental observation. We consider a RBC cluster as a cell train made of erythrocytes of length L, in which the gap d between any pair of consecutive cells is equal to or lower than 1.5 D, where D is the characteristic length of a single cell, as it is possible to see in Figure 2.4. D depends on the imposed pressure drop and can range between 6–10 μm.

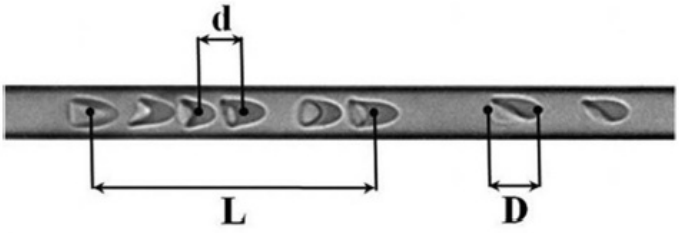

Figure 2.4: Red blood cell cluster parameters.

There is not a prevailing shape of the erythrocytes in a cluster, so it is possible to observe parachute-like morphologies, either axisymmetric or slipper-like shapes, in other words all the typical shapes observed both *in vivo* and *in vitro* on isolated cells [64, 81] (Figure 2.4). RBC clustering is also associated with local fluctuations of the hematocrit, as it is clearly shown in Figure 2.5. This finding is in agreement with qualitative observations of blood flow in microcapillaries *in vivo* and *in vitro* [71, 72].

Figure 2.5: Hematocrit fluctuations in microcirculation. The arrows show the same cell while traveling across the field of view.

Hence, our experimental model reproduces some important features of RBC flow behavior *in vivo*, both at the single and the collective cell level. In our experimental campaign, the two key parameters are the hematocrit, here fixed at 10%, and the imposed pressure drop (ΔP) across the small silica pieces of microcapillaries (the length is $\approx$2 mm). Hereafter, we present results that certainly show the importance of ΔP in the RBC aggregation occurrence. Firstly, the dimension of RBC trains and the morphology of the red blood cells (shape and deformation) have been investigated as a function of the flow strength and the number of erythrocytes included in the clusters. How does pressure drop influence the cluster dimension? In Figure 2.6, the cluster length (L) is plotted as a function of the number of RBCs per cluster

(N_{RBC}) at four different values of ΔP, close to the physiological range in microcirculation, which is 15–35 mmHg in vessels of the same dimension we used (capillary level). A linear increase of L with N_{RBC}, which is well fit by the continuous lines in Figure 2.6, is found at any ΔP. The slope of each linear fit increases with ΔP until a plateau at higher pressure drops is reached, where data superimpose on each other whatever the value of N_{RBC}. Error bars in the presented figures represent the standard deviation of the measurements, which is mainly caused by the size distribution of RBCs. Standard deviations have been calculated on a basis of at least 50 clusters with the same number of red blood cells. An evident conclusion is that there is a critical value of ΔP (estimated to be ≈50 mmHg) above which L remains the same for each N_{RBC}.

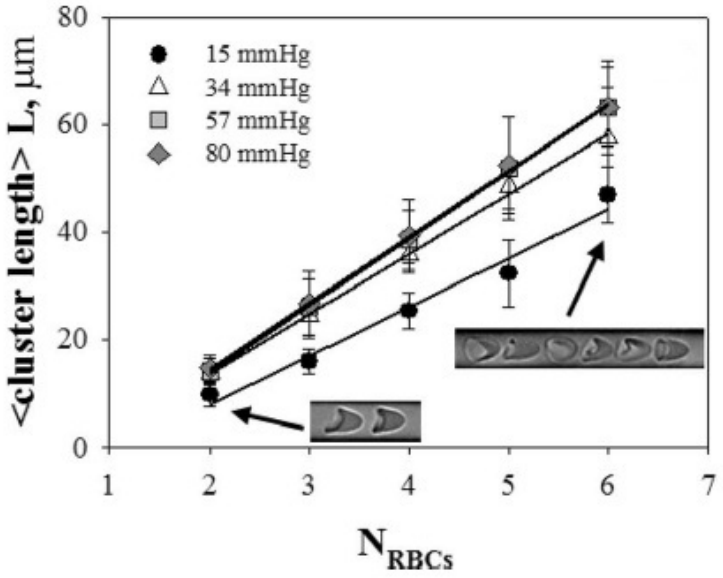

Figure 2.6: Clusters length as a function of RBC number per cluster.

The same trend is shown in Figure 2.7, where L is plotted as a function of the imposed pressure drop. It is evident that L increases with the number of erythrocytes and ΔP up to a plateau level, suggesting the presence of a critical length. What can we hypothesize about those experimental results? It is convincing that such plateau level corresponds to the fact that the average intercellular distance d in a cluster stays constant beyond a critical ΔP value even though deformation of single RBCs increases [22, 64]. This limiting value of d can be estimated as equal to $L/(N_{RBC} - 1)$ and is equal to 14.7, 13.1, and 12.6 μm for N_{RBC}=2, 4, and 6, respectively.

To prove this hypothesis, we measured the actual average distance d between the centers of mass of consecutive cells in a cluster and RBC defor-

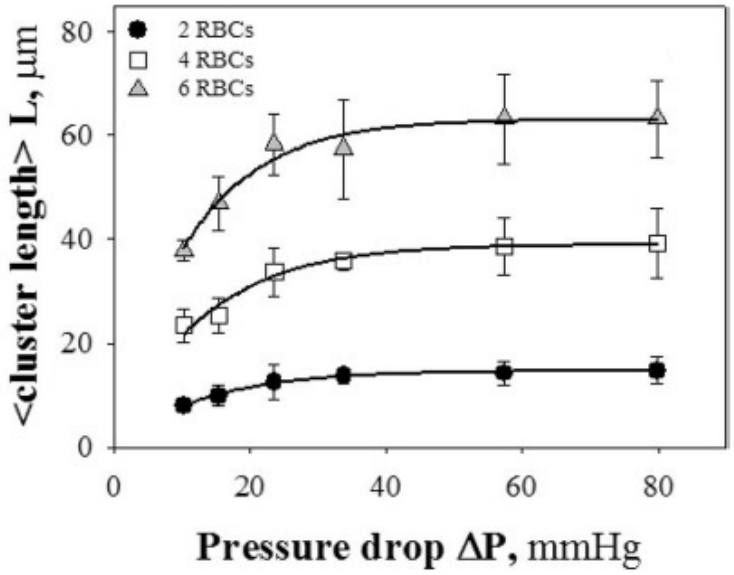

Figure 2.7: Clusters length as a function of the imposed pressure drop for different numbers of RBCs.

mation in a cluster. The results are presented in the following of this section. In Figure 2.8, the relative distances d_{I-J} between consecutive RBCs in a aggregate (for instance, d_{I-II} corresponds to the distance between the first and the second cell) are reported as a function of the number of cells N_{RBC} forming the cluster and three different pressure drops. In order to avoid the presentation of too many data, only the relative distances of the first four erythrocytes in a cluster are reported. The data in Figure 2.8 show that the distance d_{I-J} increases with ΔP at a given N_{RBC}, while there is no significant variation with cell position in the cluster and with the number of cells N_{RBC} composing the cluster.

	10 mmHg			34 mmHg			80 mmHg		
N_{RBCs}	$d_{I\text{-}II}$	$d_{II\text{-}III}$	$d_{III\text{-}IV}$	$d_{I\text{-}II}$	$d_{II\text{-}III}$	$d_{III\text{-}IV}$	$d_{I\text{-}II}$	$d_{II\text{-}III}$	$d_{III\text{-}IV}$
2	8.3 ± 1.2			11.1 ± 1.5			14.2 ± 2.2		
3	8.4 ± 1.3	8.4 ± 1.8		11.4 ± 1.4	10.8 ± 1.9		13.7 ± 2.8	14 ± 3	
4	8.4 ± 1.4	8.6 ± 2.1	9.7 ± 2.3	11.7 ± 2.4	10.9 ± 2.8	12.1 ± 2.6	14.2 ± 2.6	13.1 ± 3.5	13.3 ± 3.3
5	8.6 ± 2	8.9 ± 3	9.1 ± 2.4	12 ± 2.6	11.2 ± 2.4	11.4 ± 2.4	13.6 ± 2.9	13.5 ± 2.7	12.3 ± 3.3
6	8.8 ± 1.9	8.4 ± 2.6	8.4 ± 2.4	11.5 ± 2.2	10.9 ± 3	11.3 ± 2.6	12.9 ± 2.8	12.8 ± 2.8	12.5 ± 2.7
7	8.7 ± 1.4	8.6 ± 2.9	8.5 ± 1.3	11.6 ± 3.5	12.1 ± 2.5	11.6 ± 3.1	13.4 ± 2.6	11.8 ± 3.3	13.8 ± 2.7

Figure 2.8: Average distance between consecutive cells in a cluster as a function of the number of cell forming the cluster at three different pressure drops.

In Figure 2.9, the average intercellular distance d (calculated as the average value of the distances d_{I-J} for each N_{RBC}; i.e., for N_{RBC}=3 d is the average value of d_{I-II}, d_{II-III}) is plotted as a function of NRBCs at three different values of the imposed pressure drop. In this graph, the independence of d on N_{RBCs} is apparent for at least the two lower values of ΔP, 10 and 34 mmHg. For the higher pressure drop (80 mmHg), instead, a weak decrease of d for big clusters ($N_{RBC} \geq 5$) is noticed, though within the error bars, suggesting a possible compaction of big clusters at high ΔP.

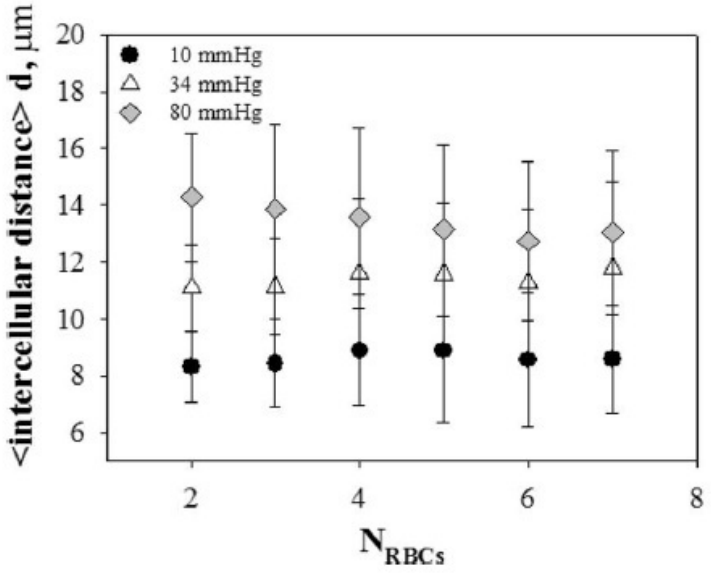

Figure 2.9: Distance between consecutive cells in clusters as a function of RBCs number per cluster.

In Figure 2.10 the average distance d between two consecutive cells in a cluster is plotted as a function of pressure drop for clusters of different N_{RBC}. The graph unquestionably shows that d increases with ΔP, apparently reaching a plateau around 60 mmHg, equal to 14.2, 13.6, and 12.7 μm for N_{RBC}=2, 4, and 6, respectively. These values are quite close to the ones estimated from Figure 2.9, thus supporting our hypothesis. In fact, at high values of pressure drops, both Figure 2.9 and Figure 2.10 show the same trend.

One of the main goal of the experimental observations is to understand which is the role that RBC deformation could play in formation, size and stability of a cluster. Two different kinds of analysis have been performed to investigate possible trends involving the morphology of erythrocytes in RBC aggregates. A qualitative analysis of RBCs shapes is performed by observing the images in the inset of Figure 2.10, where three typical examples

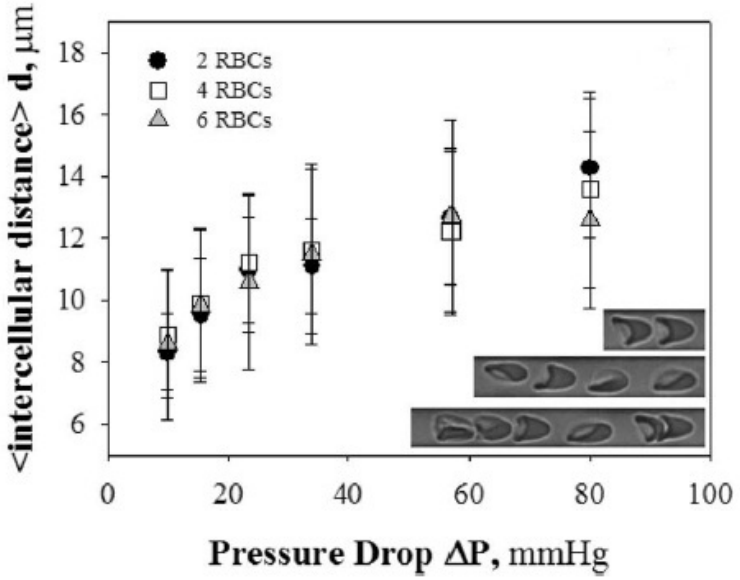

Figure 2.10: RBC distance in a cluster as a function of the imposed pressure drop (the images in the inset show clusters of 2, 4, and 6 RBCs for a ΔP=10 mmHg.

of clusters at the lower ΔP (10 mmHg) are shown to further illustrate that d is not depending on cell position in the cluster and on N_{RBC}. Another interesting feature of these pictures is that cells of different shapes, such as parachute and slipper-like, are present in a cluster. It is interesting to note that there is not a preferential position for each kind of shape (e.g., slipper-like morphologies can be found at the first, at the second, and at the third position as well). To better understand the shape changes in RBC clusters, a quantitative analysis of RBC deformation, in clusters made of 5 cells, has been performed thanks to a basic macro of the Image Pro Plus library. This software is able to notice the different levels of gray in the acquired images and detect the flowing erythrocytes.

In Figure 2.12 the deformation index (DI) (defined as the measured aspect ratio of a bounding box enclosing the cell body) of axisymmetric red blood cells is plotted as a function of pressure drop at different cell positions (e.g., I RBC means the first cell in the cluster starting from the right). The flow is from left to right. Error bars, as already specified before, represent the standard deviation of the measurements. An increasing trend is observed, as found for isolated cells [64], and no remarkable variations of cell deformation with position in the clusters are found. The pictures in the inset of Figure 2.12, which shows two examples of five RBC clusters, illustrate how clusters of equal length can exhibit cells of different deformation index

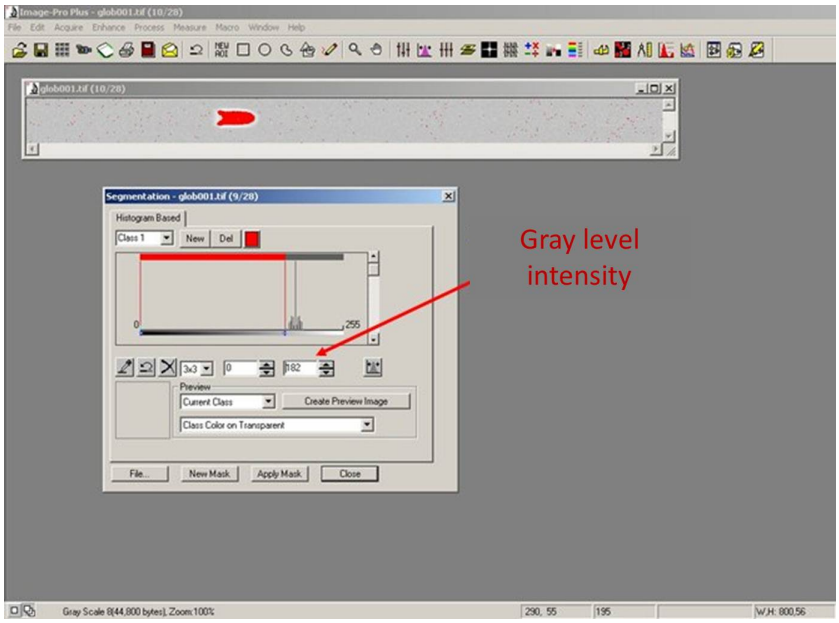

Figure 2.11: Measurement of the deformation index by Image Pro Plus.

at different positions within the cluster.

In conclusion, our analysis of cell distance and shape within a cluster provides support to the hypothesis that the main variable affecting intercellular separation and RBC deformation is ΔP, which drives cluster dimension to a plateau, whose size is dependent on N_{RBC} (as shown in Figure 2.7). The presence of a limiting cluster length suggests that the forces keeping the cells together in a cluster are of hydrodynamic nature. This point will be further discussed in the following.

To further investigate cluster formation, size, and stability, the number of RBCs in a cluster as a function of ΔP was measured at three different positions along the capillary: inlet, center, and outlet, as shown in Figure 2.13. Here, the inlet and the outlet sections are at a distance of 100 μm from the capillary ends (the whole length of the capillary was about 2 mm). At each position the distributions of N_{RBC} are shown at three values of ΔP (15, 34, and 80 mmHg). At the capillary inlet the average RBC number in a cluster is almost the same independently on ΔP. This is also shown in Table 2.1, where the average of the distribution, which is given as a function of ΔP and position, is between 2.5 and 2.9 at the capillary inlet. A possible explanation of this finding is that due to entrance effects RBC clusters are just building up at the inlet section.

On the other hand, the size distributions in the middle and outlet sections are significantly affected by the applied pressure drop. The cluster size distributions become more narrow and the average values lower by increas-

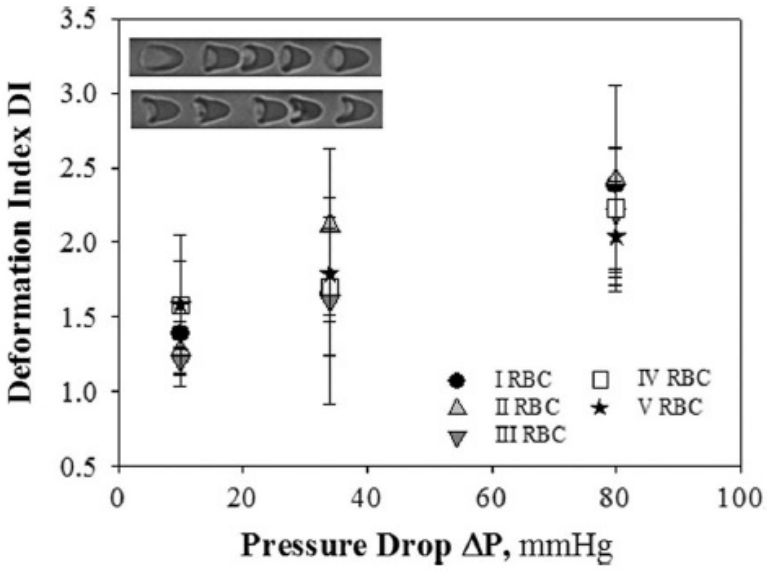

Figure 2.12: RBC deformation as a function of deltaP in five cell clusters. In the inset, typical images are shown.

	10 mmHg	**34 mmHg**	**80 mmHg**
Inlet	2.5	2.7	2.9
Middle	3.6	2.8	2.9
Outlet	5.2	3.8	2.9

Table 2.1: Average number or erythrocytes in a cluster as a function of pressure drop.

ing ΔP (see also Table 2.1). Thus, at the lower value of ΔP, larger RBC clusters are found in the middle and at the exit of the capillary. Furthermore, at ΔP=15 and 34 mmHg, the average cluster size increases from the inlet to the outlet section, and this phenomenon could be explained by the relative cell stiffness resisting shear deformations or by the resulting difference in cell shapes at different ΔP. This effect becomes negligible at ΔP=80 mmHg, where cluster size is the same at each position since pressure drop exceeds the critical ΔP value shown in Figure 2.6 and Figure 2.7. Finally, we can say that the influence of two factors on the aggregation in flow of erythtocytes in microcapillaries have been investigated. The residence time, i.e. the time that each red cell needs to flow across the microtubes, promote the RBC trains formation, but it is evident that the imposed pressure drop is the real driving force in red blood cell clustering. In fact, the higher is the value of ΔP the lower is the average RBC cluster dimension.

Finally, measurements of RBC (both isolated and within a cluster) velocity in the 10 μm diameter capillaries (the details of the experimental procedure are described elsewhere in [64]) have been also carried out in this work. The results show that there is no significant dependence of RBC velocity on cluster size. Furthermore, the difference between cluster and isolated RBC velocity is within 1%.

2.3.2 Numerical simulation

In order to elucidate the physical mechanisms leading to RBC clustering, numerical simulations in two dimensions in unbounded Poiseuille flow have been performed at the LIPhy in Grenoble, and RBCs have been modeled as vesicles (in 2D RBCs and vesicles are equivalent due to the lack of shear elasticity), taking into account bending modulus only. The simulations are based on the boundary integral method [85], already mentioned in the introductive chapter. The Stokes and continuity equations are solved together through the following integral equation for the velocity of the points x_0 of the membrane:

$$\mathbf{u}(\mathbf{x}_0) = \mathbf{u}^{\infty}(\mathbf{x}_0) + \frac{1}{4\pi\mu} \oint_{\sum_i \gamma_i} \mathbf{G}(\mathbf{x} - \mathbf{x}_0) \cdot \mathbf{f}(\mathbf{x})\, ds(\mathbf{x}),$$

where μ is water viscosity, $\mathbf{f}$(x) is the membrane force, accounting for bending and inextensibility as

$$\mathbf{f} = -k \left[\frac{d^2 c}{ds^2} + \frac{1}{2} c^3 \right] \mathbf{n} + \theta c \mathbf{n} + \frac{d\theta}{ds} \mathbf{t}$$

and G is a Green's function given by

$$G_{ij}(\mathbf{x} - \mathbf{x}_0) = -\delta_{ij}\, ln|\mathbf{x} - \mathbf{x}_0| + \frac{(\mathbf{x} - \mathbf{x}_0)_i (\mathbf{x} - \mathbf{x}_0)_j}{|\mathbf{x} - \mathbf{x}_0|^2}$$

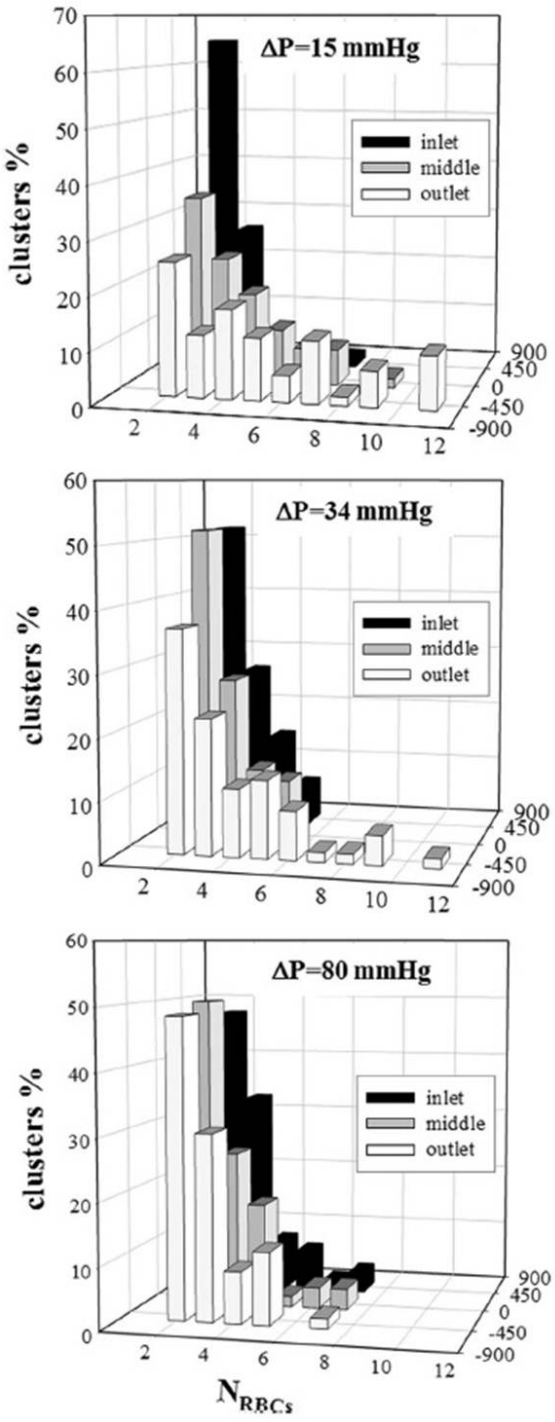

Figure 2.13: Distribution of the number of RBCs in a cluster at different positions along the capillary and at three different values of pressure drop.

Here, **n** and **t** are the normal and tangential vectors, c the membrane curvature, k the bending modulus and θ the Lagrange multiplier associated with the inextensibility constraint. γ_i represents the surface of the ith vesicle. In order to simulate RBC behavior, the vesicle reduced area (i.e., the ratio between the area of the vesicle and the area of a circle of equal perimeter) is fixed to 0.7, which is the average value for RBCs. Computed clusters of 2, 4, and 6 vesicles are shown in Figure 2.14 next to the experimental images of RBCs for similar values of the imposed pressure drop.

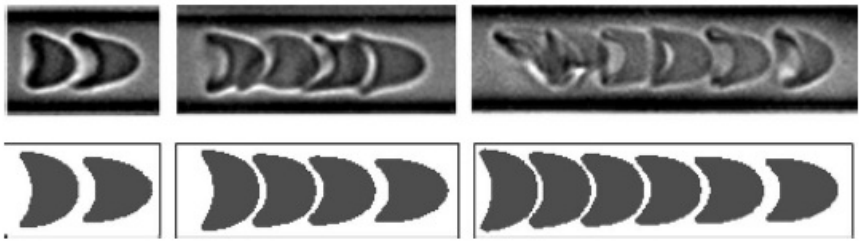

Figure 2.14: Comparison of numerical simulations with experimental images of RBCs at the same flow conditions.

The corresponding values of Ca, which is the dimensionless capillary number, defined as $\mu \mathrm{v}_{max} r^2/k$ [83] (where μ is water viscosity, v_{max} is the Poiseuille maximum velocity, r is the tube radius and k is the RBC bending rigidity, taken as 10.19 N/m [59]), are around 1000, both for experiments and simulations. It can be seen that the predicted cluster morphology bears a quite appealing resemblance with that observed in the experiments. The numerical simulations show that vesicles, at the same reduced area as RBCs, form stable clusters due to the sole hydrodynamical interactions, since our calculations are based on equally sized RBCs. However, it has been often evoked in literature [82] that clusters form due to size polydispersity of RBCs. Since the largest cells are endowed with the lower velocities [64], they would slow down the faster moving cells, thus eliciting cell clustering. Our experimental data of single cell and cluster velocity provide a strong evidence against the above mentioned hypothesis of cluster formation just based on a slowing down effect. Nevertheless, in order to test possible effects of RBC size polydispersity, we have numerically investigated cluster stability upon a variation of the size of vesicles in the less favorable situation, i.e., when a small RBC-like vesicle is in the front position. In fact, due to its reduced size, it would, in principle, move faster than the neighbors, except if it is bound to the cluster by hydrodynamical interactions. We observed that the clusters maintain their stability within a certain variation of the mean radius R of the first vesicle with respect to the radius R_0 of the others. On the other side, the width of this range decreases with increasing vesicle number in the cluster, as indicated in Table 2.2, where N is the number of

vesicles and R* is the minimal R/R0 allowing the RBCs to form one single cluster.

		R*	
N	Ca = 10	Ca = 100	Ca = 1000
2	0.94	0.94	0.94
4	0.96	0.95	0.95
6	0.98	0.97	0.96

Table 2.2: Minimal value of R* as a function of Ca and N.

These results are interesting inasmuch as the standard deviation of the distribution of RBCs radii is around 4% (11%–15% in volume), which is indeed in agreement with values from the literature (the standard deviation of cell volume has been reported as equal to 16% (21)). In fact, the data in Table 2.2 allow to predict the existence of unstable RBC clusters for the parameters (N, Ca) corresponding to R* > 0.96. The vesicle shapes for the three configurations corresponding to the limiting cases of Table 2.2 at Ca = 1000 are represented in Figure 2.15.

Figure 2.15: Stable clusters with a smaller vesicle at the front (in dark gray).

To gain further insight about the mechanisms governing cluster formation, the velocity field around the vesicles (Figure 2.16) has been analyzed by numerical simulations in recent studies. This analysis reveals that a single vesicle in a Poiseuille flow generates a hydrodynamic disturbance formed by two recirculation vortices: one clockwise in the lower half-plane (vesicles move from right to left), the other counterclockwise in the upper half-plane [170]. The two-dimensional numerical results presented here compare nicely to the experimental observations. Nevertheless, these results should be confirmed by three-dimensional simulations.

2.4 Conclusions

In this chapter, the aggregability in flow of red blood cells in microvascularity has been investigated by *in vitro* experiments and supported by 2D numerical simulations. The effect of both flow strength and residence time on RBCs clusters formation in microcapillaries has been observed. A qualitative and quantitative analysis of aggregates dimension and a statistical

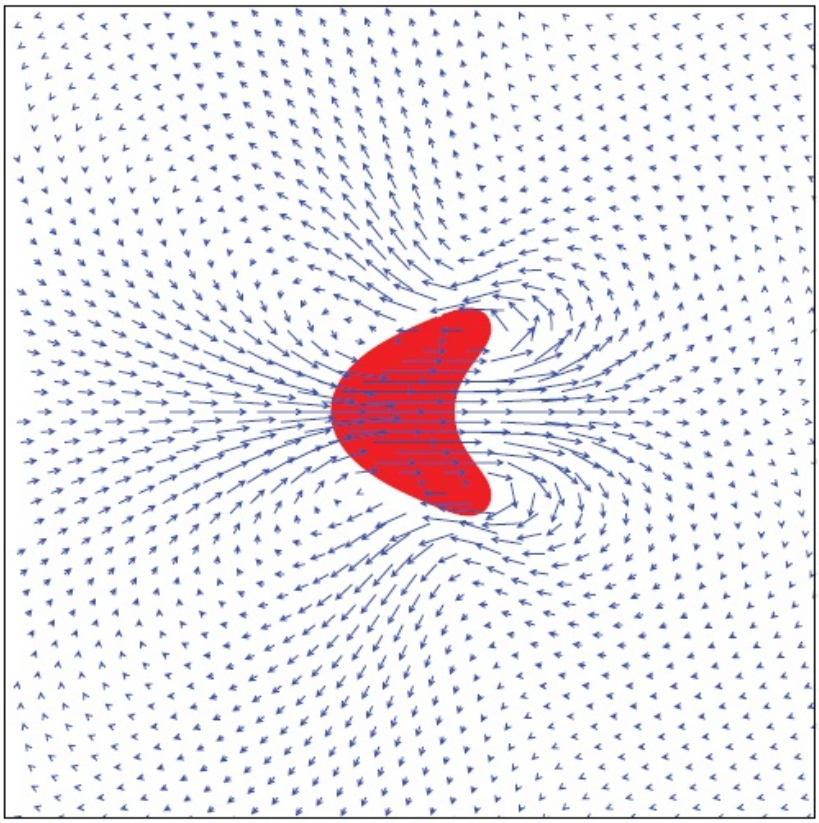

Figure 2.16: Perturbation of the velocity field caused by a single vesicle in an unbounded Poiseuille flow ($\alpha = 0.70$, N = 1, Ca = 10, stationary state). Evident attraction and repulsion zones (in front of the vesicle and on its back, respectively) are noticeable [170].

distribution of dynamic trains of erythrocytes in flow are provided. Since no additional interactive forces are noticed, we show that RBC clustering in microconfined Poiseuille flow is due only to hydrodynamic interactions between consecutive cells. Furthermore, it is well shown how size polydispersity of erythrocytes within the physiological range does not affect cluster stability. By shedding light on a still not well investigated phenomenon like RBC clustering, this work aspire to improve our knowledge about microvascular events where cell aggregation play a significant role (i.e. the process of thrombus formation and clotting in microcirculation). For instance, numerical simulations are currently under development in Grenoble to have a more precise definition of RBC clusters in microvessels and to explain the mechanisms that lead to their formation as a function of initial position and spatial distribution in the capillaries. Furthermore, experiments have been recently carried out to investigate RBCs clustering in case of rigified cells, as it happens in happens in some widespread diseases (e.g. diabetes).

Chapter 3

Flow reduction in polymer brush coated microchannels

3.1 Introduction

It is now well established from literature that *in vitro* experiments are useful in order to understand the behavior in flow of red blood cells, but the lack of the endothelial layer is still a significant limit that marks the difference with *in vivo* observations. This chapter will focus on the attempt to recreate a bio-inspired polymer layer, in order to simulate the presence of the endothelial glycocalyx and make *in vitro* experimental investigations reproduce almost physiological conditions.

3.1.1 Polymer brushes

Polymer brushes are ultra-thin layers made of macromolecules. They refer to polymeric assemblies (Figure 3.1) tethered by one end to an underlying solid substrate (e.g. a surface or an interface) either through covalent attachment or physical adsorption [95, 96, 172]. The brush chains are in sufficient proximity so that their unperturbed dimensions in a good solvent are altered. The close proximity (it depends on the grafting density, σ) causes the overlap of adjacent chains and, thus, significantly alters the nominal normal dimensions of individual polymer chains. In fact, they extend or alter their normal radius of gyration (R_g) to avoid unfavorable interactions ($R_g \propto 1/\sqrt{\sigma}$). Polymer chain-composed layers, that extend along a direction normal to the grafting surface, can exhibit properties totally different from chains in solution. This make polymer brush an interesting field for novel properties and applications.

In the 1950s, polymer brushes first attracted the attention of researchers, when the flocculation of colloidal particles had been prevented by grafting polymer macromolecules on them [171]. The first theoretical studies on

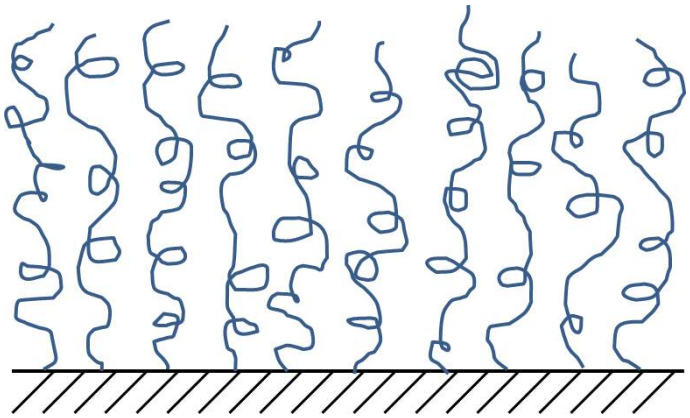

Figure 3.1: Example of end-grafted polymer brush systems.

polymer brushes were reported by Alexander ([173]) and de Gennes ([139]) almost 10 years later. The advent of new techniques with easy and rapid protocols (user-friendly chemistry) promoted a wide interest of the scientific community in producing and characterizing brush coatings both theoretically and experimentally. Several groups have performed detailed studies on polymer brushes from the early 1990s and helped to create an increased awareness of these type of structures [174, 175].

Polymer brushes can be elaborated with tight control over their thickness, grafting density, molecular structure and chemical composition. In this section covalent anchoring is chosen to produce polymer layers, thanks to its intrinsic stability in different solvent conditions. Essentially, there are two main techniques [95] to tether brushes (Figure 3.2):

- *grafting-to* technique. It involves the chemical reaction of preformed, functionalized polymers with a reactive group (for instance thiols, silanes, amino or carboxylic groups) on surfaces containing complementary functional groups, in order to attach the polymer chains onto different substrates [176]. The main advantages of this kind of techniques lie in simple protocols and a more accurate characterization of the produced layers. The synthesis can take place in a polymer solution or melt and, in general, at higher polymer concentrations correspond a higher grafting density too. However, often polymer brush with a relative low grafting density are realized by the *grafting-to* technique. This particular feature is probably due to steric repulsion between the grafted chains and the additional incoming macromolecules still present in the solution. In turn, this effect preclude the access of new polymer chains to active sites on the surface.

- *grafting-from* technique. It is an *in situ* polymerization, where the reaction occurs exclusively at the surfaces of substrates previously mod-

ified by specific initiators and immersed in a monomer solution. Thus, the main difference with the *grafting-to* technique is that here the reaction starts on the surface and not in a preformed polymer solution. The *grafting-from* methodology introduces versatility and reliability. Moreover, it is useful to produce high grafting density polymer brushes, because of the pronounced swelling properties of the chains due to the monomer solution. In this case, the growth of chains is not limited by the diffusion of monomer unless a very high grafting density is approached. The complications in *grafting-from* techniques usually involve the initiator, if it has limitation in surface coverage or if it is not efficient, and the rate of diffusion of monomers to active polymerization sites. Finally, this kind of synthesis can be implemented with almost all available polymerization techniques. In this section we will use the atom transfer radical polymerization (ATRP) method ([127]).

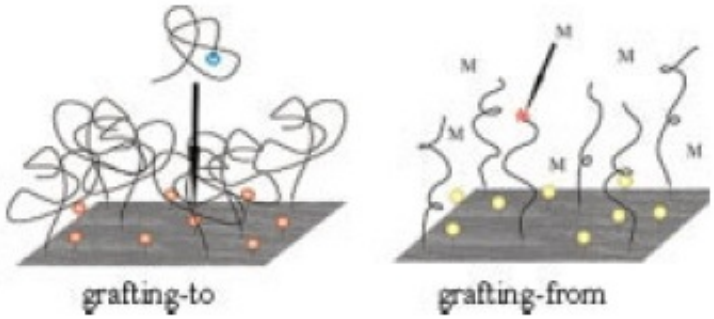

Figure 3.2: Conceptual illustration of the grafting-to and grafting-from approaches used to produce polymer brushes [172].

The already mentioned versatility of the *grafting* techniques allow us to realize tethered polymer layers fully compatible with a wide variety of technologically relevant organic, polymeric and inorganic substrates, such as cellulose [128], polystirene [129], nylon [130], poly(methylmethacrylate) [131], poly(dimethylsiloxane) [132]. Since polymer brushes are an extremely versatile way to tune surface or interface physico-chemical properties [86, 87], they can find a wide range of applications:

- *wetting* [88]
- *friction* [89]
- *adhesion of biological objects (for instance cells or proteins)* [90]
- *manipulation of flow in micro- or nanofluidics* [91, 92, 93]

Moreover, the so called thermosensitive polymers are becoming very important. They exhibit a lower critical solution temperature when mixed with a solvent, thus attracting a growing interest in the last decade for their use in designing intelligent surfaces or interfaces. The properties of such polymer-coated surfaces , like wettability, adhesion, and friction, can be deeply altered by an external thermal stimulus [115]. Thermoresponsive polymer brushes have also been used as microflow valves within microcapillaries [116] and the synthesis of various polymer brush coatings were performed in μm id capillary by atom transfer radical polymerization [92]. Recently, polymer brushes have been used in combination with soft-lithography techniques to create complex three-dimensional pattern to allow the capture and release of medicine and nanoparticles [117].

This chapter will be mainly focused on the study of the flow in polymer brush coated tubes. As regards nanofluidics, the manipulation of flow has been studied both experimentally and numerically in recent years. In this situation, brushes are comparable in thickness with the typical size of the nanochannel section, and are basically used as molecular gates controlling transports phenomena. As far as microfluidics is concerned, the use of polymer brushes have been viewed mostly as a means to alter hydrodynamic boundary conditions. It is surprising that the question of the overall resistance to flow in microchannel bearing a polymer brush on its inner walls has received rather little attention and one of the main goals of this thesis is just to shed light on this innovative topic.

3.1.2 Biocompatible polymer brushes as endothelial glycocalyx model

Observation and investigation of the flow resistance in "hairy" capillaries is interesting not only for hydrodynamic reasons, but for the improvement in understanding of blood flow mechanisms in the microvascular system too. As a consequence, the accurate study of blood flow dynamics in microvasculature could lead to the design of advanced microfluidic devices for point-of-care testings, as touched on in the introduction of this thesis. Indeed, it is well established that the lumen of blood vessels is lined by a layer made of glycopolymers bound to the membrane of the endothelial cells forming the vessels walls [7, 13]. This layer is referred to as endothelial glycocalyx (EG) or simply glycocalyx. The EG has a thickness variable in the range of 100–1000 nm (it depends on the diameter and the position of the vessels), and is exposed to the flow of plasma and blood cells. Beyond its biochemical and mechanotransduction functions [9], the glycocalyx is also expected to play a hydrodynamic role and to affect the resistance to flow, in particular in microvessels with dimensions comparable to the size of erythrocytes (i.e. ≤ 10 μm). In the last two decades, several experimental investigation have been performed and it was clearly noticed that *in vivo* blood flow resistance

of small vessels is significantly larger than expected from *in vitro* studies [105]. Moreover, a difference in flow resistance was detected during *in vivo* measurements of blood velocity in microvessels, in which the glycocalyx was either preserved or degraded by enzymatic cleavage [14]. Therefore, it is plausible to suggest that the glycocalyx presence is responsible for the observed hemorheological differences between *in vivo* and *in vitro* investigations. However, the necessity to have a deeper comprehension of blood flow dynamics in physiological conditions is paralleled by the difficulties in performing precise experiments. In fact, controlling flow parameters under tight control and monitoring thickness and state of the glycocalyx is still extremely challenging. Still, several scientific efforts are focused on this topic, since a better knowledge of the hydrodynamic role of the endothelial surface layer is important both for physico-biological reasons (glycocalyx dysfunctions are involved in vascular diseases [9]), and in the perspective of developing microfluidic-based blood assays that account properly for the interactions between walls and the corpuscolar part of blood.

The main goal of this experimental campaign was to check the possibility of mimicking the mechanical and physiological properties of the EG by means of an artificial biocompatible system. This prompted us to adopt a bio-inspired approach to this issue, and to investigate the flow in microchannels lined with a synthetic brush of macromolecules of well-controlled thickness. The majority of the experiments was performed at the LIPhy of Grenoble. Here in the following, we report on the design of channels made of glass capillary of 10 μm inner diameter, coated with polymer brushes elaborated by the so-called "grafting-from" technique. We present measurements of velocity profiles for pressure driven flows of water in such "hairy" capillaries. We show that the flow reduction induced by the presence of the brush is unexpectedly greater than what could be anticipated from simple geometric arguments on reduction of the available capillary lumen, or from predictions by models describing the brush layer as a poro-elastic boundary, as proposed in a previous theoretical study [133].

3.2 Materials and methods

3.2.1 Materials

Fused silica capillary tubing with an internal diameter (I.D.) of 10 μm was obtained from Polymicro Technologies (USA) in rolls of 10 m and cut at the desired length. Silicon wafers bearing a native oxide layer (ACS France) and freshly cleaved mica sheets (JBG Metafix, France) have been used as flat substrates for ex situ brush characterization. The monomer, hydroxyethylmethacrylate (HEMA 97%, Sigma-Aldrich), was passed through a column packed with activated microbeads (Inhibitor Remover, Sigma) in order to remove the polymerization inhibitor prior to use. Copper chlo-

ride (CuCl, 97%, Alfa Aesar), 2,2'-bipyridyl (Bpy, 99+%, Acros Organics), 3-aminopropyl-triethoxysilane (APTES, 98%, Merck), triethylamine (TEA), 2-bromo-2-methylpropionyl bromide (BMPB, 98%, Acros Organics) and dichloromethane (DCM) were used as received. Aqueous solutions were prepared in ultra-pure water (18.2 MΩ).

3.2.2 Samples preparation

The so-called "grafting-from" technique was selected in order to produce "hairy" microcapillaries. PHEMA brushes were grown both inside microcapillaries and on silicon wafers by surface-initiated Atom Transfer Radical Polymerization (ATRP), according to a protocol already developed and described in literature [115]. In a ATRP polymerization, glass or silica surfaces are pre-treated and coated by molecules of a chemical initiator, that let the reaction start and catch on. This "grafting-from" technique is quite adaptable, since it is possible to process several different polymers. In this experimental investigation, PHEMA was chosen for three fundamental reasons: it is easy to be processed, it has a hydrophilic character, and it has significant swelling properties in wet conditions. Below, the five fundamental steps of polymerization are presented in detail:

1. A piece of microcapillary of about 4 cm was cut, one of its ends fitted inside and glued to a luer-type connector using a UV setting glue (NOA 81, Norland). This allowed us to connect the capillary to a membrane pump that was used to flush the needed solutions into the sample at the various steps described below.

2. Capillaries and silicon substrates were first cleaned in a 1 M sodium hydroxide aqueous solution for 5 minutes and rinsed with water.

3. An aqueous solution of APTES (10^{-3}M) was prepared and stirred for 2 hours in order to hydrolyze the ethoxysilane groups. The solution was subsequently passed through a 0.2 mm membrane filter in order to remove possible APTES large aggregates. The filtered solution was then pumped into the capillary during 30 seconds, after which pumping was stopped and the APTES solution left inside the capillary for 10 minutes. In parallel, a clean oxidized silicon sample was immersed in the APTES solution for the same amount of time. Samples were then rinsed with water and dried.

4. The APTES treated surfaces were then placed in a solution of 2-bromo-2-methylpropionyl bromide (250 μL) and triethylamine (1.25 mL) in dichloromethane (20mL) for 10 minutes, then successively rinsed with pure dichloromethane, ethanol and water before being dried. This step is very important, since it leads to bromine-terminated surfaces from which atom transfer polymerization can be initiated.

5. A solution of HEMA (4 mL) in ultrapure water (10 mL) was placed in a round flask. A second flask was used to mix 20 mg of CuCl and 50 mg of Bpy. The two flasks, sealed with rubber septae, were separately purged with argon gas for 30 minutes. The monomer solution was then transferred to the flask containing the copper catalyst and stirred for 5 minutes under argon atmosphere. The dark brown solution obtained after mixing was then transferred into a sealed flask containing a Br-functionalized flat silicon sample and a capillary, the later being connected to the membrane pump through the sealing septum. The aqueous solution was pumped into the capillary for 1–2 minutes, then left inside without flow for a prescribed amount of time and at a temperature fixed in the range between 25 and 100 °C. After polymerization, samples were rinsed with water, dried, and characterized as described below.

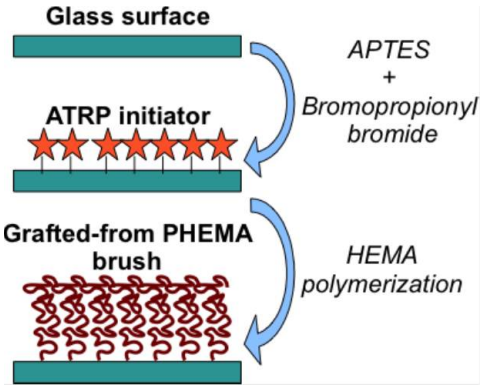

Figure 3.3: Schematic sketch of the pHEMA brush production by ATRP.

The areal density of initiator is determined during steps 3) and 4), and as a consequence the brush grafting density (σ). On the contrary, step 5) closely influences the polymerization index (N, the number of monomer units per chains), and thus the length of the grafted chains. These two parameters determine the dry thickness (h_{dry}) of a brush as $h_{dry}/\sigma = Na^3$, with a being the monomer size. We optimized the ATRP reaction, in order to produce brushes with the same grafting density and different chain lengths.

3.2.3 Characterization techniques

The main chemico-physical characteristics of the PHEMA brushes we produced, have been investigated both on silicon wafers and inside "hairy" tubes. First of all, polymer brushes were systematically characterized by ellipsometry measurements of their dry thickness on flat silicon wafers. Their swollen thickness in water was inferred from Surface Forces measurements,

since it is fundamental to quantify the tendency to elongate in wet conditions. In the end, an in situ investigation of the brush growth on the inner surface of microcapillaries has been performed by means of Electron Microscopy images of their cross section and a further elemental analysis, in order to check desirable similar results as on silicon wafers. Below, a description in detail of the apparatus we used and the acquiring techniques is presented.

Ellipsometry

Ellipsometry measurements were performed at the LIPhy in Grenoble on a rotating quarterwave plate home-built instrument working at 70 °C incidence angle and 632 nm wavelength. Data analysis was done assuming a multilayer model including a silicon substrate, a silicon oxide layer (with a thickness of 2 nm and a refractive index equal to 1.46), and an outermost polymer layer of refractive index 1.51 and thickness to be determined.

Surface Force Apparatus

The measurements by Surface Force Apparatus were performed In Grenoble, as for the characterization by ellipsometry. SFA experiments were performed on a home-built instrument [135], according to a protocol described in details in [115]. In a few words, a pair of freshly cleaved mica sheets ($\approx$ 1–5 μm in thickness) were glued onto cylindrical lenses with radius of curvature $\approx$ 1 cm. After plasma activation on its surface, a PHEMA brush was grown on one of the mica samples, strictly following the ATRP grafting technique described in the previous section. The brush-coated mica sheet was then fixed on the SFA, facing the bare mica sample. The gap between the two surfaces was filled with ultra-pure water. Afterwards, the surfaces were then approached at low velocity ($\approx$ 1 nm*s^{-1}), while monitoring the force and the distance between the mica substrates by means of multiple beam interferometry, that was used and described in detail in previous works in literature [115].

Scanning Electron Microscopy and EDX elemental analysis

Small fragments of the PHEMA brushes-coated capillaries (about 2-3 mm in length) were cut to conduct an observation by means of Scanning Electron Microscopy (SEM, FEI inspect), equipped with an advanced chamber vacuum technology. Some of their ends were roughly cut perpendicularly to the channel axis, in order to image the sample cross-section, while the others were simply crushed to obtain an irregular transverse section exposing the internal surface of the polymer-lined channels. Preliminarily, the samples were placed horizontally on an adhesive support and coated by a thin layer of gold (the presence of a good conductor is necessary to perform efficient observation by SEM) by plasma assisted deposition for 20 minutes.

The support was then placed into the vacuum chamber of the microscope for imaging. The brush-coated samples were observed at different magnification. In a following stage, we have also performed elemental analysis, using the energy-dispersive X-ray (EDX) spectroscopy microanalysis facility of the SEM. The electron beam was directed on the inner surfaces of the microcapillaries and the eventual presence of Silicon, Oxygen and Carbon amounts was checked.

3.2.4 Experimental apparatus for flow measurements

Pressure driven flow inside brush-coated capillaries was investigated using a home-built flow cell (Figure 3.4). In the following, a detailed description of its main components is provided. The cornerstone of the flow cell is certainly a sheet of polydimethylsiloxane (PDMS) of 1 mm in thickness and 24×60 mm of lateral dimensions. In the middle of this PDMS sheet a channel of 5 cm in length is cut, exhibiting a central constriction as represented in Figure 3.4. This particular configuration allow to place two 3–4 mm long segments of microcapillaries (one bare and one coated with a brush) on each side of the central constriction and hold them by adhesion. The set of PDMS plate and capillary samples is then sandwiched between a 24×60 mm glass coverslip and a polycarbonate plate of the same lateral dimensions and a thickness of 5 mm. The sandwich is mounted in an aluminum frame and then lightly pressed, in order to properly seal the channel.

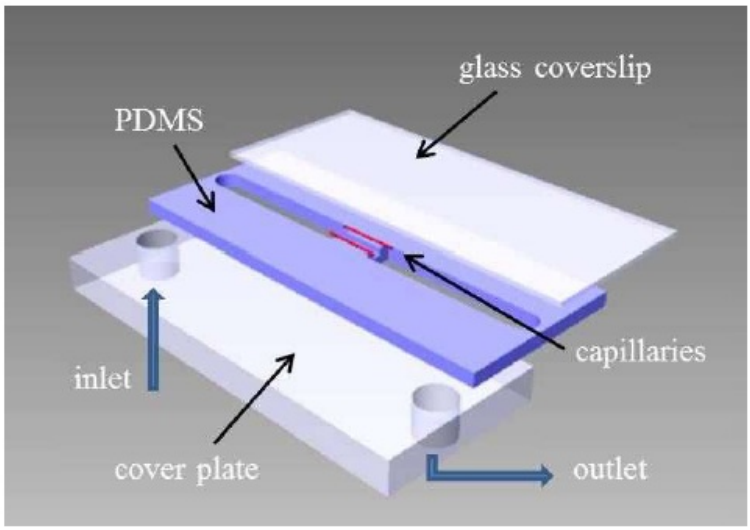

Figure 3.4: Sketch of the cell used for flow measurements.

A dilute aqueous suspension of fluorescent nanoparticles (Fluoro-Max, Thermo Scientific, 200 nm diameter latex beads) was fed to the flow cell by means of flexible tubing connected to a 50 mL glass syringe, used as

an upper reservoir on a vertical rail, and collected at the exit in a glass reservoir. As for the flow cell used to observe the red blood cell flow, the pressure drop inside the microcapillaries is regulated by adjusting the height difference between the liquid surfaces in the two reservoirs, which can be set in the range 150–400 mm. The flow cell was positioned on the stage of an inverted epifluorescence microscope (Olympus IX 70). The flow observation was performed thanks to a 100× oil immersion objective (NA = 1.3). The objective was focused at the mid-plane of the circular microcapillaries, and the fluorescence intensity coming from particles flowing in the midplane was detected with a cooled CCD camera (Sensicam, PCO Imaging). This setup allowed us to acquire time-lapse sequences of flowing particles at a frame rate up to 50 Hz over a region of 15×90 μm along the channel axis, with a resolution in space of 0.5 μm (the latter value was determined by the pixel binning required to obtain a good signal to noise ratio using low exposure times). The acquired sequences, constituted by almost 600 images, were subjected to an off-line analysis by means of the Manual Tracking plugin of the ImageJ freeware, in order to detect nanoparticles velocity as a function of their lateral position in the capillary mid-plane. Therefore, velocity profiles inside the microtubes were measured by tracking the fluorescent nanoparticles and then interpreted.

3.3 Results and discussion

3.3.1 Samples characterization

Brush growth

A basic question prompted us to characterize the PHEMA samples we produced: how do polymerization conditions influence brush growth? In the following we will try to shed light on this question, by measuring brush dry thickness by ellipsometry, as a function of reaction time and temperature. In Figure 3.5, the PHEMA brush growth is plotted as a function of the reaction time at three different temperatures. At room temperature a fast initial increase of the thickness is noticed within the first 20–30 minutes, followed by a significant slowdown of the kinetics. After almost 3 hours of polymerization, a plateau is reached at about 75 nm. Thanks to literature search, it was possible to verify that this trend is typically in agreement with earlier results obtained by growing PHEMA brushes in pure water, in which the poor "living" character of ATRP of HEMA in water is highlighted [138].

A classic method to increase reaction kinetics is to increase the ambient temperature (T). Therefore, the PHEMA layers growth has been probed at higher temperatures. Figure 3.5 clearly shows how, as T is increased, the initial brush growth displays a broader linear increase with time, extended over the first hour of reaction. For instance, at T = 90 °C, the plateau is

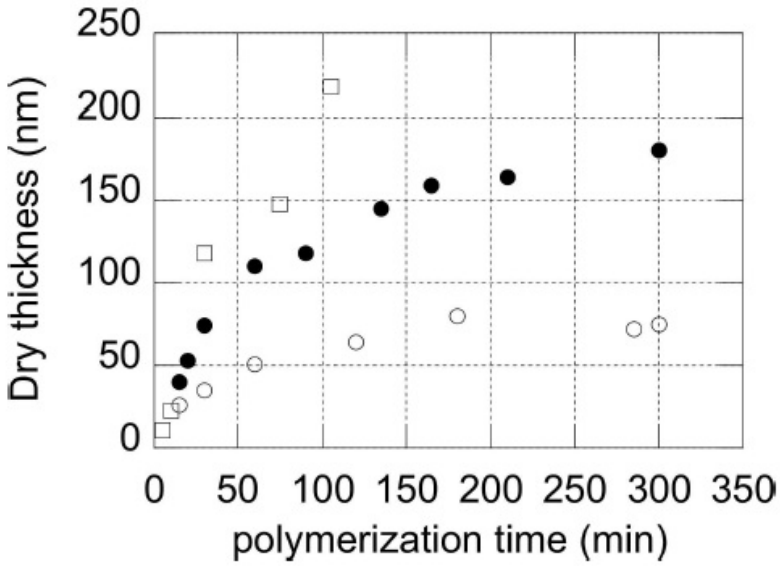

Figure 3.5: Brush growth kinetics measured at room temperature (∘), T = 55 °C (•) and T = 90 °C ().

reached in correspondence to a brush thickness (h_{dry}) ≥ 200 nm. Even if it is not possible to have a meticulous control of the kinetics, it seems that the higher is the temperature of polymerization the larger is the linear increase of brush growth with time, with a significant delay in reaching the plateau value.

In addition to the quantitative analysis made by ellipsometry, a qualitative characterization of the polymer-coated inner surfaces of the microcapillaries has been performed by SEM. The direct observation of tube sections is found to be extremely difficult, most likely due to the probable damages caused to the PHEMA thin layers while cutting or polishing the sample fragments. We succeeded only once to acquire a satisfactory image of a clearly visible PHEMA coating on a capillary cross-section and this picture is presented in Figure 3.6. The panels a) and b) show the comparison between the "hairy" microtube and a bare one, where the polymer layer is not noticeable. Taking in account the dimensions of the image, the dry thickness can be estimated to be around 200 nm. This is consistent with the ellipsometric value (≈ 195 nm) measured ex situ on a silicon wafer sample produced along with the investigated capillary. These results strongly suggest that brush growth occurs in a very similar way either on flat silicon surfaces and inside the microcapillaries. In fact, we rule out that the curvature of microcapillaries can affect the growth of polymer brushes because of steric reasons, since the PHEMA brushes thickness is not comparable to the tubes diameter. In conclusion, the thickness measured by ellipsometry can be safely used as

reference values for each brush elaborated.

Elemental analysis provided another important qualitative characterization. In contrast to the SEM imaging inside the capillaries, this kind of analysis was easier to perform and several samples have been analyzed. The spectra acquired observing the transverse sections of bare capillaries display only Silicon (Si) and Oxygen (O) peaks. On the contrary, brush-coated samples undoubtedly show a peak associated with the presence of Carbon in addition to the ones of O and Si. This suggests that the inner walls of "hairy" microcapillaries are really lined by an added organic coating. In the panel c) of Figure 3.6, the ratio of the Carbon to Silicon peak intensities is presented for different brush thickness. The plausible depth of analysis of EDX testing being 1 μm, we have to consider that all the acquired spectra are averaged over the brush thickness and the underlying glass substrate and so the elemental analysis can provide only a qualitative probe. Therefore, an increase of C/Si ratio indicates the presence of a larger Carbon amount, qualitatively in agreement with the increasing PHEMA brush thickness detected ex situ.

Brush swelling in water

Since the main topic of this chapter is to investigate what is the effect of a polymer brush coating on the flow resistance in microchannels, it is necessary to understand the properties of brushes when surrounded by a liquid (i.e. water, in the present experiments). Below, the swelling of PHEMA coating immersed in ultra pure water is estimated by means of Force vs Distance curves, measured by Surface Force Apparatus (SFA). First of all, we wanted to check if the brushes grown on plasma-activated mica samples have the same density and, subsequently, width as those produced on flat silicon wafers under the same grafting conditions. Therefore, the dry thickness on mica surfaces have been measured in the SFA. Next, the facing mica sheets were immersed in water and approached quasi-statically, while precisely monitoring both the distance between the two mica substrates and the interaction force.

In Figure 3.7 the Force-Distance curve measured with a brush of h_{dry} = 110 nm is presented. It is evident how the repulsive interaction forces become detectable below a given intersurface distance, and progressively increase as the surfaces approach further. Such forces are of steric origin and correspond to the repulsion due to compression of the brush [134, 139]. It means that the onset of repulsion that it is possible to observe in Figure 3.7 represents the point in which the bare mica surface comes into contact with the facing polymer coating. Therefore, the distance between the mica substrates can be reasonably considered as the swollen thickness of the PHEMA brushes. In this case, the onset of repulsion is situated in correspondence of $h_{swell} \approx 225$ nm, suggesting a probable swelling ratio almost equal to $\alpha =$

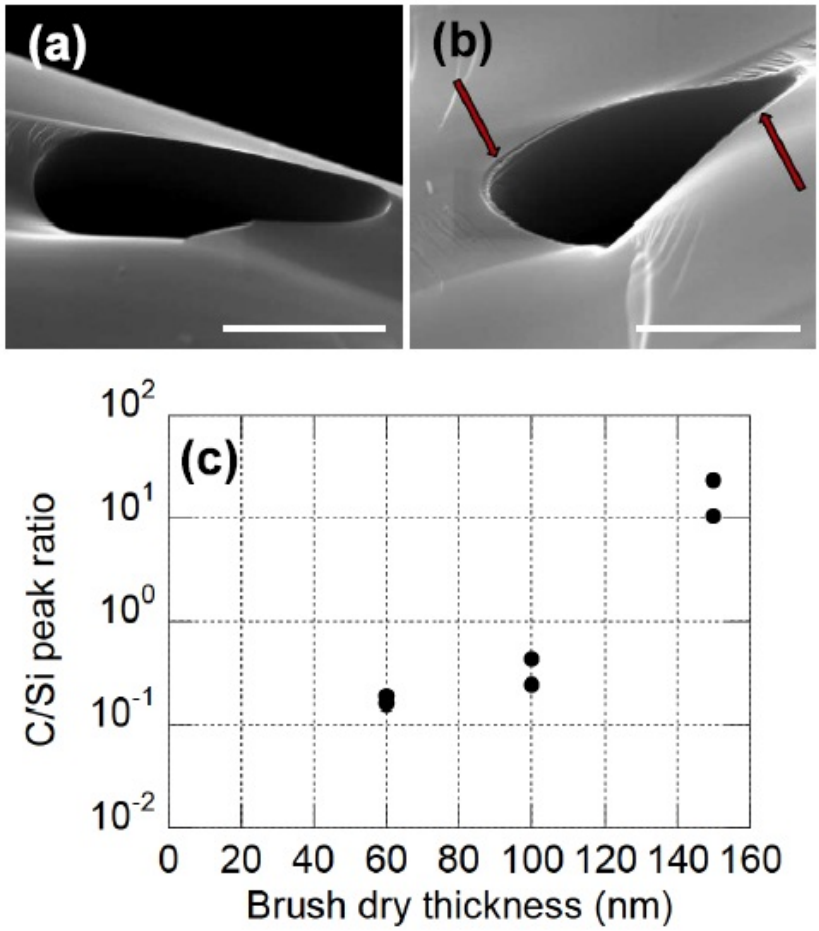

Figure 3.6: Observation of a crushed cross-section with a finite incident angle with respect to the capillary axis. a) SEM image of a bare microcapillary. b) SEM image of a brush-coated capillary. The arrow indicates the polymer layer, not visible in panel a). The scale bar in both images is equal to 5 μm. c) Evolution of the C/Si ratio as a function of the ellipsometric brush thickness.

$h_{swell}/h_{dry} \approx 2$. It is credible to hypothesize the constancy of the swelling ratio α, independently of the length of the grafted chains. In order to probe the veracity of this hypothesis, we measured the Forse vs Distance curve for PHEMA brushes with same grafting density and different thickness. For instance, in the inset of Figure 3.7 there is a comparison between the experimental results obtained for $h_{dry} = 110$ nm and $h_{dry} = 40$ nm. It is evident either the thinner and the thicker brushes displays the same value of $h_{swell}/h_{dry} \approx 2$. So, in the following, the value of the swelling ratio descending from the dry thickness measured by ellipsometry will be $\alpha = 2$ for each h_{dry}.

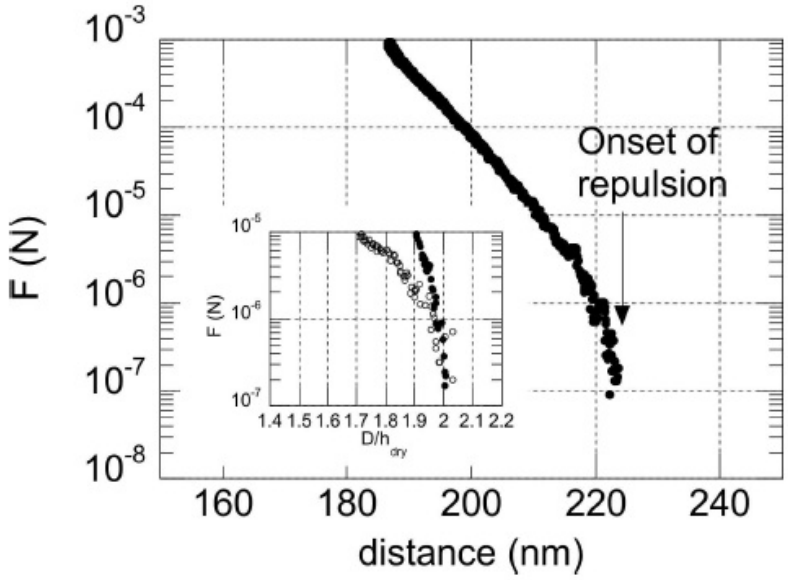

Figure 3.7: Force vs Distance curve measured by SFA with a PHEMA brush immersed in water ($h_{dry} = 110$ nm). In the inset the forse vs distance normalized by h_{dry} is plotted to show the onset repulsion for two different brushes. (•): $h_{dry} = 110$ nm; (○): $h_{dry} = 40$ nm.

3.3.2 Flow velocity in brush-coated capillaries

In this section, the attention will be focused on evaluating the effect of PHEMA grafted brushes on the flow velocity inside the microcapillaries. In Figure 3.8, the velocity profiles obtained either for bare and "hairy" capillaries is plotted as a function of the radial position in the mid-plane of the tube. Each profile has been normalized by the maximum velocity expected from Poiseuille theory in a channel of 10 μm diameter ($V_{max} = \Delta P R^2/(4\eta L)$), in order to favor the comparison between theory and results. In general, an overall downward shift of the normalized velocity profiles ($\tilde{V}(r)$

$= V(r)/V_max$) is noticed when the inner walls of microcapillaries are coated by polymer brushes. In particular, we observed that the flow reduction is larger with the increasing brush thickness. The typical Poiseuille flow profile is kept in brush-coated microchannels, at least in the central part of the tubes. However, space and velocity resolution of our experimental setup do not allow us to measure the velocity in proximity of the lined walls of the capillary, where it is probable to find pronounced deviations of the flow profile from the parabolic shape.

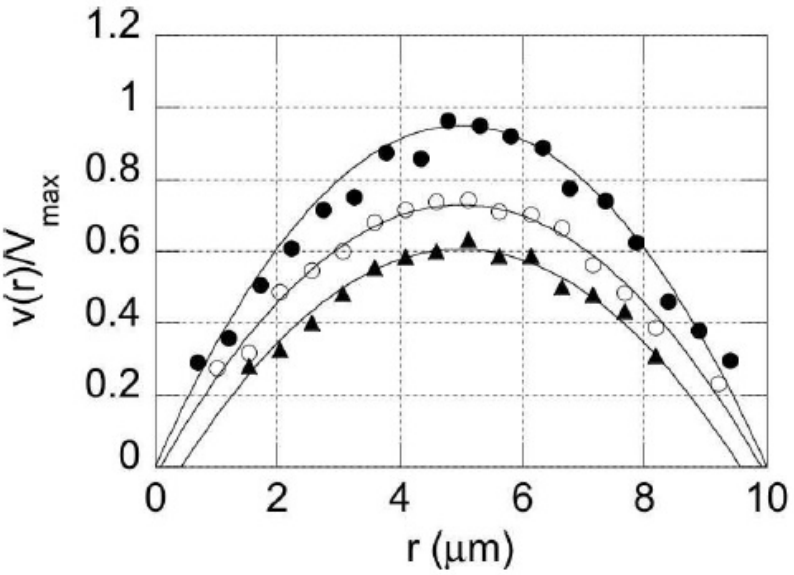

Figure 3.8: Normalized velocity profiles as a function of the radial position r in the mid-plane of the capillary. (•) bare capillary; (○) h_{swell} = 240 nm; () h_{swell} = 390 nm. Lines are parabolic fits of the data points.

The velocity profile in microcapillaries has been determined for different swollen thickness of the brushes, ranging from 45 to 400 nm. For the sake of comparison, we computed the relative variation $\Delta\tilde{V}/\tilde{V}_{max}$, where $\tilde{V}_{max}$ is the normalized central velocity measured in a reference bare 10 μm diameter capillary and $\Delta\tilde{V}$ is the difference in normalized maximum velocities between bare and brush-lined samples. In Figure 3.9 the trend of $\Delta\tilde{V}/\tilde{V}_{max}$ is plotted as a function of h_{swell}. It is quite clear that there is a roughly linear proportionality between the flow reduction and the increasing brush thickness. A maximum velocity decrease of up to has been measured for the thickest PHEMA coating we produced, which have a swollen thickness filling $\approx$ 4% of the nominal capillary lumen.

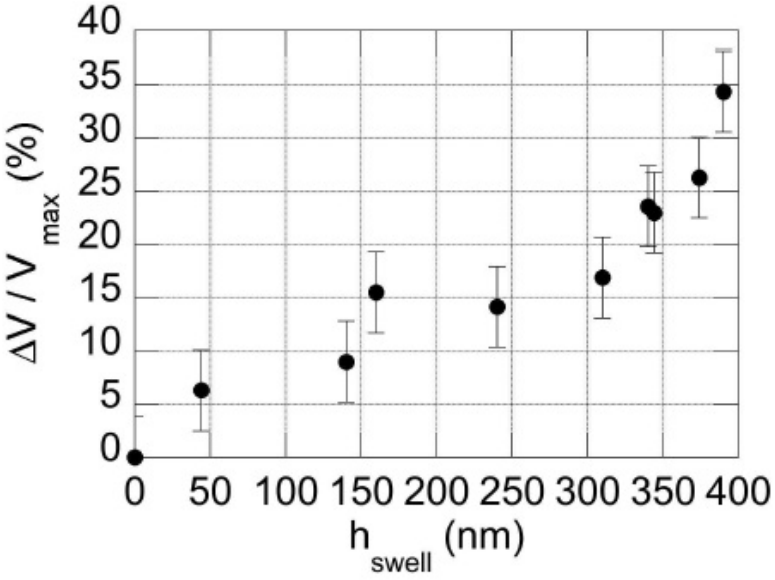

Figure 3.9: $\Delta\tilde{V}/\tilde{V}_{max}$ as a function of h_{swell}. Error bars correspond to the uncertainty on the velocity measurements.

3.3.3 Interpretation of experimental results

The results reported in Figure 3.8 and Figure 3.9 are, to the best of our knowledge, the first ones showing the quantitative effect on flow velocity of grafted brushes of various thicknesses and they encourage an intense discussion in order to interpret the experimental outcomes in the light of contemporary theoretical models. A slowdown of flow speed at a given pressure drop (ΔP) in the presence of a grafted polymer coating is *a priori* not surprising. In fact, adding a thin rigid layer on the microchannel walls, the other flow parameters being established, reduces its available lumen and thus induces a velocity drop. In that respect, our results are qualitatively consistent with a recent study [93] dealing with the flow in chemically modified capillaries. Now, the main open question about the effect reported in Figure 3.9 is: is the downward shift of flow velocity simply due to the decrease of the nominal capillary diameter or another explication has to be taken into account?

The first step to understand our results was looking for theoretical studies that propose a model similar to the grafted brushes system. In that regard, we first attempt to interpret our outcomes within the framework proposed in a previous theoretical work by Damiano *et al.* [133], that addresses the question of the flow of erythrocytes in microvessels lined by endothelial glycocalyx. In this study, a grafted polymer brush is described as a thin poro-elastic layer coating the nominal inner walls of a microchannel.

Indeed, it is intuitive to predict that the flow properties inside this porous medium can affect the overall velocity profile in the capillaries, since a brush is made of elastic chains, for which the flowing fluid is a good solvent. In Damiano's model, the flow rate and the shape of the velocity profile inside the brush depend essentially on the ratio (R - d)/R, where R is the bare channel radius and d the thickness of the poro-elastic layer, and on the parameter $\delta^2 = \eta/(\mathrm{R}^2\mathrm{K})$, where η is the viscosity of the fluid inside the porous layer and K is the hydraulic resistivity of the layer. This theory introduces the limit case of $\mathrm{K} \to \infty$, which corresponds to a no flow condition inside the polymer layer of thickness d. In such a limit case, the velocity profile is simply the one predicted by Poiseuille theory in a channel of radius R - d. In Figure 3.10, the measurements on $\Delta\tilde{V}/\tilde{V}_{max}$, already presented before, are compared with the flow reduction expected from a radius reduction of $\mathrm{d} = \mathrm{h}_{swell}$ (i.e. $\Delta\tilde{V}/\tilde{V}_{max} \approx 2\Delta\mathrm{R}/\mathrm{R} = 2\mathrm{h}_{swell}/\mathrm{R}$). It is evident that the simple "no flow" assumption inside the brush is not enough to account for our experimental observations and leads to systematically underestimate the flow reduction. Moreover, it follows that a porous layer of finite resistivity, as well as for Damiano's model, will lead to a bigger underestimate of the experimental results.

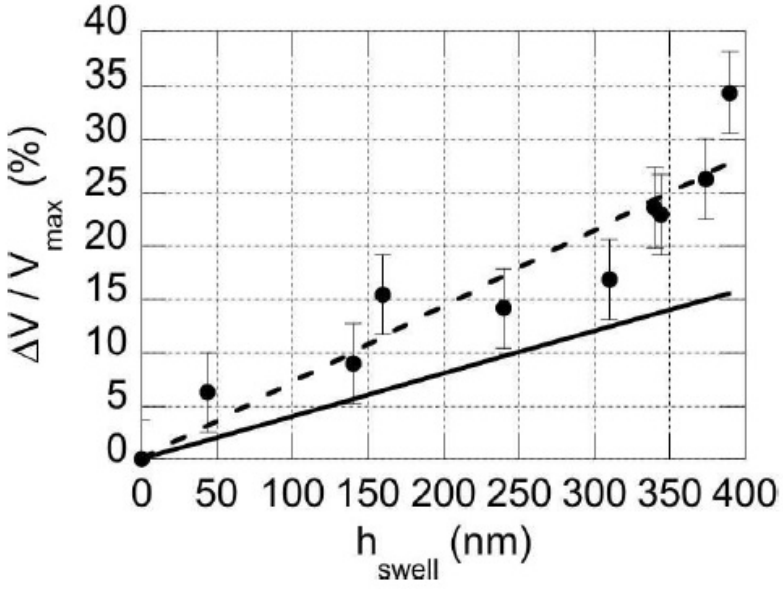

Figure 3.10: $\Delta\tilde{V}/\tilde{V}_{max}$ as a function of h_{swell}. The symbols represent experimental measurements, the continuous line is the prediction assuming the no flow condition in a shell of thickness h_{swell}, and the dashed line is the best linear fit to the data obtained with $\mathrm{h}_{eff} = 1.8\ \mathrm{h}_{swell}$.

In fact, the swelling ratio α of PHEMA brushes would be significantly

higher than 2, in order to account for such a strong flow reduction using the Damiano's model. Such a discrepancy between experimental outcomes and theoretical previsions raises an important open question about the real thickness of brush coatings in the presence of shear flow. Indeed, it is plausible to predict a higher value of h_{swell} under shear, due to an additional stretching of polymer chains, since our estimations by SFA have been measured in quasi-static conditions and the absence of flow. This have been the topic of several works in the past decades either from the theoretical and experimental point of view. Considering theoretical studies, there is no consensus on whether a shear flow could vary [142] or leave unchanged [143] the thickness of a polymer brush. On the contrary, experimental works provide a more convincing answer to our issue. No significant differences in brush thickness has been detected by neutron reflectivity in the presence of shear stresses [144], and these results have been confirmed by numerical simulations too [145]. So, it is reasonable to hypothesize that chain stretching in the presence of shear flow is compensated by a simultaneous tilting, thus leaving brush thickness globally unaffected and excluding the possibility of an additional swelling to account for our investigations.

In the following, two possible mechanisms that may provide an explanation to our observations are examined. The first one is associated to the possible polydispersity of chain length in the brushes we produced. Indeed, it is plausible to predict the presence in the layer of a small amount of chains longer than the overall value measured during the characterization. Their contribution on the noticed flow reduction is difficult to detect by Surface Force Apparatus, since measurements were performed in quasi-static conditions and force sensitivity is limited. However, there is a high probability that these longer chains contribute to flow resistance under shear, over an "effective" brush thickness larger than the one estimated by SFA. Now, in order to account for our measurements of $\Delta\tilde{V}/\tilde{V}_{max}$ on the basis of such an effective thickness h_{eff}, and assuming as above that the brush behaves as an impenetrable layer in which no flow occurs, a value of $h_{eff} \approx 1.8\ h_{swell}$. In Figure 3.10, the dashed line obtained using $h_{eff} \approx 1.8\ h_{swell}$ is consistent with our experimental results. Such an estimate of a possible h_{eff} is quite surprising, since it is almost twice the value detected by SFA. Moreover, it is difficult to find an agreement between this estimate and the overall shape of Force-Distance curves showed in Figure 3.7. In fact, the rather well defined onset of repulsion forces is consistent with the presence of a monodisperse brush, as predicted by previous theoretical studies [139]. All things considered, we think that even if PHEMA brushes polydispersity is likely to play an important role in the enhanced frictional drug observed in our investigations, this effect is not sufficient to fully explain the experimental data.

The second possible mechanism we want to present, relies on recent observations obtained in simulations by molecular dynamics of polymer

brushes under shear flow [146, 147]. These innovative simulations propose a cyclic stretching-recoil motion of the chain macromolecules under the dual effect of advection in flow and thermal fluctuations. As a consequence, the alternation of stretching and recoil phases causes a backwards flow in the area occupied by the brush. It means that there is a region with a thin depth where the flow is opposite in direction to that induced by the imposed pressure gradient. The possibility that the oscillatory motion of the elastic polymer chains and the resulting near-wall secondary flows could deeply affect the increase of flow resistance inside "hairy" microcapillaries is quite convincing.

One of the goals of this work, beyond observing the flow in polymer brush-coated microcapillaries, was to verify the possibility of recreating an *in vitro* system able to mimic physiological conditions in human microvessels. Therefore, at the end of this section, it is interesting to highlight how our experimental results can be successfully compared with earlier measurements of *in vivo* blood flow in microvessels. Pries *et al.* [14] measured the flow velocity in mice vessels of nominal diameter equal to 20 μm: they compared the flow rate in an intact vessel with the one measured in a venule where the endothelial glycocalyx was removed by enzymes. The difference of flow velocity of up to 30% detected in this study is consistent, in terms of order of magnitude, with the results we obtained with a PHEMA brush thickness closest to a plausible glycocalyx depth (for $h_{swell} \approx 400$ nm, a $\Delta\tilde{V}/\tilde{V}_{max} \approx 35\%$ was obtained). It is striking to notice that this work focuses only on the flow of pure water, while the experiments of Pries have been performed on whole blood. This suggest that a large part of the flow reduction due to the presence of the glycocalyx arises from a slowdown of the suspending plasma in which Red Blood Cells (RBCs) flow and that direct interactions between RBCs and vessel walls do not entirely control blood flow resistance in microvessels.

3.4 Conclusions

In this chapter, the design of microcapillaries coated with hydrophilic polymer brush (PHEMA) by ATRP has been reported. The kinetics of brushes growth and their swelling properties have been investigated by means of ellipsometry, Surface Force Apparatus and *in situ* electron microscopy coupled with EDX elemental analysis, in order to provide the best possible characterization of our samples. Afterwards, we probed the effect of PHEMA brushes on the flow of water inside the "hairy" microchannels. We have shown that a grafted polymer coating causes a flow reduction, which is roughly proportional to the brush thickness and quite larger than expected from a simple reduction of the channel available lumen. Two plausible mechanisms are proposed to explain such a large brush-induced resistance: the brush

polydispersity and the cyclic stretching-recoil motion of the grafted chains under shear, that creates flow perturbations close to the microtubes wall region. Our experimental campaign was animated by two main purposes: the better understanding of the mechanisms governing *in vivo* microvascular system and the further design of microdevices for clinical testings of vascular diseases in microcirculation. Thus, the results of present study can be considered quite encouraging and open the way to additional investigation, in order to produce synthetic microchannels which account for the effect of the glycocalyx, for *in vitro* observation of hemodynamics.

Chapter 4

Red blood cell flow in polymer brush-coated microcapillaries: the role of glycocalyx in microcirculation *in vivo*

4.1 Introduction

The following and final chapter of this thesis is dedicated to the observation and investigation of the flow of red blood cells in polymer brush-coated glass microcapillaries. Since in the previous two chapters we focused the attention on the role of erythrocytes in microcirculation and we noticed the effect of polymer coatings on the flow properties in microchannels, it seems immediate to check if RBCs properties in flow are modified by the presence of polymer brushes. In fact, the development of an artificial system able to simulate the presence of the endothelial glycocalyx would help to understand the mechanisms leading many vascular diseases, in which both blood cell disfunctions and endothelium damages can be involved Moreover, the set up of such microdevices would allow to carry out diagnostic analysis elaborating small amount of blood in dynamic conditions, instead of the static ones in usual clinical tests, and experiment innovative methods for drug delivery.

4.1.1 Endothelial glycocalyx: properties and main functions

The glycocalyx layer (EG), located on the inner surface of the vascular endothelium, is a network of proteoglycans and glycoproteins with a thickness ranging from 100 to 1000 nm [8]. The depth usually depends on the vessel

size, but can be affected by pathological factors too [177]. Its properties [8, 9] have been already listed and detailed previously, so we will only provide a general overview in the following. The EG is fundamental in the vascular mechanotransduction of translating biomechanical stimuli such as shear stress into biochemical signals on the endothelial cells (ECs) of the vessels wall. Moreover, it plays a fundamental role in the vasculature determining vascular permeability, mediating blood cell-vessel wall interactions and shear stress sensing, enabling balanced signaling, regulating clotting and complement cascade, controlling the interaction between leukocyte and endothelial cells, fulfilling a vasculo-protective function and influencing the microvascular hematocrit [1, 8, 19]. So far, the effect of the glycocalyx on capillary hematocrit has been attributed to the fact that the actual lumen available to plasma and red blood cells (RBCs) flow is reduced [14].

4.1.2 Red blood cell flow in microvascularity: the interaction with glycocalyx

RBCs play a key role in human body by delivering oxygen and removing CO_2 from tissues [13]. Their behavior under microconfined conditions has been the subject of several investigations both *in vivo* and *in vitro*, as recently reviewed [59, 97]. The flow of RBCs have been imaged *in vitro*, in order to better understand some of their fundamental properties in flow (e.g. velocity, deformability, aggregability) and develop innovative microdevices for the study of vascular pathologies, either in silica microcapillaries and in PDMS microchannels [98]. Since it seems plausible that oxygen and nutrients delivery takes place in microcirculation, the attention have been focused on capillaries and channels with dimension comparable to cell size during last years. RBCs observation were performed in microtubes with inner diameter up to 10 μm by using a high speed camera, either in steady-state [64, 99, 141] and in transient conditions [100]. From the theoretical point of view, many works are focused on RBCs flow in microcapillaries [22, 67], including numerical simulations of RBC shape in microcapillaries [83, 102, 103], and through micropores [67, 101] .

Both theoretical and experimental works deal with one of the most important geometric features associated with RBC confined flow, i.e. the geometry of the suspending fluid layer separating the cell body from the confining walls. Indeed, the increase of cell length with the flow strength is paralleled by a decrease of cell width. Hence, at a given capillary diameter, the layer thickness is an increasing function of cell velocity, with a leveling off until an apparent plateau is reached [104]. On the other hand, at a given velocity, the larger is the capillary diameter the higher is the layer thickness value [104]. Even if this behavior is noticed either *in vivo* and *in vitro* observations, RBC deformation and consequently the fluid layer thickness are quantitatively different in artificial devices than in real microvessels, due to the presence of

endothelial glycocalyx on the inner walls of *in vivo* capillaries.

The glycocalyx is considered the main factor leading to the lower flow resistance and the increased hematocrit found in glass microcapillaries as compared to microvessels *in vivo* [105]. Recent experimental studies clearly show that alterations of the glycocalyx have consequences in microvascular permeability disorders, and are associated to several diseases, such as diabetes, ischemia and atherosclerosis [1, 8, 177]. Given the physiopathological role played by the glycocalyx layer on blood flow, various techniques have been employed to experimentally measure its dimensions, mechanical properties and moreover its effect on the microcirculation [106], but these measurements are typically limited to relatively large microvessels (i.e. diameter larger than 100 μm. At the same time, theoretical and numerical studies were carried on to model the glycocalyx layer and its interaction with blood cells [20, 21, 43, 107].

To our knowledge, a quantitative experimental study of the effect of glycocalyx on RBC fluid dynamic behavior under microconfined shear flow is not currently available. To this end, polymer brush are potentially fundamental in order to investigate hemodynamics and design *in vivo*-mimicking artificial systems, thanks to their mechanical properties (high elasticity and resistance), their high biocompatibility and pronounced versatility in order to develop microfluidic devices. The goal of this chapter is to provide an experimental investigation on the behavior of RBC flowing in microcapillaries with diameter of 10 μm, lined with polymer brushes, the latter used as a model of endothelial glycocalyx.

4.2 Materials and methods

4.2.1 Experimental apparatus

Fused silica capillaries (Polymicro Technologies, USA) with 10 μm inner diameter have been lined with a layer of polymer brush [140], as described in details in chapter 3. The polymer that has been chosen to coat the microcapillaries is poly-Hydroxy Ethyl Methacrylate (PHEMA), a non thermoresponsive polymer, easy to processed and useful for its hydrophilic property, that allows the brush swelling during water flow inside the tubing. The brush-coated capillaries, with different thickness of polymer coating, ranging from 28 to 190 nm (the range of thickness was chosen in order to have layers consistent or at least comparable to the endothelial glycocalyx in human microvessels), were placed on a coverslip placed into the flow cell already described and used in chapter 2 [64, 99, 100, 141]. The flow cell was connected by two flexible tubing to two glass reservoirs, where the RBC suspension was fed in. By adjusting the distance between the liquid menisci in the two reservoirs, it was possible to regulate the pressure drop across the silica microcapillaries. The flow cell was placed on a motorized stage of

an inverted microscope (Zeiss Axiovert 100) and the images of the flowing RBC were acquired by using a high speed camera (Phantom 4.3), operating up to 1000 frames per second. The large number of images recorded were processed off-line by a custom macro based on the library of commercial software (Image Pro Plus) to measure the velocity and the deformation index (defined as the ratio between of the long side and the short side of a box enclosing the cell) of single RBC, as it was already described in chapter 2.

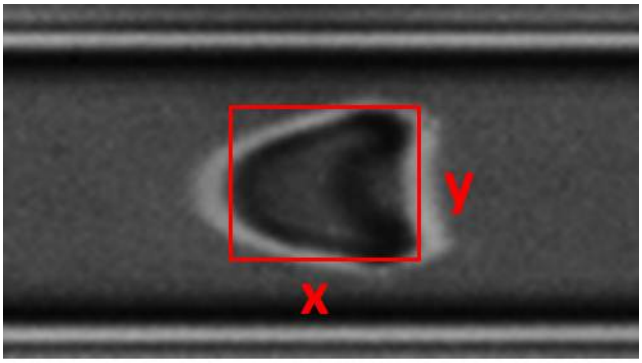

Figure 4.1: Box enclosing a red blood cell. The deformation index is defined as the ratio between its long and short side.

4.2.2 Blood samples

As already described in chapter 2, fresh venous blood samples were drawn from healthy consenting donors, collected into EDTA test-tubes and used within 4 hours form collection. The samples were diluted with anticoagulant ACD (0.6% citric acid, 1.1% anhydrous dextrose, 2.3% sodium citrate, 96% water) supplemented with BSA (Bovine serum Albumin), until a 0.1% RBC concentration by volume. RBC viability was checked before each experiment by observing cell morphology under static conditions at high magnification (100x objective).

4.3 Results and discussion

4.3.1 Red blood cell velocity

As known from the literature [64], at a given pressure drop, RBC velocity increases with microcapillary diameter. Furthermore, in the previous chapter, an increase of the flow resistance with the thickness of the polymer layer has been unequivocally measured in brush-coated microcapillaries [140]. Therefore, a slowing down of RBC velocity in "hairy" capillaries is expected in comparison with bare tubes, due to the double effect of the decrease of the

available lumen and the increase of the friction at the walls. This hypothesis is consistent with the experimental results presented in Figure 4.2, where RBC velocity is plotted as a function of pressure drop for bare and 170 nm hairy capillary. A percentage decrease of RBCs velocity (ΔV) of about 20% is found in 170 nm "hairy" capillary. This value of ΔV is in good agreement with the flow velocity slowing down measured in chapter 3 in microtubes coated by PHEMA brushes of comparable thickness [140].

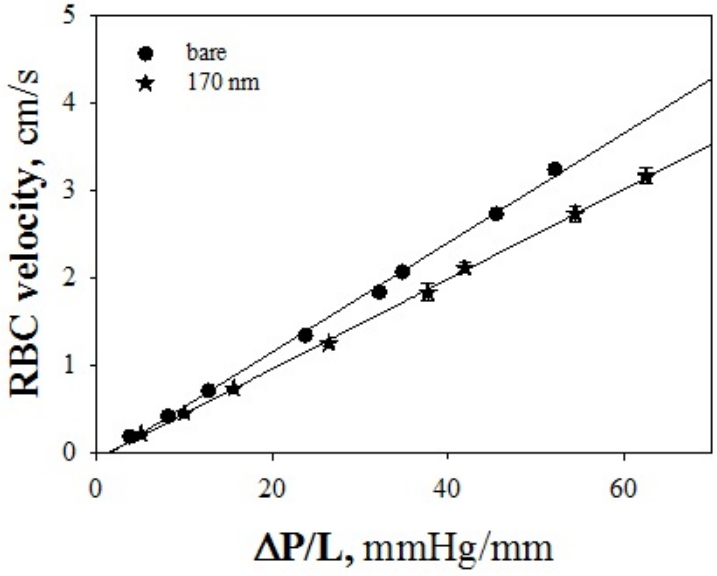

Figure 4.2: RBC velocity in bare and in 170 nm brush coating capillaries as a function of the imposed pressure drop.

RBC velocity in capillaries coated with brushes of different dry thickness (h_{dry}) is plotted in Figure 4.3 as a function of the imposed pressure drop. Although it would have been plausible to expect a direct proportionality between the velocity of red blood cells and the thickness of polymer layers (as it has been detected in chapter 3 for the flow velocity [140]), it is evident that the slowing down of flowing RBCs does not depend on the PHEMA brush thickness in the range we explored ($h_{dry} \approx$ 70–190 nm). One possible explication of this unexpected outcome relies in the choice of relatively high pressure gradients for our observations. In fact, as already mentioned in the introduction of this chapter, the depth of the suspending fluid layer between cells and walls is an increasing function of RBCs velocity, thus avoiding a direct contact between RBCs and polymer chains at high ΔP.

Therefore, we performed the same experiments at low pressure drops ($0 \leq \Delta P/L \leq 8$ mmHg/mm). As for *in vivo* flow conditions in microcirculation, in which RBCs interact with endothelial glycocalyx [20, 21], at low ΔP red

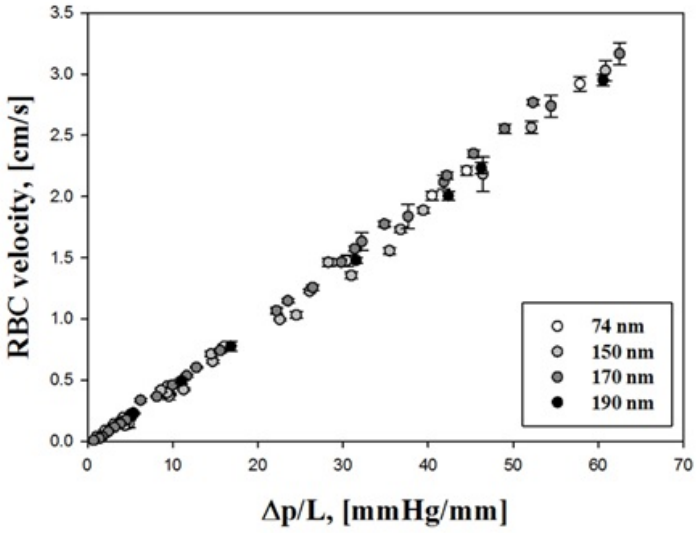

Figure 4.3: RBC velocity as a function of the imposed pressure drop both in bare and in hairy capillaries with different PHEMA brush thickness.

blood cells are less deformed and have a closer contact with the capillary walls coated by PHEMA brushes. In Figure 4.4, RBC velocity in hairy microcapillaries is plotted for both low and high values in a range of $h_{dry} \approx$ 25–190 nm (for the sake of clarity, the values related to only four thickness are reported in the diagram). We looked for an eventual critical value of the polymer layer thickness and subsequently a range where RBC speed depends on h_{dry}. Even at low values of the imposed pressure gradient, the same trend of Figure 4.3 can be observed for thicker PHEMA coatings. For thinner polymer layers ($h_{dry} < 60$ nm), the slope of the line fitting the experimental results corresponds to the bare one and, therefore, RBC velocity shows to be unaffected by the presence of polymer coatings on the inner walls of the tubes.

In Figure 4.5, the normalized difference of velocity $((V_{brush}\text{-}V_{bare})/V_{bare})$ is plotted as a function of the polymer brush thickness, in order to summarize the experimental results. An evident slowing down of RBC velocity ($\Delta V \approx$ 20–23%) has been detected in brush-coated capillaries lined by PHEMA brushes with a thickness above 70 nm. On the contrary, thin polymer layers do not show to have any effect on the flow of erythrocytes. Since the strength of the flow and the resulting depth of the fluid layer between cells and walls seem to be not crucial in the overall slowing down of RBCs in "hairy" capillaries, we attempted to provide another possible explanation to these striking results. In a work published in the 80s, Secomb *et al.* numerically solved the problem of the flow of axisymmetric red blood cells in

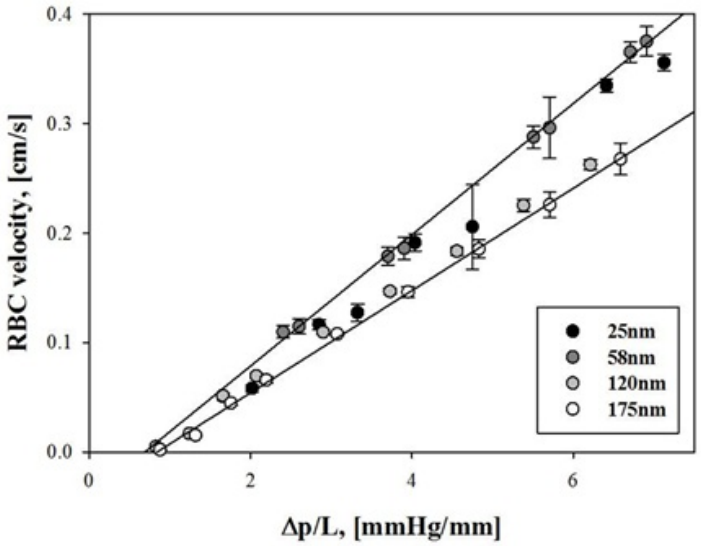

Figure 4.4: RBC velocity in hairy microcapillaries with different PHEMA brush thickness at low pressure drops.

narrow capillaries. By means of a model focusing on the lubrication theory, they strongly suggest that RBCs flowing in microtubes with diameter comparable to cell size exert an additional pressure on the capillary walls, due to the particular flow field around the erythrocyte [178]. Thus, since polymer chains of PHEMA brushes have a pronounced elastic character (they are usually modeled as a system of beads and springs in series [147]), a comparison between these two opposite effects is necessary. Unfortunately, even if the SFA measurements provide a qualitative evaluation of PHEMA coatings elasticity, a precise estimate of their elastic modulus is difficult to be carried out. However, in the light of the obtained results, it seems plausible that the additional pressure is extremely higher than the elastic force potentially exerted by the polymer chains, thus causing the crushing of the brushes on the walls in correspondence of RBCs transit.

In conclusion, the experimental measurements plausibly show that red blood cells have such a bigger dimension than PHEMA brushes thickness that their speed is affected only by the roughness of the microcapillary walls [179], due to the presence of the coating ($h_{dry} > 70$ nm). However, when density and roughness of the polymer layer are not enough ($h_{dry} < 60$ nm), RBCs simply flow like in bare microtubes. Thus, instead of a gradual slowing down of RBCs velocity with the increasing PHEMA brush thickness, an on-off behavior has been noticed. The presence of a narrow range of h_{dry} in which RBC velocity directly depends on brush thickness is not probable, since it would have a width of only 10 nm, like the diagram in Figure 4.5

clearly shows with a possible sigmoid fitting the data. Moreover, the sensitivity of our equipments do not allow to deeply investigate a range of so limited extent.

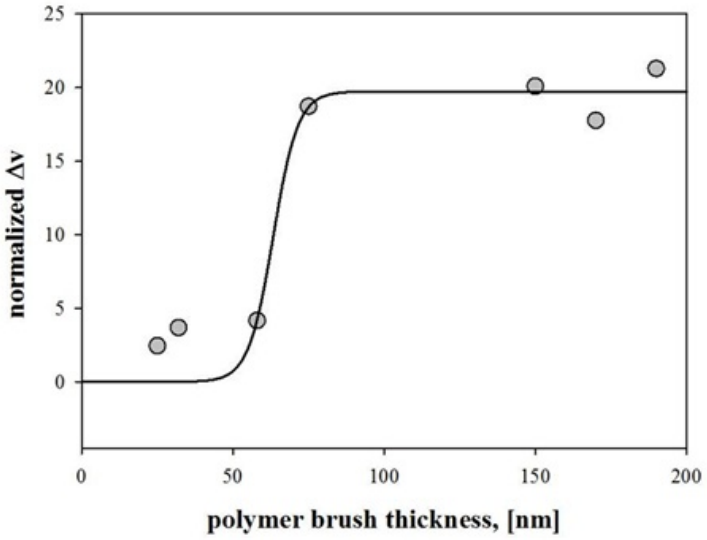

Figure 4.5: Difference of velocity in bare and hairy capillaries (ΔV), normalized by the velocity value in bare tubes, as a function of polymer coating thickness.

4.3.2 Red blood cell deformation

Since the effect of PHEMA brushes on RBCs velocity provided quite unexpected results, the following experimental analysis focused on the study of their deformability in "hairy" channels, in order to check an eventual dependence of the shape of flowing red blood cells on brush thickness. As known from the literature, there is not a predominant morphology in red blood cells flowing in microcirculation, either *in vivo* and *in vitro* conditions, except for very narrow channels. Indeed, in microcapillaries with size comparable to the ones used for our experiments (diameter $\approx$ 10 μm), it is possible to observe parachute-, bullet- and slipper-like shapes. For the sake of clarity and precision, measurements have been performed on axisymmetric cells only, like in other works in literature [64].

In Figure 4.6 (left), the deformability of axisymmetric cells is qualitatively evaluated either for a bare and a polymer coated capillary (h_{dry} = 170 nm), at similar values of cell velocities. All RBCs show the typical parachute-like shape, tending to an asymptotic configuration at increasing cell velocity. Moreover, it is evident that cells flowing in bare capillary are less deformed than ones in brush-coated capillary. A quantitative analysis of

RBC shape is presented in the right side of Figure 4.6, where cell deformation index DI (measured as the aspect ratio of a bounding box enclosing the cell body) is plotted as a function of RBC velocity both for bare tubes and capillaries coated with three different thickness of polymer layer (25, 73 and 170 nm). Error bars (such as in the previous figures) represent the standard deviation of the measurements, which is mainly due to the size distribution of RBCs in this case. For all the data sets, an increasing trend is observed, with a leveling-off of cell DI with increasing RBC velocity. These results are in very good agreement with previous results on RBC deformation in microcapillaries [64]. Although the large standard deviations, a plausible trend can be extrapolated from the measurements we obtained.Indeed, the deformation index in 170 nm coated capillary results to be higher than in bare ones, confirming the difference of the observed shapes shown in the left side of Figure 1, and intermediate decreasing values of DI were detected at lower layer thickness. In fact, it is clear that the thicker is the PHEMA brush coating and the higher is the deformation of erythrocytes. The deformation index (DI) of cells in 25 nm "hairy" capillary superimpose the one of bare capillary, indicating that RBC flow is not affected by the presence of such a thin layer and suggesting a plausible critical value of h_{dry} below which the shape of flowing red blood cells is no more depending on the PHEMA coatings lining the glass microtubes.

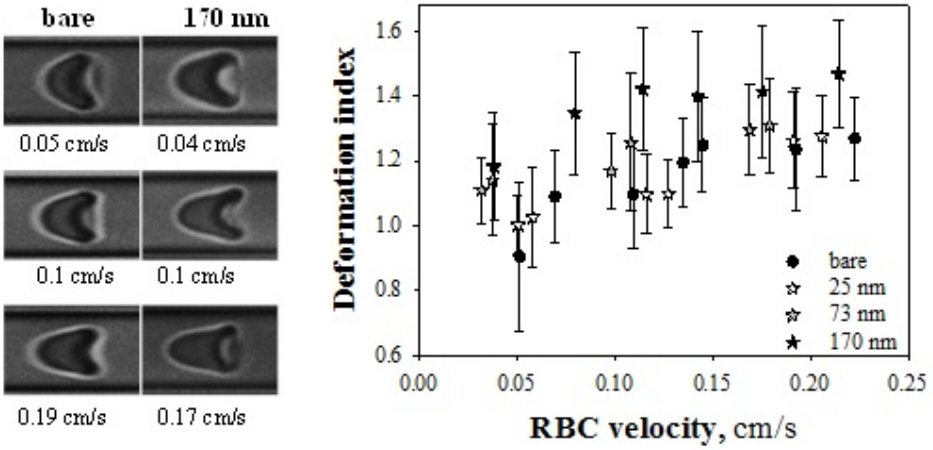

Figure 4.6: RBC deformation both in bare and hairy capillaries. On the left, a qualitative effect of brush coatings on RBC shape is shown. On the right, the trend of deformation index DI is presented as a function of red blood cell velocity.

As regards the progressive increase of RBCs deformation, how can this particular behavior be related to the on-off situation noticed for the velocity of red cells? In the range $70 < h_{dry} < 190$ nm, where an overall slowing

down of red blood cells is measured ($\Delta V \approx 20$–23%), the erythrocytes tend to spontaneously modify their shape in order to keep the speed unchanged. This is quite striking, since previous works *in vitro* [64] showed how the DI value depends on the flow strength and, consequently, the RBCs velocity. Moreover, another interesting cause for reflection is provided by the already cited work [178], written by Secomb *et al.* in 1986. The theoretical model proposed in this study suggests a value of the ratio between the RBC speed and the average flow velocity in a 10 μm capillary equal to 1.5 at each imposed pressure gradient. The outcomes of our experimental investigation do not agree with this hypothesis, since at the gradual slowing down of the flow velocity with the increasing polymer layer thickness do not correspond a progressive decrease of the speed of erythrocytes. Thus, $V_{RBC} / <V_{flow}> \neq 1.5$ at each value of the fixed pressure drop in the "hairy" capillaries we produced. Thus, the reasons of these striking results deserve to be deeply faced.

4.4 Conclusions

In this chapter we investigated the flow of red blood cells in 10 μm capillaries lined by PHEMA polymer brushes, the latter used as a possible model of glycocalyx in human microvessels. RBC velocity and deformability in microcapillaries bearing different brush thickness ($28 < h_{dry} < 190$ nm) have been measured at various imposed pressure drops, in order to shed light on the mechanisms leading blood flow in microvascular system. An identical significant slowing down of the erythrocytes has been detected in "hairy" tubes ($\Delta V \approx 20$–23%) for each value of the PHEMA coating thickness, when $h_{dry} > 70$ nm. On the contrary, we did not notice any difference in RBCs velocity between bare and brush-coated microchannels in correspondence of lower values of h_{dry}. The interpretation of the obtained experimental results suggests that red blood cells are plausibly slowed down because of the roughness of the brush-coated inner walls of the microcapillaries. When roughness and density of the produced brushes are not sufficiently significant, cells behave like in bare microtubes. Unlike the on-off situation observed for RBCs speed, the deformation index of the erythrocytes clearly reveals a different and gradual trend with the increasing polymer layer thickness. In fact, the measurements show that the thicker is the PHEMA brush and the higher is the deformation of red blood cells. As a consequence, it is plausible that red blood cells modify their shape during the flow in "hairy" microcapillaries, in order to keep their velocity unchanged. These results encourage further experimental and theoretical efforts, in order to better understand RBC properties in flow. For example, it seems necessary to combine the experimental investigation on this topic with theoretical models and eventually numerical simulations. Moreover, it could be important to investigate the behavior

of red blood cells in brush-coated capillaries with diameters smaller than cell size for checking mechanical properties of the polymer coatings. The real optimum would be to design and set up an innovative system based on microfluidics, where real endothelial cells line the inner surfaces of artificial channels. This will be fundamental to completely understand the role of glycocalyx in microvascularity and develop innovative microdevices able to simulate biological conditions and provide medical treatments for vascular diseases.

Chapter 5

Conclusions

5.1 Achieved results

This work of thesis has been developed in collaboration between the Dipartimento di Ingegneria Chimica of Federico II University in Napoli and the Laboratoire Interdisciplinaire de Physique (LIPhy) of Joseph Fourier University in Grenoble. It consisted of the study of red blood cells flow in microcirculation, mainly by means of *in vitro* imaging techniques, paralleled by numerical simulations and theoretical interpretation. The experimental campaign was essentially carried out in three phases:

1. In first instance, the aggregability of red blood cells flowing in microvascularity has been investigated by *in vitro* measurements on 10 μm silica capillaries. Qualitative and quantitative analysis of clusters dimension as a function of ΔP have been performed thanks to optical microscopy and following elaboration of the acquired images by suitable softwares. Moreover, RBCs aggregation has been observed in correspondence of different positions in the capillary (inlet, middle, outlet) and a statistical distribution of the trains of erythrocytes has been provided. In summary, the effect of both flow strength and residence time on RBC clusters formation in microtubes has been investigated and the results clearly showed that the imposed pressure gradient is the driving force of RBC aggregation in dynamic conditions. We showed that RBC clustering in microconfined Poiseuille flow is due only to hydrodynamic interactions between consecutive cells, since no additional interactive forces have been noticed by our measurements. Furthermore, our experimental results clearly reveal how size polydispersity of erythrocytes within the physiological range does not affect cluster stability, as hypothesized in previous studies. The obtained outcomes have been supported by 2D numerical simulations, that confirmed the trend already described for RBC clusters morphology and formation.

2. The increasing interest developed around the microcirculatory system prompted us to work on the realization of an artificial device, that would be able to mimic *in vivo* conditions. In fact, the second part of this project of thesis focused on the production of 10 μm glass microcapillaries coated with hydrophilic polymer brush (PHEMA) by *grafting-from* technique (ATRP). The kinetics of brushes growth and their swelling properties have been investigated by means of ellipsometry, Surface Force Apparatus and *in situ* electron microscopy coupled with EDX elemental analysis, in order to provide the best possible characterization of our samples. Then, the effect of PHEMA brushes on the flow of water inside the "hairy" microchannels have been probed. We have shown that a grafted polymer coating causes a flow reduction, which is roughly proportional to brush thickness and quite larger than expected from a simple reduction of the channel available lumen. After a lively discussion, two plausible mechanisms have been proposed to explain such a large brush-induced resistance: the brush polydispersity and the cyclic and the cyclic stretching-recoil motion of the grafted chains under shear, that creates flow perturbations in the regions close to microtube walls.

3. The last experimental part of this PhD project was dedicated to the observation of red blood cells flow in microcapillaries lined by PHEMA polymer brushes, the latter used as a possible model of glycocalyx in microcirculation *in vivo*. RBC velocity and deformability have been monitored at various imposed pressure drops in capillaries (inner diameter $\approx$ 10 μm) bearing brush of different thickness ($28 < h_{dry} < 190$ nm), in order to shed light on the mechanisms leading blood flow in microvascular system. A significant and identical slowing down of RBCs speed has been detected in "hairy" tubes ($\Delta V \approx$ 20–23%) for each value of the PHEMA coating thickness, when $h_{dry} > 70$ nm. On the contrary, we did not notice any difference in RBCs velocity between bare and brush-coated microchannels in correspondence of lower values of h_{dry}. One possible interpretation of these interesting results is that red blood cells are plausibly slowed down because of the roughness of the brush-coated inner walls of the microcapillaries. When brush chains density is not high enough and, consequently, the roughness of tube inner surfaces is not sufficiently significant, cells behave like in bare microtubes. The measurement of deformation index of the erythrocytes clearly revealed a different and gradual trend with the increasing polymer layer thickness: in fact, the thicker is the PHEMA brush and the higher is the deformation of red blood cells. Thus, considering all experimental results, it is plausible to say that red blood cells modify their shape during the flow in "hairy" microcapillaries, in order to keep their velocity unchanged and it is probable that they

have the same behavior *in vivo* too.

5.2 Possible developments

The results we obtained shed light on pioneering topics and, of course, they encourage further experimental and theoretical efforts, in order to better understand RBCs properties during the flow in physiological microvessels and develop innovative medical point-of-care testings for vascular diseases. Thus, it seems necessary to combine the experimental investigation with exhaustive theoretical models and possibly numerical simulations.

For example, as regards the RBC clustering phenomenon, both 2D and 3D numerical simulations are currently under development to have a more precise definition of RBC clusters in microvessels and to explain the mechanisms that lead to their formation as a function of initial position and spatial distribution in the capillaries. From the experimental point of view, experiments on red blood cells aggregability in microcapillaries with narrower diameters (d < 10 μm) are a fundamental item on the agenda, in order to have a global knowledge on this topic and improve the understanding of some common pathologies linked to RBC aggregation, like thrombus formation. Furthermore, experiments are going to be carried out to investigate RBCs clustering in case of rigified cells, as it happens in some widespread diseases (e.g. diabetes).

As regards the experimental campaign on polymer brush, it was animated by two purposes: the better understanding of the mechanisms governing *in vivo* microvascular system and the further design of microdevices for clinical testings of cardiac diseases in microcirculation. Thus, the results of present study can open the way to additional investigation, in order to produce synthetic microchannels which account for the effect of the glycocalyx, for *in vitro* observation of hemodynamics. It would be interesting in a next future to study the flow in "hairy" capillaries with different diameters and line the inner walls of the tubes with other biocompatible polymers. For instance, next investigation will focus on the flow of RBC in brush-coated tubes with a smaller diameter than cell size, in order to check mechanical properties of polymer coatings and how the glycocalyx is able to modify erythrocytes morphology in microvascularity. Moreover, the real goal will be to make a comparison between the properties of RBCs flowing in brush-coated channels and the ones of red cells in flow through artificial systems lined by *in vitro* grown endothelium.

Chapter 6

Acknowledgments

Se ho visto più lontano, è perché stavo sulle spalle di giganti
(I.Newton)

If I have seen further it is by standing on the shoulders of giants
(I.Newton)

It is very difficult to express all my acknowledgments in English, so I hope you do not mind if I switch to Italian language.

Nel mio piccolo, posso dire di sposare pienamente le parole del buon Isaac. In questi tre anni sono cresciuto molto, sia dal punto di vista scientifico che umano e, se son riuscito a raggiungere qualche traguardo, è stato perchè ho potuto poggiare sulle spalle solide di chi mi ha guidato e insegnato ad amare la scienza e la conoscenza in senso lato. L'elenco di tali persone nella mia vita, magari anonime e lontane dalla celebrità, è molto numeroso, per mia fortuna, e provo profonda gratitudine per tutto ciò che mi hanno trasmesso. Vorrei dedicare anche a loro questa tesi, a partire dalla mia maestra Rachele Bosco, i professori Salvatore Diodato, Pia Fimiani, fino ad arrivare ai miei docenti di liceo e università, Lucio Vecchio, Luciano Antonetti, Marisa Gallucci, Francesco Branda e Antonio D'Alessio.

Non posso che offrire il mio sincero grazie al professor Stefano Guido, che mi ha dato l'opportunità di lavorare per tre anni ad un progetto avvincente e ambizioso. In lui ho sempre trovato competenza, ingegno, curiosità, ma soprattutto umanità. In un mondo in cui contano sempre più l'autorità e l'apparire, il prof. Guido mi ha mostrato come si possano raggiungere risultati importanti usando il dialogo e la semplicità. La mia riconoscenza infinita va, senza ombra di dubbio, all'ingegner Giovanna Tomaiuolo, il ricercatore più valente, tenace e onesto che conosca. Il suo sostegno, sia scientifico che morale, è stato un pilastro che mi ha consentito di procedere spedito durante tutto il dottorato. E' grazie a Giovanna che ho imparato a lavorare in equipe, a confrontarmi con mentalità diverse dalla mia e su di lei ho po-

tuto sempre contare anche nei momenti di maggiore dubbio e confusione. In generale, vorrei rivolgere il mio grazie a tutti i colleghi e studenti del laboratorio Chemems: l'infaticabile Angelo, la verace Valentina, il brillante Dario, le pazienti Valeria, Speranza e Floriana, i neo arrivati Rosa e Antonio, Sergio, i miei tesisti e, dulcis in fundo, il mio grande amico Antonio Perazzo, ingegnere valido e uomo limpido. Sarà forse un pò tedioso leggere questa sfilza di nomi, ma una volta mi è stato detto che Dio conosce il nome di ognuno di noi, per cui mi sembrava il minimo nominare tutti coloro che hanno condiviso con me sorrisi e sfiducia in questi mesi.

Nel Novembre 2010, prima di partire alla volta di Grenoble, ero certo che non sarei sopravvissuto alla terra transalpina. Facendo un sincero mea culpa, ammetto di aver peccato di presunzione e giudizio, di aver coltivato, per anni, moltissimi preconcetti nei confronti di un popolo e una società da cui potremmo imparare in tanti ambiti. Oggi, a distanza di quasi tre anni, posso dire di essere anche io un pò Grenoblois, addirittura apprezzo la gente di montagna, la loro spontaneità, ho imparato con piacere la lingua e mi sono affezionato naturalmente ai nostri cugini francesi. Desidero ringraziare con sincerità i miei direttori di tesi al Laboratoire Interdisciplinaire de Physique, i dottori Lionel Bureau e Chaouqi Misbah. Lionel è stato sempre un esempio di dedizione e lavoro, di intelligenza e umiltà. Grazie al suo prezioso aiuto ho iniziato a sentirmi un ricercatore, ho imparato a prendermi responsabilità e usare la fantasia anche in un mondo dove tutto è precisione e raziocinio. Grazie a Chaouqi per il suo modo ancora "adolescenziale" di fare ricerca, pieno di entusiasmo e buon umore, per i suoi consigli mirati e decisivi, per la sua apertura mentale. Nel mio anno e mezzo passato al LIPhy, ho potuto conoscere persone che rimarranno indelebilmente nel mio cuore, per l'estrema gentilezza, la dedizione al lavoro, la capacità di non prendersi mai troppo sul serio. Penso, ad esempio, alla super Jessie, a tutte le signore dell'amministrazione, ai miei splendidi colleghi: Xavier, Yann, Valentina, Matthias, Caterina, Michael, Vincent, Rachel, Teodora, Othmane, Sofia.. qui devo fermarmi, la lista potrebbe diventare infinita! Grazie a tutti loro che mi hanno fatto sentire meno straniero e sempre a casa, anche quando da casa ero distante centinaia di Km. Grazie perchè mi avete insegnato la ricchezza della diversità e del rispetto reciproco, perchè mi avete donato momenti indimenticabili nella pura semplicità. Caro Filippo, credevi di esserti scampato la mozione ai sentimenti.. e invece no! Si dice che ci siano amici per una stagione, ed altri per tutta la vita. Beh, tu hai, ormai, un posto di diritto nel mio cuore. É vero, sei riuscito nell'intento di farmi comprare gli oggetti più inutili e costosi della mia esistenza, ma senza te, le nostre camminate a piedi, le riflessioni notturne, i bicchieri di vino sorseggiati alla stessa tavola, penso che i miei giorni sarebbero stati un pò più banali e vuoti, sarei stato come Totò senza Peppino, come una raclette senza patate!

I miei giganti, però, non si limitano a coloro con cui mi sono rapportato negli ultimi 3–4 anni. Winston Churchill diceva "più si riesce a guardare

indietro, più avanti si riuscirà a vedere", ed io sposo in pieno il suo pensiero. Quando penso ai miei maestri, ai pilastri della mia conoscenza, immediatamente la memoria mi rimanda all'immagine di un bambino di 5 anni, seduto al tavolo di una cucina sulle gambe di una donna bellissima e dolce. É a te, mamma, che rivolgo il mio grazie gioioso e riconoscente, per aver coltivato in me la curiosità, la pazienza, ad aver creduto in me anche quando io stesso avevo perso la fiducia. Ogni mio piccolo successo sarà sempre condiviso con te e con quel piccolo, immenso uomo di mio padre. Non andavo a dormire, se non dopo che tu fossi rientrato a casa. Quanti sacrifici hai fatto, quante nottate per l'amore alla famiglia e alla scienza. Tu cavalchi il sapere con semplicità e umiltà, tu rendi anche le cose più sofisticate, semplici come affettare il pane. Nessun comitato scientifico potrà mai avere valore maggiore di un tuo sorriso di assenso, un tuo sguardo di soddisfazione. E insieme a voi due, miei cari genitori, vorrei ringraziare tutta la mia famiglia. Prima di tutto mio fratello, che da sempre condivide con me gioie e dolori, mia nonna, mia zia Anna, zio Piero e zia Elena, i miei amatissimi cugini Lucio e Maria Paola. Mi perdonino tutti loro, ma un grazie ancor più di cuore va a un uomo che da sempre rappresenta il collante della mia famiglia e il gigante dell'amore: mio nonno Tonino. Pigro, indolente, furbo, brillante, ma soprattutto dolce e affettuoso, voglio ringraziarti per avermi fatto sempre sentire amato, per avermi sempre messo al centro delle tue attenzioni, che valgono molto più di un dottorato o un articolo pubblicato. Un giubilante grazie lo rivolgo anche a quella splendida peste della mia Chiara, che è riuscita a risvegliare in me il desiderio di mettermi in gioco, di rischiare, la voglia di dedicarmi anima e corpo che da un pò non sentivo dentro me.

In ultimo, per sugellare queste pagine, vorrei ringraziare il Signore. Non è semplice essere credenti oggi, in un mondo sempre più votato all'egocentrismo e il relativismo. Non posso definirmi un credente perfetto, non posso dire di avere una fede incrollabile, ma sono testimone, certamente, di quanto Dio ami me, di come mi abbia aiutato in questo percorso, quando ero uno studente in rovina e senza più fiducia. In questo senso, la canzone di San Damiano, ispirata a San Francesco, recita perfettamente quello che è il mio semplice grazie a Colui che da sempre mi conosce e mi ama..

Ogni uomo semplice, porta in cuore un sogno,
con amore ed umiltà potrà costruirlo;
Se con fede tu saprai vivere umilmente,
più felice tu sarai anche senza niente.
Se vorrai, ogni giorno, con il tuo sudore,
una pietra dopo l'altra alto arriverai.
Nella vita semplice troverai la strada
che la calma donerà al tuo cuore puro.
E le gioie semplici sono le più belle,
sono quelle che alla fine sono le più grandi

Dai e dai ogni giorno con il tuo sudore
una pietra dopo l'altra in alto arriverai.

Bibliography

[1] A.H.J. Salmon, S.C. Satchell, *Endothelial glycocalyx dysfunction in disease: albuminuria and increased microvascular permeability*, J Pathol 2012; 226: 562–574.

[2] W. Risau, *Development and differentiation of endothelium*, Kidney Int Suppl 1998; 67: S3–6.

[3] S.C. Satchell, F. Braet, *Glomerular endothelial cell fenestrations: an integral component of the glomerular filtration barrier*, Am J Physiol Renal Physiol 2009; 296: F947–956.

[4] K. Ichimura, R.V. Stan, H. Kurihara, et al., *Glomerular endothelial cells form diaphragms during development and pathologic conditions*, J Am Soc Nephrol 2008; 19: 1463–1471.

[5] M.E. Nesheim, F.J. Nesheim, *An experimental and mathematical model for fibrinolysis*, FASEB J 1988, 2:A1412.

[6] B. Haraldsson, J. Nystrom J, W.M. Deen, *Properties of the glomerular barrier and mechanisms of proteinuria*, Physiol Rev 2008; 88: 451–487.

[7] A.R. Pries, T.W. Secomb, P. Gaehtgens, *The endothelial surface layer*, Pflugers Arch 2000; 440: 653–666.

[8] S. Reitsma, D.W. Slaaf, H. Vink, et al., *The endothelial glycocalyx: composition, functions, and visualization*, Pflugers Arch 2007; 454: 345–359.

[9] S. Weinbaum, J.M. Tarbell, E.R. Damiano, *The structure and function of the endothelial glycocalyx layer*, Annu Rev Biomed Eng 2007; 9: 121–167.

[10] J.H. Luft, *Fine structure of capillary and endocapillary layer as revealed by ruthenium red*, Microcirc Symp Fed Proc 1966, 25: 1773–1783.

[11] B. Klitzman, B.R. Duling, *Microvascular hematocrit and red cell flow in resting and contracting striated muscle*, Am J Physiol 1979, 237: H481–H490.

[12] A.R. Pries, T.W. Secomb, P. Gaehtgens, J.F. Gross, *Blood flow in microvascular networks — experiments and simulation*, Circ Res 1990, 67: 826–834.

[13] A.S. Popel, P.C. Johnson, *Microcirculation and hemorheology*, Annu. Rev. Fluid Mech., 2005, 37, 43.

[14] A.R. Pries, T.W. Secomb, H. Jacobs, M. Sperandio, K. Osterloh, P. Gaehtgens, *Microvascular blood flow resistance: role of endothelial surface layer*, Am. J. Physiol. Heart Circ. Physiol., 1997, 273, H2272.

[15] E. Dejana, E. Tournier-Lasserve, B.M. Weinstein, *The control of vascular integrity by endothelial cell junctions: molecular basis and pathological implications*, Dev Cell 2009; 16: 209–221.

[16] N.J. Abbott, A.A. Patabendige, D.E. Dolman, et al., *Structure and function of the blood—brain barrier*, Neurobiol Dis 2010; 37: 13–25.

[17] N.J. Abbott, L. Ronnback, E. Hansson, *Astrocyte—endothelial interactions at the blood—brain barrier*, Nat Rev Neurosci 2006; 7: 41–53.

[18] H. Vink, B.R. Duling, *Identification of distinct luminal domains for macromolecules, erythrocytes, and leukocytes within mammalian capillaries*, Circ. Res. , 79: 581–89.

[19] E.R. Damiano, *The effect of the endothelial-cell glycocalyx on the motion of red blood cells through capillaries*, Microvasc. Res. 1998, 55: 77–91.

[20] T.W. Secomb, R. Hsu, A.R. Pries, *A model for red blood cell motion in glycocalyx-lined capillaries*, Am. J. Physiol. Heart Circ. Physiol 1998, 274: H1016–22.

[21] T.W. Secomb, R. Hsu, A.R. Pries, *Motion of red blood cells in a capillary with an endothelial surface layer: effect of flow velocity*, Am. J. Physiol. Heart Circ. Physiol. 2001, 281: H629–36.

[22] T.W. Secomb, R. Skalak, N. Ozkaya, J.F. Gross, *Flow of axisymmetric red blood cells in narrow capillaries*, J. Fluid Mech. 1986, 163: 405–23.

[23] P. Algenstaedt, C. Schaefer, T. Biermann, A. Hamann, B. Schwarzloh, H. Greten, W. Ruther, N. Hansen-Algenstaedt, *Microvascular alterations in diabetic mice correlate with level of hyperglycemia*, Diabetes 2003, 52: 542–549.

[24] I. Rubio-Gayosso, S.H. Platts, B.R. Duling, *Reactive oxygen species mediate modification of glycocalyx during ischemia–reperfusion injury*, Am. J. Physiol. Heart. Circ. Physiol. 2006, 290: H2247–H2256.

[25] H. Vink, A.A. Constantinescu, J.A. Spaan, *Oxidized lipoproteins degrade the endothelial surface layer: implications for platelet–endothelial cell adhesion*, Circulation 2000, 101: 1500–1502.

[26] A.R. Pries, T.W. Secomb, *Blood flow in microvascular networks*, Handbook of Physiology 2008: section 2, The Cardiovascular System, vol. IV, Microcirculation, 2nd edn, ed. Tuma RF, Duran WN & Ley K, pp. 3–36. Academic Press, San Diego.

[27] A.R. Pries, T.W. Secomb, P. Gaehtgens, *Structure and hemodynamics of microvascular networks: heterogeneity and correlations*, Am. J. Physiol. Heart. Circ. Physiol. 1995, 269, H1713–H1722.

[28] B.R. Duling, D.H. Damon, *An examination of the measurement of flow heterogeneity in striated muscle*, Circ. Res. 1987, 60, 1–13.

[29] T.W. Secomb, A.R. Pries, *The microcirculation: physiology at the mesoscale*, J. Physiol. 2011, 589.5: pp 1047–1052.

[30] T.W. Secomb, *Theoretical models for regulation of blood flow*, Microcirculation 2008, 15, 765–775.

[31] A.H. Goodman, R. Einstein, H.J. Granger, *Effect of changing metabolic rate on local blood flow control in the canine hindlimb*, Circ. Res. 1978, 43, 769–776.

[32] P.C. Johnson, *Autoregulation of blood flow*, Circ. Res. 1986, 59, 483–495.

[33] S.S. Segal, *Regulation of blood flow in the microcirculation*, Microcirculation 2005, 12, 33–45.

[34] T.W. Secomb, R. Hsu, E.T. Ong, J.F. Gross, M.W. Dewhirst, *Analysis of the effects of oxygen supply and demand on hypoxic fraction in tumors*, Acta Oncol 1995, 34 , 313–316.

[35] C.H. Wang, A.S. Popel, *Effect of red blood cell shape on oxygen transport in capillaries*, Math. Biosci. 1993, 116: 89–110.

[36] P.C. Johnson, *Overview of the microcirculation*, Microcirculation 2008, Academic Press.

[37] P.B. Canham, A.C. *Burton, Distribution of size and shape in populations of normal human red cells*, Circ. Res. 1968, 22: 405–422.

[38] R.E. Waugh, M. Narla, C.W. Jackson, T.J. Mueller, T. Suzuki, G.L. Dale, *Rheologic properties of senescent erythrocytes: Loss of surface area and volume with red blood cell age*, Blood 1992, 79: 1351–1358.

[39] H.K. Gerald Lim, M. Wortis, R. Mukhopadhyay, *Red blood cell shapes and shape transformations: Newtonian mechanics of a composite membrane*, Soft Matter 2008, 4: 83.

[40] R.M. Hochmuth, R.E. Waugh, *Erythrocyte membrane elasticity and viscosity*, Annu. Rev. Physiol. 49 (1987) 209–219.

[41] A.R. Pries, T.W. Secomb, P. Gaehtgens, *Biophysical aspects of blood flow in the microvasculature*, Cardiovascular Research 1996, 32: 654-667.

[42] M. Sugihara-Seki, B. M. Fu, *Blood flow and permeability in microvessels*, Fluid Dynamics Research 2005, 37: 82-132.

[43] T.W. Secomb, R.Hsu and A.R. Pries, *Blood Flow and Red Blood Cell Deformation in Nonuniform Capillaries: Effects of the Endothelial Surface Layer*, Microcirculation 2002, 9: 189, 196.

[44] G. Tomaiuolo, *Blood—mimicking fluid for biotechnological applications. Fluidodynamic behavior of red blood cells and droplets under confined shear flow*, PhD thesis 2009.

[45] S. Hénon, G. Lenormand, A. Richert, F. Gallet, *A new determination of the shear modulus of the human erythrocyte membrane using optical tweezers*, Biophys. J. 1999, 76: 1145–1151.

[46] E.A. Evans, *Bending elastic modulus of red blood cell membrane derived from buckling instability in micropipet aspiration tests*, Biophys. J. 1983, 43: 27–30.

[47] E.A. Evans, R. Waugh, L. Melnik, *Elastic area compressibility modulus of red cell membrane*, Biophys. J. 1976, 16: 585–595.

[48] W.C. Hwang, R.E. Waugh, *Energy of dissociation of lipid bilayer from the membrane skeleton of red blood cells*, Biophys. J. 1997, 72: 2669–2678.

[49] M. Puig-de-Morales-Marinkovic, K.T. Turner, J.P. Butler, J.J. Fredberg, S. Suresh, *Viscoelasticity of the human red blood cell*, Am. J. Physiol. Cell. Physiol. 2007, 293: C597–C605.

[50] Y.-Z. Yoon, J. Kotar, G. Yoon, P. Cicuta, *The nonlinear mechanical response of the red blood cell*, Phys. Biol. 2008, 5: 036007.

[51] O.K. Baskurt, H.J. Meiselman, *Blood Rheology and Hemodynamics*, Seminars in Thrombosis and Hemostasis 2003, 29(5), 435–447.

[52] C. Alonso, A.R. Pries, P. Gaehtgens, *Time-dependent rheological behaviour of blood flow at low shear in narrow horizontal tubes*, Biorheology 1989, 26; 229-246.

[53] P.S. Lingard, *Capillary Pore Rheology of Erythrocytes. I. Hydroelastic Behaviour of Human Erythrocytes*, Microvascular Research 1974, 8: 53–63.

[54] A.S. Popel, P.C. Johnson, *Microcirculation and hemorheology*, Annu. Rev. Fluid Mech. 2005, 37: 43–69.

[55] R. Pal, *Rheology of concentrated suspensions of deformable elastic particles such as human erythrocytes*, Journal of Biomechanics 2003, 36: 981–989.

[56] T.C. Pearson, R.R.C. Path, *Hemorheology in the Erythrocytoses*, The Mount Sinai Journal of Medicine 2001, 68(3): 182–191.

[57] T.W. Secomb, *Flow-dependent rheological properties of blood in capillaries*, Microvascualr Research 1987, 34: 46–58.

[58] S. Chien, S. Usami, R. Skalak, Blood flow in small tubes, in: Handbook of Physiology: The Cardiovascular System IV, American Physiological Society, Bethesda, MD, 1984.

[59] S. Guido, G. Tomaiuolo, *Microconfined flow behavior of red blood cells in vitro*, C. R. Physique 2009, 10: 751–763.

[60] L.T. Chen, L. Weiss, *The role of the sinus wall in the passage of erythrocytes through the spleen*, Blood 1973, 41: 529–537.

[61] N. Watanabe, D. Sakota, K. Ohuchi, S. Takatani, *Deformability of red blood cells and its relation to blood trauma in rotary blood pumps*, Artif. Organs. 2007, 31: 352–358.

[62] R. Skalak, P.I. Branemark, *Deformation of Red Blood Cells in Capillaries*, Science 1969, 164: 717–719.

[63] G.Tomaiuolo, M. Simeone, S. Guido, R. Ciancia, C. Rinaldi, V. Martinelli, B. Rotoli, *A methodology to study the deformability of red blood cells flowing in microcapillaries in vitro*, Ann Ist Sup SanitÃ 2007, 43: 186–192.

[64] G. Tomaiuolo, M. Simeone, V. Martinelli, B. Rotoli, S. Guido, *Red blood cell deformation in microconfined flow*, Soft Matter 2009, 5: 3736–3740.

[65] S. Shattil, B. Furie, H. Cohen, L. E. Silverstein, P. M. Glave, M. Strauss, *Hematology: Basic Principles and Practice*, Churchill Livingstone, Philadelphia, 2000.

[66] S. Chen, B. Gavish, S. Zhang, Y. Mahler, and S. Yedgar, *Monitoring of erythrocyte aggregate morphology under flow by computerized image analysis*, Biorheology 1995, 32(4), 487.

[67] I. V. Pivkin and G. E. Karniadakis, *Accurate coarse-grained modeling of red blood cells*, Phys. Rev. Lett. 2008, 101(11), 118105.

[68] N. Wohner, *Role of cellular elements in thrombus formation and dissolution*, Cardiovasc. Hematol. Agents Med. Chem. 2008, 6(3), 224.

[69] V. T. Turitto, H. J. Weiss, *Red blood cells: Their dual role in thrombus formation*, Science 1980, 207(4430), 541.

[70] J. Wan, W. D. Ristenpart, H. A. Stone, *Dynamics of shear-induced ATP release from red blood cells*, Proc. Natl. Acad. Sci. U.S.A. 2008, 105(43), 16432.

[71] P. Gaehtgens, C. Dührssen, and K. H. Albrecht, *Motion, deformation, and interaction of blood cells and plasma during flow through narrow capillary tubes*, Blood Cells 1980, 6(4), 799.

[72] J. L. McWhirter, H. Noguchi, G. Gompper, *Flow-induced clustering and alignment of vesicles and red blood cells in microcapillaries*, Proc. Natl. Acad. Sci. U.S.A. 2009, 106(15), 6039.

[73] R. Fahraeus, *The suspension stability of the blood*, Physiol. Rev. 1929, 9: 241–274.

[74] R. Fahraeus, T. Lindqvist, *The viscosity of the blood in narrow capillary tubes*, Am. J. Physiol. 1931, 96: 562–568.

[75] G. Bugliarello, J.W.Hayden, *Detailed characteristic of the flow of blood in vitro*, Transaction of the Society of Rheology, VII 1963, 209–230.

[76] H.H. Lipowsky, Microvascular rheology and hemodynamics, Microcirculation 2005, 12: 5–15.

[77] V.P. Zharov, E.I. Galanzha, Y. Menyaev, V.V. Tuchin, *In vivo high-speed imaging of individual cells in fast blood flow*, J. Biomed. Opt. 2006, 11: 054034.

[78] J. Seki, H.H. Lipowsky, *In vivo and in vitro measurements of red cell velocity under epifluorescence microscopy*, Microvasc. Res. 1989, 38: 110–124.

[79] U. Bagge, P.I. Branemark, R. Karlsson, R. Skalak, *Three—dimensional observations of red blood cell deformation in capillaries*, Blood Cells 1980, 6: 231–239.

[80] P. Gaehtgens, C. Duhrssen, K.H. Albrecht, Motion, deformation, and interaction of blood cells and plasma during flow through narrow capillary tubes, Blood Cells 1980, 6: 799–812.

[81] M. Abkarian, M. Faivre, R. Horton, K. Smistrup, C. A. Best-Popescu, H. A. Stone, *Cellular-scale hydrodynamics*, Biomed. Mater. 2008, 3(3), 034011.

[82] G. W. Schmid—Schönbein, S. Usami, R. Skalak, and S. Chien, *The interaction of leukocytes and erithrocytes in capillary and postcapillary vessels*, Microvasc. Res. 1980, 19(1), 45.

[83] B. Kaoui, G. Biros, C. Misbah, *Why do red blood cells have asymmetric shapes even in a symmetric flow?*, Physical Review Letters, 10/2009; 103(18):188101.

[84] K. H. Albrecht, P. Gaehtgens, A. Pries, and M. Heuser, *The Fahraeus effect in narrow capillaries (i.d. 3.3 to 11.0 micron)*, Microvasc. Res. 18(1), 33 (1979).

[85] G. Ghigliotti, T. Biben, and C. Misbah, *Rheology of a dilute two-dimensional suspension of vesicles*, J. Fluid Mech. 653, 489 (2010).

[86] F. Zhou, W.T.S. Huck, *Surface grafted polymer brushes as ideal building blocks for smart surfaces*, Phys. Chem. Chem. Phys., 2006, 8, 3815.

[87] R. Barbey, L. Lavanant, D. Paripovic, N. Schuwer, C. Sugnaux, S. Tugulu, H.A. Klok, *Polymer brushes via surface-initiated controlled radical polymerization: synthesis, characterization, properties, and applications*, Chem. Rev., 2009, 109, 5437.

[88] M. Motornov, S. Minko, K.J. Eichhorn, M. Nitschke, F. Simon, M. Stamm, *Reversible Tuning of Wetting Behavior of Polymer Surface with Responsive Polymer Brushes*, Langmuir 2003, 19, 8077.

[89] L. Spirin, A. Galuschko, T. Kreer, K. Binder, J. Baschnagel, *Polymer—Brush Lubricated Surfaces with Colloidal Inclusions under Shear Inversion*, Phys. Rev. Lett. 2011, 106, 168301.

[90] M. A. Cole, N. H. Voelcker, H. Thissen, H. J. Griesser, *Stimuli—responsive interfaces and systems for the control of protein—surface and cell-surface interactions*, Biomaterials 2009, 30, 1827.

[91] A.J. Wang, J.J. Feng, J. Fan, *Covalent modified hydrophilic polymer brushes onto poly(dimethylsiloxane) microchannel surface for electrophoresis separation of amino acids*, J. Chromatogr. A 2008, 1192, 173.

[92] A.N. Constable, W.J. Brittain, *Characterization of polymer brushes in capillaries*, Coll. Surf. A 2007, 308, 123.

[93] A.N. Constable, W.J. Brittain, *Modification of flow through silica microcapillaries via polymer brushes*, Coll. Surf. A 2011, 380, 128.

[94] I. Lokuge, X. Wang, P. W. Bohn, *Temperature-controlled flow switching in nanocapillary array membranes mediated by poly(Nisopropylacrylamide) polymer brushes grafted by atom transfer radical polymerization*, Langmuir 2007, 23, 305.

[95] R. Advincula, W.J. Brittain, K.C. Caster, J. Rühe, *Polymer Brushes: Synthesis, Characterization, Applications*; Eds.; VCH—Wiley: Weinheim, 2004.

[96] O. Azzaroni, *Polymer Brushes Here, There, and Everywhere: Recent Advances in Their Practical Applications and Emerging Opportunities in Multiple Research Fields*, JOURNAL OF POLYMER SCIENCE PART A: POLYMER CHEMISTRY 2012, 50, 3225–3258.

[97] X. Li, P. M. Vlahovska and G. E. Karniadakis, *Continuum- and particle-based modeling of shapes and dynamics of red blood cells in health and disease*, Soft Matter, 2013, 9, 28–37.

[98] G. Tomaiuolo, M. Barra, V. Preziosi, A. Cassinese, B. Rotoli and S. Guido, *Microfluidics analysis of red blood cell membrane viscoelasticity*, Lab Chip, 2011, 11, 449–454.

[99] G. Tomaiuolo, D. Rossi, S. Caserta, M. Cesarelli and S. Guido, *Comparison of two flow-based imaging methods to measure individual red blood cell area and volume*, Cytometry. Part A : the journal of the International Society for Analytical Cytology, 2012, 81.

[100] G. Tomaiuolo and S. Guido, *Start-up shape dynamics of red blood cells in microcapillary flow*, Microvascular Research, 2011, 82, 35–41.

[101] T. Secomb and R. Hsu, *Analysis of red blood cell motion through cylindrical micropores: effects of cell properties*, Biophys J, 1996, 71, 1095–1101.

[102] H. Noguchi and G. Gompper, *Shape transitions of fluid vesicles and red blood cells in capillary flows*, Proc Natl Acad Sci U S A, 2005, 102, 14159–14164.

[103] C. Pozrikidis, *Numerical Simulation of the Flow-Induced Deformation of Red Blood Cells*, Ann Biomed Eng, 2003, 31, 1194–1205.

[104] R. Hochmuth, R. Marple and S. Sutera, *Capillary blood flow. I. Erythrocyte deformation in glass capillaries*, Microvasc Res, 1970, 2, 409–419.

[105] A. Pries, T. Secomb, T. Gessner, M. Sperandio, J. Gross and P. Gaehtgens, *Resistance to blood flow in microvessels in vivo*, Circ Res, 1994, 75, 904–915.

[106] M. B. Kim and I. H. Sarelius, *Distributions of wall shear stress in venular convergences of mouse cremaster muscle*, Microcirculation, 2003, 10, 167–178.

[107] J. Zhang, P. C. Johnson and A. S. Popel, *Effects of Erythrocyte Deformability and Aggregation on the Cell Free Layer and Apparent Viscosity of Microscopic Blood Flows*, Microvascular Research, 2009, 77, 265–272.

[108] S. T. Milner, Science, *Polymer Brushes*, 1991, 251, 905–914.

[109] K. Binder, T. Kreer and A. Milchev, *Polymer brushes under flow and in other out—of—equilibrium conditions*, Soft Matter, 2011, 7, 7159–7172.

[110] J. Klein, Science, *Repair or replacement? A joint approach*, 2009, 323, 47–48.

[111] P. Mansky, Y. Liu, E. Huang, T. P. Russell and C. Hawker, *Controlling Polymer-Surface Interactions with Random Copolymer Brushes*, Science, 1997, 275, 1458–1460.

[112] G. Storm, S. O. Belliot, T. Daemen and D. D. Lasic, *Surface modification of nanoparticles to oppose uptake by the mononuclear phagocyte system*, Advanced Drug Delivery Reviews, 1995, 17, 31–48.

[113] A. Hucknall, A. J. Simnick, R. T. Hill, A. Chilkoti, A. Garcia, M. S. Johannes, R. L. Clark, S. Zauscher and B. D. Ratner, *Versatile synthesis and micropatterning of nonfouling polymer brushes on the wafer scale*, Biointerphases, 2009, 4, FA50–57.

[114] A.J. Wang, J.J. Xu and H.Y. Chen, *In—situ grafting hydrophilic polymer on chitosan modified poly (dimethysiloxane) microchip for separation of biomolecules*, Journal of Chromatography A, 2007, 1147, 120–126.

[115] I. B. Malham and L. Bureau, *Density effects on collapse, compression, and adhesion of thermoresponsive polymer brushes* Langmuir, 2009, 26, 4762–4768.

[116] N. Idota, A. Kikuchi, J. Kobayashi, K. Sakai and T. Okano, *Microfluidic Valves Comprising Nanolayered Thermoresponsive Polymer—Grafted Capillaries* Advanced Materials, 2005, 17, 2723–2727.

[117] J. Yom, S. M. Lane and R. A. Vaia, *Multi—component hierarchically structured polymer brushes*, Soft Matter, 2012, 8, 12009–12016.

[118] P. Connoly, *A comprehensive review on the opportunities of point-of-care systems for the clinical diagnostics market*, Biosensors Bioelectronics, 1995, 10, 1–6.

[119] A.J. Tüdos, G.A.J. Besselink, R.B.M. Schasfoort, *Trends in miniaturized total analysis systems for point-of-care testing in clinical chemistry*, Lab on a chip, 2001, 1, 83–95.

[120] A. Manz, N. Graber and H.M. Widmer, *Miniaturized total chemical analysis systems: A novel concept for chemical sensing*, Sens. Actuators B, 1990, 1, 244–248.

[121] N.E. Drenck, *Point-of-care testing in critical care medicine: the clinician view*, Clin. Chim. Acta, 2001, 307, 3–7.

[122] M.P. Hudson, R.H. Christenson, L.K. Newby, A.L. Kaplan and E.M. Ohman, *Cardiac markers: point of care testing*, Clin. Chim. Acta, 1999, 284, 223–237.

[123] J. H. Nichols, *Management of Point-of-Care Testing*, Blood Gas News 1999, 8, 4–14.

[124] D. A. Adams and M. Buus-Frank, *Point-of-care technology: the i-STAT system for bedside blood analysis*, J. Pediatr. Nurs., 1995, 10, 194–198.

[125] P. Stubbs and P. O. Collinson, *Point-of-care testing: a cardiologist's view*, Clin. Chim. Acta, 2001, 311, 57–61.

[126] C.H. Ahn, J.W. Choi, G. Beaucage, J.H. Nevin, J.B. Lee, A. Puntambekar and J.Y. Lee, *Disposable smart lab on a chip for point-of-care clinical diagnostics*, Proceedings of the IEEE, vol. 92, no. 1, January 2004.

[127] K. Matyjaszewski, P.J. Miller, N. Shukla, B. Immaraporn, A. Gelman, B.B. Luokala, T.M. Siclovan, G. Kickelbick, T. Vallant, H. Hoffmann,

T. Pakula, *Polymers at interfaces: Using atom transfer radical polymerization in the controlled growth of homopolymers and block copolymers from silicon surfaces in the absence of untethered sacrificial initiator*, Macromolecules 1999, 32, 8716–8724.

[128] J. Lindqvist, D. Nyström, E. Östmark, P. Antoni, A. Carlmark, M. Johansson, A. Hult, E. Malmström, *Intelligent Dual-Responsive Cellulose Surfaces via Surface-Initiated ATRP*, Biomacromolecules 2008, 9, 2139–2145.

[129] D. Bontempo, N. Tirelli, G. Masci, V. Crescenzi, J.A. Hubbell, *Atom Transfer Radical Polymerization as a Tool for Surface Functionalization*, Macromol. Rapid Commun. 2002, 23, 418–422.

[130] F.J. Xu, J.P. Zhao, E.T. Kang, K.G. Neoh, J. Li, *Functionalization of nylon membranes via surface-initiated atom-transfer radical polymerization*, Langmuir 2007, 23, 8585–8592.

[131] J. Liu, T. Pan, A.T. Woolley, M.L. Lee, *Surface-modified poly(methyl methacrylate) capillary electrophoresis microchips for protein and peptide analysis*, Anal. Chem. 2004, 76, 6948–6955.

[132] O. Azzaroni, S.E. Moya, A.A. Brown, Z. Zheng, E. Donath, W.T.S. Huck, *Polyelectrolyte brushes as ink nanoreservoirs for microcontact printing of ionic species with poly(dimethyl siloxane) stamps*, Adv. Funct. Mater. 2006, 16, 1037–1042.

[133] E.R.Damiano, B.R. Duling, K. Ley, T.C. Skalak, *Axisymmetric pressure-driven flow of rigid pellets through a cylindrical tube lined with a deformable porous wall layer*, J. Fluid Mech., 1996, 314, 163.

[134] I.B. Malham, L. Bureau, *Density Effects on Collapse, Compression, and Adhesion of Thermoresponsive Polymer Brushes*, Langmuir 2010, 26, 4762.

[135] L. Bureau, *Surface force apparatus for nanorheology under large shear strain*, Rev. Sci. Instrum. 2007, 78, 065110.

[136] W. Helfrich, *Elastic properties of lipid bilayers: theory and possible experiments*, 1973 Z. Naturforschung 28 693–703.

[137] U. Seifert, *Configurations of fluid membranes and vesicles* , 1997 Advances in Physics 46 13–137.

[138] D.M. Jones, W.T.S. Huck, *Controlled surface-initiated polymerizations in aqueous media*, Adv. Mater. 2001, 13, 1256.

[139] P.G. de Gennes, *Conformations of polymers attached to an interface*, Macromolecules 1980, 13, 1069.

[140] L. Lanotte, S. Guido, C. Misbah, P. Peyla and L. Bureau, *Flow reduction in microchannels coated with a polymer brush* Langmuir, 2012, 28, 13758–13764.

[141] G. Tomaiuolo, L. Lanotte, G. Ghigliotti, C. Misbah and S. Guido, Physics of Fluids, *Red blood cell clustering in Poiseuille microcapillary ow* 2012, 24, 051903–051908.

[142] J.L Barrat, *A possible mechanism for swelling of polymer brushes under shear*, Macromolecules 1992, 25, 832.

[143] Y. Rabin, S. Alexander, *Stretching of grafted polymer layers*, Europhys. Lett, 1990, 13, 49.

[144] R. Ivkov, P.D. Butler, S.K. Satija, L.J. Fetters, *Effect of solvent flow on a polymer brush: A neutron reflectivity study of the brush height and chain density profile*, Langmuir 2001, 17, 2999.

[145] L. Miao, H. Guo, M.J. Zuckermann, *Conformation of polymer brushes under shear: Chain tilting and stretching*, Macromolecules 1996, 29, 2289.

[146] M. Muller, C. Pastorino, *Cyclic motion and inversion of surface flow direction in a dense polymer brush under shear*, Europhys. Lett 2008, 81, 28002.

[147] F. Leonforte, J. Servantie, C. Pastorino, M. Muller, *Molecular transport and flow past hard and soft surfaces: computer simulation of model systems*, J. Phys. Condens. Matter 2011, 23, 184105.

[148] A. Laadhari, P. Saramito and C. Misbah, *Vesicle tumbling inhibited by inertia*, Phys. Fluids, 24:031901.

[149] T. Biben, A. Farutin and C. Misbah, *Three-dimensional vesicles under shear flow: Numerical study of dynamics and phase diagram*, 2011 Phys. Rev. E 83(3) 031921.

[150] C. Misbah, *Vacillating breathing and tumbling of vesicles under shear flow*, 2006 Phys. Rev. Lett. 96 028104.

[151] P.M. Vlahovska and R.S. Gracia, *Dynamics of a viscous vesicle in linear flows*, 2007 Phys. Rev. E 75 016313.

[152] A. Farutin and C. Misbah, *Symmetry breaking of vesicle shapes in Poiseuille flow*, 2011 Phys. Rev. E 84(1) 011902.

[153] D. Barthés-Biesel and J.M. Rallison, *The time dependent deformation of a capsule freely suspended in a linear shear flow*, 1981 J. Fluid Mech., 113 251–267.

[154] R. Finken, S. Kessler and U. Seifert, *Micro-capsules in shear flow*, 2011 Phys. Cond. Mat. 23 184113.

[155] P. Gires, G. Danker and C. Misbah, *Hydrodynamic interaction between two vesicles in a linear shear flow: Asymptotic study*, 2012 Phys. Rev. E. 86, 011408.

[156] C. Pozrikidis, *Boundary Integral and Singularity Methods for Linearized Viscous Flow*, 1992 (Cambridge University Press, Cambridge, UK).

[157] S.K. Veerapaneni, D. Gueyffier, D. Zorin and G. Biros, *A boundary integral method for simulating the dynamics of inextensible vesicles suspended in a viscous fluid in 2D*, 2009 J. Comp. Phys. 228 2334–2353.

[158] E. Lac, A. Morel and D. Barthés-Biesel, *Hydrodynamic interaction between two identical capsules in simple shear flow*, 2007 J. Fluid Mech. 573 149–169.

[159] H. Wang, T. Lei, L. Huang and Z. Yao, *A parallel fast multipole accelerated integral equation scheme for 3D Stokes equations*, 2004 Int. J. Numer. Methods Eng. 70 812–839.

[160] C. Peskin, *Numerical analysis of blood flow in the heart*, 1977 J. Comp. Phys 25 220–252.

[161] A.Z.K. Yazdani and P. Bagchi, *Three-dimensional numerical simulation of vesicle dynamics using a front-tracking method*, 2011 Phys. Rev. E 84(2) 026314.

[162] M. Ismail and A. Lefebvre-Lepot, *A Necklace Model for Vesicles Simulations in 2D*, 2012 arXiv:1202.3034v1 [math-ph].

[163] T. Biben, K. Kassner and C. Misbah, *Phase-field approach to three-dimensional vesicle dynamics*, 2005 Phys. Rev. E 72 041921.

[164] D. Jamet and C. Misbah, *Thermodynamically consistent picture of the phase-field model of vesicles: elimination of the surface tension*, 2008 Phys. Rev. E 78(4) 041903.

[165] E. Maitre, C. Misbah, P. Peyla and A. Raoult, *Comparison between advected-field and level-set methods in the study of vesicle dynamics*, 2012 Physica D 243 1146–1157.

[166] I.V. Pivkin and G.E. Karniadakis, *Accurate coarse-grained modeling of red blood cells*, 2008 Phys. Rev. Lett. 101(11) 118105.

[167] A. Lamura, G. Gompper, T. Ihle and D.K. Roll, *Multi-particle-collision Dynamics: Flow around a Circular and a Square Cylinder*, Institut fuer Festkoerperforschung Scientific Report 2001/2002, Forschungszentrum Juelich.

[168] J.L. McWhirter, H. Noguchi and G. Gompper, *Flow-induced clustering and alignment of vesicles and red blood cells in microcapillaries*, 2009 PNAS 106 6039–6043.

[169] J. Clausen and C. Aidun, 2010 Phys. Fluid 23 123302–123311.

[170] G. Ghigliotti, H. Selmi, L. El Asmi, and C. Misbah, *Why and how does collective red blood cells motion occur in the blood microcirculation?*, Phys. Fluids 24, 101901 (2012).

[171] M. Van der Waarden, J Colloid Sci 1950, 5, 535.

[172] W.J. Brittain and S. Minko, *A Structural Definition of Polymer Brushes*, J. POLYM. SCI. PART A: POLYM. CHEM.: VOL. 45 (2007).

[173] S. Alexander, *ADSORPTION OF CHAIN MOLECULES WITH A POLAR HEAD A SCALING DESCRIPTIONJ*, Phys (Paris) 1977, 38, 983.

[174] S.T. Milner, *Polymer Brushes*, Science 1991, 251, 905.

[175] I. Szleifer, M.A. Carignano, Adv Chem Phys 1996, 94, 165.

[176] M. Tirrell, S. Patel, G. Hadziioannou, *Polymeric amphiphiles at solid-fluid interfaces: Forces between layers of adsorbed block copolymers*, Proc Natl Acad Sci USA 1987, 84, 4725.

[177] A.I. Barakat and D.K. Lieu, *Differential Responsiveness of Vascular Endothelial Cells to Different Types of Fluid Mechanical Shear Stress*, Cell Biochemistry and Biophysics, Volume 38, 2003.

[178] T.W. Secomb, R. Skalak, N. Ozkaya and J.F. Gross, *Flow of axisymmetric red blood cells in narrow capillaries*, J . Fluid Mech. (1986), vol. 163, pp. 405–423.

[179] S.W. Park, M. Intaglietta, D.M.Tartakovsky, *Impact of endothelium roughness on blood flow*, Journal of Theoretical Biology, 300 (2012) 152–160.

[180] G.A. Truskey, F. Yuan, D.F. Katz, *Transport Phenomena in Biological Systems*, 2004, Pearson Prentice Hall Bioengineering, Upper Saddle River, New Jersey 07458.

Appendix A

Publications

1. Giovanni Ausanio, Cornelia L. Hison, Vincenzo Iannotti, Luca Lanotte, and Luciano Lanotte, *Magneto-piezoresistance in elastomagnetic composites*, Journal of Applied Physics 110, 063903 (2011).
   [**doi: 10.1063/1.3634120**]

2. Giovanna Tomaiuolo, Luca Lanotte, Giovanni Ghigliotti, Chaouqi Misbah, and Stefano Guido, *Red blood cell clustering in Poiseuille microcapillary flow*, Physics of Fluids 24, 051903 (2012).
   [**http://dx.doi.org/10.1063/1.4721811**]

3. Luca Lanotte, Stefano Guido, Chaouqi Misbah, Philippe Peyla, and Lionel Bureau, *Flow Reduction in Microchannels Coated with a Polymer Brush*, Langmuir 2012, 28, 13758–13764.
   [**http://dx.doi.org/10.1021/la302171a**]

4. Luca Lanotte, Claudio Bilotti, Luigi Sabetta, Giovanna Tomaiuolo, and Stefano Guido, *Dispersion of sepiolite rods in nanofibers by electrospinning*, Polymer 54 (2013) 1295–1297.
   [**http://dx.doi.org/10.1016/j.polymer.2013.01.009**]

5. Giovanni Ausanio, Vincenzo Iannotti, Luca Lanotte, and Luciano Lanotte, *Optimization of the coupling between piezoresistivity and magnetoelasticity in an elastomagnetic composite to sense a spatial gradient of the magnetic field*, Eur. Phys. J. B (2013) 86: 51.
   [**DOI: 10.1140/epjb/e2012-30657-1**]

Appendix B

Conferences

1. L. Lanotte, G. Tomaiuolo, L. Bureau, C. Misbah, S. Guido, *Microcapillari rivestiti da polymer brush come modello per simulare il glycocalyx*, Emoreologia e Microcircolo: dalla ricerca alla clinica, ISS, December 13th, 2012, Roma, Italy.

2. L. Lanotte, G. Tomaiuolo, L. Bureau, C. Misbah, S. Guido, *Flow behaviour of red blood cells in microcapillaries coated with a polymer brush*, BIOMICS Topical Team of the European Space Agency, November 5th–6th, 2012, Napoli, Italy.

3. G. Tomaiuolo, L. Lanotte, S. Caserta, A. Cassinese, S. Guido, *Studio in vitro della deformabilità e dell'aggregabilità di globuli rossi in flusso microconfinato tramite metodi di analisi dell'immagine*, Convegno GRICU 2012, September 16–19, 2012, Montesilvano (PE), Italy.

4. G. Tomaiuolo, L. Lanotte, S. Caserta, S. Guido, *Realizzazione di un apparato di electrospinning per la produzione di microtubi in policaprolattone*, Convegno GRICU 2012, September 16–19, 2012, Montesilvano (PE), Italy.

5. L. Lanotte, L. Bureau, S. Guido, C. Misbah, *Flow in hairy microcapillaries*, 13th Condensed Matted Meeting of the French Physical Society, mini-colloquium on Nanofluidics – Liquids at Interfaces, August 27–31, 2012, Montpellier, France.

6. G. Tomaiuolo, L. Lanotte, V. Preziosi, S. Caserta, A. Cassinese, C. Misbah, S. Guido, *Microconfined flow to measure red blood cell viscoelastic properties*, ICR 2012 – XVIth International Congress on Rheology, August 5–10, 2012, Lisbon, Portugal.

7. G. Tomaiuolo, L. Lanotte, S. Guido, *A novel technique for the analysis of red blood cell deformation and clustering in vitro*, Joint meeting of the European Society of Microcirculation (ESM) and the Society

of Microcirculation and Vascular Biology (GfMVB), October 13–16, 2011, Munich, Germany.

8. L. Lanotte, L. Bureau, G. Tomaiuolo, C. Misbah, S. Guido, *Flow of red blood cells in hairy microcapillaries*, Joint meeting of the European Society of Microcirculation (ESM) and the Society of Microcirculation and Vascular Biology (GfMVB), October 13–16, 2011, Munich, Germany.